

Amphibian distributions and extinction risk in China under climate and land use
change

by

Youhua Chen

A thesis submitted in partial fulfillment of the requirements for the degree of

Doctor of Philosophy

in
CONSERVATION BIOLOGY

Department of Renewable Resources
University of Alberta

Abstract

Species extinctions are inevitable, irreversible and a time-delayed process that is accelerating due to the warming climate and the loss of habitats worldwide. The most threatened vertebrate group in terrestrial ecosystems is amphibians. In this thesis, I assess potential range shifts and extinction risks of amphibians in China, and test whether the current distribution of protected areas is effective in protecting amphibian habitats both today and under conditions imposed by climate and land use change in the future. This was done by use of circular statistics, metapopulation models, climate velocity algorithms and ensemble species distribution modeling. Overall, I found: (1) large conservation (protected area) gaps were found throughout China and especially the southern parts of Tibet and the Hengduan Mountains, an amphibian diversity hotspot vulnerable to climate change and human activities; (2) correlations between directional range shift of species and climate velocity were evident with range shifts of amphibians in China being mostly tri-directional in pattern, preferring northern, eastern or northeastern directions for different dispersal scenarios and climatic data used; (3) relaxation time of extinction debt for amphibians in China was related to the strength of the Allee effect, forest cover change and the trade-off between colonization and emigration rates. Metapopulation models, with and without Allee effects, estimated average time to half extinction for endemic amphibians of China to be 44.9 and 71.8 years, respectively. Collectively, this thesis research identifies

regional conservation needs of amphibians, fuels the development and application of novel statistical methods in the estimate of species extinction, and paves the ways for future studies on extinction debt modeling.

Acknowledgements

I am very fortunate to work with Prof. Fangliang He and under his supervision, to conduct research on biodiversity conservation and ecological modeling. Without his excellent mentorship, great support and many encouragements, this thesis would not have been possible.

I sincerely thank my supervisory committee members, Profs. Mark Lewis and Scott E. Nielsen, for their helpful advice and constructive comments on my research over the past years. I appreciate Profs. Mark Poesch, Matthew Wheatley and David M. Green for giving helpful comments on my projects as well. My thesis greatly benefited with discussions and assistance from current and past members in Profs. He and Nielsen's labs and my friends, including, but not limited to Drs. Jian Zhang, David R. Roberts, Xiaofeng Ruan, Dingliang Xing and Shushi Peng.

Finally, I acknowledge the financial support from the China Scholarship Council (CSC). Without the CSC support over the past several years, it would have been challenging for me, as an international student, to study abroad. After years of hard work and diligence overseas, I now feel it is time for me to go back China, meet my parents, and work for my home country.

Table of Contents

Chapter 1 General Introduction	1
Amphibian biology	1
Contemporary diversity and distribution patterns of amphibians in China.....	3
Biogeographic processes that influence amphibian diversity and distribution in China	4
Amphibian extinction risks and correlating factors in China.....	7
Aims and structure of this thesis.....	10
Literature cited.....	12
Chapter 2 Assessing the effectiveness of China's protected areas to conserve current and future amphibian diversity	19
Summary	19
Introduction	20
Materials and Methods	23
<i>Distributional data</i>	23
<i>Bioclimatic and land use data</i>	25
<i>Species distribution modeling (SDM)</i>	28
<i>Climate velocity and residence time of climate</i>	31
<i>Computation of phylogenetic diversity and phylogenetic endemism.....</i>	32
<i>Reference sites and indices of protected area effectiveness</i>	33
<i>Identifying conservation gaps</i>	38
Results	39
Discussion	41
Literature cited	45
Figures	57
Supporting Information.....	64
Chapter 3 Directionality and spacing of climate-driven changes in amphibian ranges in China	97
Summary	97

Introduction	98
Materials and Methods	102
<i>Distributional and climatic data</i>	102
<i>Species distribution models (SDMs)</i>	103
<i>Dispersal modeling</i>	103
<i>Climate velocity and range shift of the species</i>	105
<i>Circular statistics for testing range-shift hypotheses</i>	106
Results	111
Discussion	113
<i>Amphibian range-shift patterns</i>	113
<i>Climate velocity as a range-shift predictor</i>	116
<i>Applying circular statistics in future range change assessments and conservation</i>	117
Literature cited	119
Tables	128
Figures	129
Supporting Information	131
Chapter 4 Predicting the extinction debt for amphibians in China due to deforestation	141
Summary	141
Introduction	142
Materials and Methods	146
<i>Distribution data</i>	146
<i>Forest data</i>	146
<i>Metapopulation models</i>	148
<i>Time point triggering extinction debts</i>	152
<i>Time to half extinction</i>	152
<i>Comparisons of different metapopulation models and forest scenarios</i>	154
Results	154
Discussion	157

Literature cited	161
Figures	169
Supporting Information	174
Chapter 5 Discussion and conclusions	190
Limitations	191
Conservation challenges	192
Literature cited	193
Bibliography	195

List of Figures

- Fig. 2-1.** Distribution of grid cells (in green color) that are used to represent current protected areas of China (A), range map-derived hotspots of richness (B), occurrence-derived hotspots of richness (C), range map-derived complementary sites (D) and occurrence-derived complementary sites (E) at $0.25^\circ \times 0.25^\circ$ spatial resolution. Grid cells are identified as protected areas when at least 50% of their area is currently protected (in red color), which are superimposed in the maps.....57
- Fig. 2-2.** Predicted change using range maps at the $0.25^\circ \times 0.25^\circ$ spatial resolution of species richness (A), corrected weighted endemism (B), phylogenetic diversity (C) and phylogenetic endemism (D) between current and 2070s in protected areas (PAs) versus reference sites (unprotected areas: non-PAs; richness hotspots: RH; complementary sites: CS). Error bars indicate the 95% confidence interval. “*” and “NS” above each histogram for reference sites indicates that the comparison between PAs and reference sites is significant ($P < 0.05$) or non-significant ($P > 0.05$), respectively based on a *t* test.59
- Fig. 2-3.** Residence time of climate using range maps at the $0.25^\circ \times 0.25^\circ$ spatial resolution in protected areas (PAs) versus reference sites (unprotected areas: non-PAs; richness hotspots: RH; complementary sites: CS) and in species’ partial ranges within protected versus unprotected areas. Error bars indicate the 95% confidence interval. In A and B, “*” indicates that the comparison between PAs and each reference site is significant ($P < 0.05$) using a *t* test. In C, “*” indicates the comparison of residence time of climate in species’ partial ranges covered by protected areas versus unprotected areas is significant ($P < 0.05$).60
- Fig. 2-4.** Predicted change using range maps at the $0.25^\circ \times 0.25^\circ$ spatial resolution between the current time and the 2070s, in proportion of natural habitat in protected areas (PAs) versus reference sites (unprotected areas: non-PAs; richness hotspots: RH; complementary sites: CS) and in species’ partial ranges covered by protected versus unprotected areas. Error bars indicate the 95% confidence interval. In A, “*” indicates that the comparison between PAs and each reference site is significant ($P < 0.05$) through a *t* test. In B, “*” indicates the comparison of potential change of proportion of natural habitat in species’ partial ranges covered by protected areas versus unprotected areas is significant ($P < 0.05$).61
- Fig. 2-5.** Distribution of the top 10% of conservation gaps (in red color) that are not covered by the current distribution of protected areas (in green color) using a $0.25^\circ \times 0.25^\circ$ spatial resolution and range map data. Two blue rectangles indicate the two large recommended conservation areas discussed in the text.62
- Fig. 2-6.** Comparison of the top 10% of conservation gaps (GAs) versus current

protected areas (PAs) of China, as measured by different effectiveness indices.....63

Fig. 2-S1. Distribution of grid cells (in green colors) that are used to represent current protected areas of China (A), range map data set-derived richness hotspots (B), occurrence data set-derived richness hotspots (C), range map-derived complementary sites (D) and occurrence-derived complementary sites (E) at $0.1^\circ \times 0.1^\circ$ spatial resolution. Grid cells are identified as protected areas when at least 50% of their areas are covered by the polygons of current protected areas, which are superimposed in the maps.....70

Fig. 2-S2. Distribution of grid cells (in green colors) that are used to represent current protected areas of China (A), range map-derived richness hotspots (B), occurrence-derived richness hotspots (C), range map-derived complementary sites (D) and occurrence-derived complementary sites (E) at $0.5^\circ \times 0.5^\circ$ spatial resolution. Grid cells are identified as protected areas only when at least 50% of their areas are covered by the polygons of current protected areas, which are superimposed in the maps.....72

Fig. 2-S3. Comparison of effectiveness indices in protected areas (PAs), unprotected areas (non-PAs), richness hotspots (RH) and complementary sites (CS) at $0.25^\circ \times 0.25^\circ$ spatial resolution using occurrence data. These indices include: potential change in species richness (A), corrected weighted endemism (B), phylogenetic diversity (C), phylogenetic endemism (D), residence time of temperature (E), residence time of precipitation (F), and change of total suitable habitat over time (G). Additionally, comparisons of residence time of climate (H) and change of suitable habitat (I) in species' partial ranges covered by protected versus unprotected areas were provided. Error bars indicate the 95% confidence interval. “**” and “NS” indicate that the comparison between PAs and each kind of the reference sites through a *t*-test is significant ($P < 0.05$) and non-significant ($P > 0.05$) respectively.....74

Fig. 2-S4. Comparison of effectiveness of diversity indices in protected areas (PAs), unprotected areas (non-PAs), richness hotspots (RH) and complementary sites (CS) at $0.5^\circ \times 0.5^\circ$ spatial resolution using range map data set. These indices include: potential change of species richness (A), corrected weighted endemism (B), phylogenetic diversity (C), phylogenetic endemism (D), residence time of temperature (E), residence time of precipitation (F), and change of total suitable habitat over time (G). Additionally, comparisons of residence time of climate (H) and change of suitable habitat (I) in species' partial ranges covered by protected versus unprotected areas are provided. Error bars indicate the 95% confidence interval. “**” and “NS” indicate that the comparison between PAs and each kind of the reference sites through a *t*-test is significant ($P < 0.05$) and non-significant ($P > 0.05$) respectively.....76

Fig. 2-S5. Comparison of effectiveness of diversity indices in protected areas (PAs), unprotected areas (non-PAs), richness hotspots (RH) and complementary sites (CS) at $0.5^\circ \times 0.5^\circ$ spatial resolution using occurrence data. These indices include: potential change of species richness (A),

corrected weighted endemism (B), phylogenetic diversity (C), phylogenetic endemism (D), residence time of temperature (E), residence time of precipitation (F), and change of total suitable habitat over time (G). Additionally, comparisons of residence time of climate (H) and change of suitable habitat (I) in species' partial ranges covered by protected versus unprotected areas are provided. Error bars indicate the 95% confidence interval. “*” and “NS” indicate that the comparison between PAs and each kind of the reference sites through a *t*-test is significant ($P<0.05$) and non-significant ($P>0.05$) respectively.....78

Fig. 2-S6. Comparison of effectiveness of diversity indices in protected areas (PAs), unprotected areas (non-PAs), richness hotspots (RH) and complementary sites (CS) at $0.1^\circ \times 0.1^\circ$ spatial resolution using range map data set. These indices include: potential change of species richness (A), corrected weighted endemism (B), phylogenetic diversity (C), phylogenetic endemism (D), residence time of temperature (E), residence time of precipitation (F), and change of total suitable habitat over time (G). Additionally, comparisons of residence time of climate (H) and change of suitable habitat (I) in species' partial ranges covered by protected versus unprotected areas are provided. Error bars indicate the 95% confidence interval. “*” and “NS” indicate that the comparison between PAs and each kind of the reference sites through a *t*-test is significant ($P<0.05$) and non-significant ($P>0.05$) respectively.....80

Fig. 2-S7. Comparison of effectiveness indices in protected areas (PAs), unprotected areas (non-PAs), richness hotspots (RH) and complementary sites (CS) at $0.1^\circ \times 0.1^\circ$ spatial resolution using occurrence data. These indices include: potential change of species richness (A), corrected weighted endemism (B), phylogenetic diversity (C), phylogenetic endemism (D), residence time of temperature (E), residence time of precipitation (F), and change of total suitable habitat over time (G). Additionally, comparisons of residence time of climate (H) and change of suitable habitat (I) in species' partial ranges covered by protected versus unprotected areas are provided. Error bars indicate the 95% confidence interval. “*” and “NS” indicate that the comparison between PAs and each kind of the reference sites through a *t*-test is significant ($P<0.05$) and non-significant ($P>0.05$) respectively.....82

Fig. 2-S8. Top 10% of conservation gaps (in red color) identified using different distribution data and across three spatial scales. A) range map-derived conservation gaps at $0.1^\circ \times 0.1^\circ$ spatial scale; B) occurrence-derived conservation gaps at $0.1^\circ \times 0.1^\circ$ spatial scale; C) occurrence-derived conservation gaps at $0.25^\circ \times 0.25^\circ$ spatial scale; D) range map-derived conservation gaps at $0.5^\circ \times 0.5^\circ$ spatial scale; E) occurrence-derived conservation gap sat $0.5^\circ \times 0.5^\circ$ spatial scale.84

Fig. 2-S9. Comparison of effectiveness of diversity indices in protected areas (PAs) and top 10% of conservation gap areas (GA) at $0.1^\circ \times 0.1^\circ$ spatial resolution using range map data set. These indices include: potential change of species richness (A), corrected weighted endemism (B), phylogenetic diversity (C),

phylogenetic endemism (D), residence time of temperature (E), residence time of precipitation (F), and change of total suitable habitat over time (G). Additionally, comparisons of residence time of climate (H) and change of suitable habitat (I) in species' partial ranges covered by protected versus unprotected areas are provided. Error bars indicate the 95% confidence interval. “*” and “NS” indicate that the comparison between PAs and GAs through a *t*-test is significant ($P<0.05$) and non-significant ($P>0.05$) respectively. 86

Fig. 2-S10. Comparison of effectiveness of diversity indices in protected areas (PAs) and top 10% conservation gap areas (GA) at $0.1^\circ\times0.1^\circ$ spatial resolution using occurrence data set. These indices include: potential change of species richness (A), corrected weighted endemism (B), phylogenetic diversity (C), phylogenetic endemism (D), residence time of temperature (E), residence time of precipitation (F), and change of total suitable habitat over time (G). Additionally, comparisons of residence time of climate (H) and change of suitable habitat (I) in species' partial ranges covered by protected versus unprotected areas are provided. Error bars indicate the 95% confidence interval. “*” and “NS” indicate that the comparison between PAs and GAs through a *t*-test is significant ($P<0.05$) and non-significant ($P>0.05$) respectively. 88

Fig. 2-S11. Comparison of effectiveness of diversity indices in protected areas (PAs) and top 10% conservation gap areas (GAs) at $0.25^\circ\times0.25^\circ$ spatial resolution using occurrence data set. These indices include: potential change of species richness (A), corrected weighted endemism (B), phylogenetic diversity (C), phylogenetic endemism (D), residence time of temperature (E), residence time of precipitation (F), and change of total suitable habitat over time (G). Additionally, comparisons of residence time of climate (H) and change of suitable habitat (I) in species' partial ranges covered by protected versus unprotected areas are provided. Error bars indicate the 95% confidence interval. “*” and “NS” indicate that the comparison between PAs and GAs through a *t*-test is significant ($P<0.05$) and non-significant ($P>0.05$) respectively. 90

Fig. 2-S12. Comparison of effectiveness of diversity indices in protected areas (PAs) and top 10% conservation gap areas (GAs) at $0.5^\circ\times0.5^\circ$ spatial resolution using range map data set. These indices include: potential change of species richness (A), corrected weighted endemism (B), phylogenetic diversity (C), phylogenetic endemism (D), residence time of temperature (E), residence time of precipitation (F), and change of total suitable habitat over time (G). Additionally, comparisons of residence time of climate (H) and change of suitable habitat (I) in species' partial ranges covered by protected versus unprotected areas are provided. Error bars indicate the 95% confidence interval. “*” and “NS” indicate that the comparison between PAs and GAs through a *t*-test is significant ($P<0.05$) and non-significant ($P>0.05$) respectively. 92

- Fig. 2-S13.** Comparison of effectiveness of diversity indices in protected areas (PAs) and top 10% conservation gap areas (GAs) at $0.5^\circ \times 0.5^\circ$ spatial resolution using occurrence data set. These indices include: potential change of species richness (A), corrected weighted endemism (B), phylogenetic diversity (C), phylogenetic endemism (D), residence time of temperature (E), residence time of precipitation (F), and change of total suitable habitat over time (G). Additionally, comparisons of residence time of climate (H) and change of suitable habitat (I) in species' partial ranges covered by protected versus unprotected areas are provided. Error bars indicate the 95% confidence interval. “*” and “NS” indicate that the comparison between PAs and GAs through a *t*-test is significant ($P < 0.05$) and non-significant ($P > 0.05$) respectively. 94
- Fig. 2-S14.** Comparison on the predicted richness derived from different data sets (range maps versus museum occurrence records) for climatic model MIROC and two RCPs at $0.25^\circ \times 0.25^\circ$ spatial resolution. Spatial correlation test is conducted by using Dutilleul's modified *t*-test. The comparisons are very similar at the other two spatial scales and all of them are significant and thus are omitted for simplicity. 96
- Fig. 3-1.** Shift of range centers of amphibians of China under climate change using universal unlimited dispersal (A), stochastic limited dispersal (B) and deterministic limited dispersal (C) scenarios respectively. Mean directions are given in the titles of the subplots. Length of each line indicates the relative shift distance of geographic centroids of a species' range in the future. Directions are measured in a counterclockwise manner starting from the due East. Individual directions of species are binned together on the circle if they are close to each other to show the density. 129
- Fig. 3-2.** Associations between range shift directions and distances of species versus the mean directions and scalar values of climate velocity in species' current ranges for MIROC+RCP8.5 climatic data set across different dispersal scenarios. Circular-circular correlation (Eq. 3-7), circular-linear correlation (Eq. 3-6) and conventional Pearson's product-moment correlation were applied to subplots A, B-C and D respectively. Significance of the correlations was conducted through a permutation test and marked with asterisks. B3, B8, B14, B15 and B18 indicate the bioclimatic variables Bio3, Bio8, Bio14, Bio 15 and Bio18 respectively. 130
- Fig. 3-S1.** Climate velocity maps of the five bioclimatic variables based on MIROC+RCP8.5 climatic dataset for building SDMs for amphibians of China. Units for the legends are km/year. 134
- Fig. 3-S2.** Shift of range centers of amphibians of China for MIROC+RCP2.6 climatic data set using universal unlimited dispersal (A), stochastic limited dispersal (B) and deterministic limited dispersal (C) scenarios respectively. Mean directions are given in the titles of the subplots. Length of each line indicates the relative shift distance of geographic centroids of a species' range in the future. Directions are measured in a counterclockwise manner starting

from the due East. Individual directions are binned together on the circle if they are close to each other.	135
Fig. 3-S3. Shift of range centers of amphibians of China for BCC+RCP2.6 climatic data set using universal unlimited dispersal (A), stochastic limited dispersal (B) and deterministic limited dispersal (C) scenarios respectively. Length of each line indicates the shift distance of geographic centroids of a species' range in the future. Mean directions are given in the titles of the subplots. Length of each line indicates the relative shift distance of geographic centroids of a species' range in the future. Directions are measured in a counterclockwise manner starting from the due East. Individual directions are binned together on the circle if they are close to each other.	136
Fig. 3-S4. Shift of range centers of amphibians of China for BCC+RCP8.5 climatic data set using universal unlimited dispersal (A), stochastic limited dispersal (B) and deterministic limited dispersal (C) scenarios respectively. Mean directions are given in the titles of the subplots. Length of each line indicates the relative shift distance of geographic centroids of a species' range in the future. Directions are measured in a counterclockwise manner starting from the due East. Individual directions are binned together on the circle if they are close to each other.	137
Fig. 3-S5. Associations between range shift direction and shift distance of species versus the mean direction and scalar values of climate velocity in species' current ranges for MIROC+RCP2.6 climatic data set across different dispersal scenarios. Circular-circular correlation (Eq. 3-7), circular-linear correlation (Eq. 3-6) and conventional Pearson's product-moment correlation were applied to subplots A, B-C and D respectively. Significance of the correlations was conducted through a permutation test and marked with asterisks. B3, B8, B14, B15 and B18 indicate the bioclimatic variables Bio3, Bio8, Bio14, Bio 15 and Bio18 respectively.	138
Fig. 3-S7. Associations between range shift direction and shift distance of species versus the mean direction and scalar values of climate velocity in species' current ranges for BCC+RCP8.5 climatic data set across different dispersal scenarios. Circular-circular correlation (Eq. 3-7), circular-linear correlation (Eq. 3-6) and conventional Pearson's product-moment correlation were applied to subplots A, B-C and D respectively. Significance of the correlations was conducted through a permutation test and marked with asterisks. B3, B8, B14, B15 and B18 indicate the bioclimatic variables Bio3, Bio8, Bio14, Bio 15 and Bio18 respectively.	140
Fig. 4-1. Extinction debt process for species occupancy of forests and the corresponding quantities measured by the metapopulation models used for the present study.....	169
Fig. 4-2. Projected future forest cover dynamic across the whole territory of China based on the harmonized data sets from four integrated assembly scenarios.	170
Fig. 4-3. Relationship between estimated extinction-colonization ratio and the	

range size observed for the amphibian species in the no-Allee metapopulation model.....	171
Fig. 4-4. Comparisons on the number and relaxation time of species that will be subjected to extinction debt processes at different future time periods (measured by every twenty years; A), across different forest cover scenarios (B) and over different metapopulation models (C). At last, a comparison on time to half extinction across different metapopulation models was presented as well (D). Error bars indicate standard errors, and different letters “a-c” above the bars in (D) indicate the significance of the model through two-sample <i>t</i> -tests.....	172
Fig. 4-5. Spatial extinction debt patterns of forest-dwelling endemic amphibians in China in terms of both magnitude (A) and mean time to half extinction (B) by combining the distributions from all the 27 species that are prone to future extinction (detected at least one time from the results of the 20 combinations of different forest cover scenarios and metapopulation models).	173

List of Tables

Table 2-S1. A list of amphibian species of China used for the present study.....	64
Table 2-S2. A list of data-deficit amphibian species of China those are not included for the present study	68
Table 2-S3. Twelve reclassified land use (LU) classes derived from Globio3 data set for the present study.....	69
Table 3-1. Associations of range shift distances, directions and latitudinal centroids of current distribution of amphibians of China for MIROC+RCP8.5 climatic data set. Subscripts “a” and “b” denote the circular-circular correlation (Eq. 3-7) and circular-linear correlation (Eq. 3-6) respectively. Significance of the correlations was conducted through a permutation test with 1000 runs.....	128
Table 3-S1. Associations of range shift distances, directions and latitudinal centroids of current distribution of amphibians of China for MIROC+RCP2.6 climate data set. Subscripts “a” and “b” denote the circular-circular correlation (Eq. 3-7) and circular-linear correlation (Eq. 3-6) respectively. Significance of the correlations was conducted through a permutation test.....	131
Table 3-S2. Associations of range shift distances, directions and latitudinal centroids of current distribution of amphibians of China for BCC+RCP2.6 climate data set. Subscripts “a” and “b” denote the circular-circular correlation (Eq. 3-7) and circular-linear correlation (Eq. 3-6) respectively. Significance of the correlations was conducted through a permutation test.....	132
Table 3-S3. Associations of range shift distances, directions and latitudinal centroids of current distribution of amphibians of China for BCC+RCP8.5 climate data set. Subscripts “a” and “b” denote the circular-circular correlation (Eq. 3-7) and circular-linear correlation (Eq. 3-6) respectively. Significance of the correlations was conducted through a permutation test.....	133
Table 4-S1. Estimated extinction-colonization ratios for different metapopulation models (with or without Allee effects) for each amphibian species using equations (Eq. 4-7, 4-9 and 4-10) in the main text.....	177
Table 4-S2. Future time periods triggering delayed extinctions of 27 endemic amphibians of China for the 20 combinations of different forest cover scenarios and metapopulation models.	184

Chapter 1 General Introduction

Amphibian biology

Amphibians are one of the major vertebrate groups on Earth, with nearly 7000 species worldwide. Amphibians are very sensitive to changes in the surrounding environment (Wake, 1991, 2007; Alroy, 2015); at a global scale, approximately 40% of amphibian species are threatened with extinction (Primack, 2014). This percentage of threatened taxa is the highest among all vertebrate groups. In comparison, approximately 30% of mammals, 30% of reptiles and 20% of birds worldwide are threatened with extinction based on recent reports of the International Union for Conservation of Nature (IUCN) (Primack, 2014). All current evidence indicates the conservation crisis of amphibians in a changing world, in which climate change and land use conversion are occurring rapidly (Wake, 1991, 2007).

The class *Amphibia* originated from certain sarcopterygian fish during the Devonian Period, or approximately 350 million years ago. Contemporary amphibians have three main orders: *Anura* (frogs and toads), *Caudata* (salamanders), and *Gymnophiona* (caecilians). The order *Anura* contains 53 families, with a total number of approximately 6200 species globally. The order *Caudata* has over 600 species and 9 families. Finally, the order *Gymnophiona* contains 10 families, in which approximately 200 species have been recorded. The *Gymnophiona* species inhabit only tropical areas, while the *Caudata* species live in temperate areas in the Northern

Hemisphere (some species in this order can extend their distributional ranges to arctic or tropical zones) (Fei *et al.*, 2012). In contrast, the distributional ranges of Gymnophiona and Anura species are much broader. Except for Antarctica, Anura species inhabit all continents and most of the continental islands worldwide. Over 80% of the species in this order are distributed in tropical and temperate zones (Fei *et al.*, 2012).

The following are some important morphological and physiological characteristics of amphibians: 1) they have moist skin without hair, feathers or scales (Bartlett & Bartlett, 2006); 2) similarly to reptiles, amphibians are ectotherms; 3) most species have an aquatic larval or tadpole stage and a terrestrial adult stage (though some species are aquatic throughout their lifespans); and 4) most species are nocturnal to better avoid predators and search for prey without losing too much water through the skin (Bartlett & Bartlett, 2006).

The life-history cycle of amphibians can be divided into several stages with distinct appearances. In frogs and toads, these stages typically include the egg, tadpole, froglet, and adult stages. In salamanders and caecilians, the stages are egg, larva, and adult. Amphibians must live in rivers, streams or ponds during the young growth stages before metamorphosis. Tadpoles are herbivorous; thus, they have long intestines for better digestion. However, during metamorphosis before becoming an adult for the species from the order Anura, the tail of a tadpole is resorbed and the intestine is shortened to allow for digestion of animal matter (Bartlett & Bartlett,

2006). In terms of the dispersal ability of amphibians, current field records are scarce. However, because of their aquatic-terrestrial transient life cycles and ectothermic lifestyles, amphibians are hypothesized to be dispersal-limited organisms (Smith & Green, 2005). Amphibians can live up to several decades based on reports of captive individuals of certain species (Goin *et al.*, 1978).

Contemporary diversity and distribution patterns of amphibians in China

There are approximately 420 amphibian species found in China, of which approximately 70% are endemic (Fei, 1999; Fei *et al.*, 2012). Regarding the taxonomic classification of these species, China has only one species belonging to the order Gymnophiona, approximately 70 species belonging to 3 families of the order Caudata and approximately 350 species belonging to 9 families of the order Anura (Fei *et al.*, 2012). The only Gymnophiona species is *Ichthyophis bannanicus*, which can be found in the southern tropical edges of the Yunnan, Guangxi and Guangdong Provinces (Fei *et al.*, 2012).

Two zoogeographic realms, the Oriental and the Palaearctic (Chen & Srivastava, 2015), have a demarcation boundary crossing mainland China. In general, the Oriental Realm covers Central, Southern, and Southwestern China, whereas the Palaearctic Realm includes the remaining parts of the country (i.e., the Qinghai-Tibet Plateau and Northern and Northeastern China). A high amphibian diversity and endemism are typically found in areas that belong to the Oriental Realm and which are characterized

by a series of mountainous ranges. Two islands, Hainan and Taiwan, are also within the Oriental Realm and have a great number of endemic amphibian species (Chen & Bi, 2007; Fei *et al.*, 2012). In contrast, the amphibian diversity in China in areas covered by the Palaearctic Realm is much lower (Fei *et al.*, 2012), though a few exceptions are found at the transitional margins. For example, certain species from tropical or temperate habitats have been recorded in the southern or southeastern edges of Tibet (a part of the Palaearctic Realm).

The precise demarcation between the Oriental and Palaearctic Realms remains controversial (Chen, 2004; Chen & Srivastava, 2015). Based on the reptilian distribution, Chen and Srivastava (2015) recently argued that 35°N should be the delineation boundary between these two zoogeographic realms in Eastern China. Nonetheless, the transition from the Oriental to the Palaearctic Realms in China should be strongly associated with the Pleistocene glaciation history, which will be discussed in more detail below.

Biogeographic processes that influence amphibian diversity and distribution in China

The glacial-interglacial cycles during the Pleistocene period are a key factor that explains the current distribution patterns of amphibians and determines the delineation of the Oriental and Palaearctic zoogeographic realms in China. This evidence has been widely supported by many phylogeographic and biogeographic studies on

different taxa in China, including frogs, plants and mammals (Zhang, 2004; Gong *et al.*, 2008; You *et al.*, 2010; Dong *et al.*, 2012; Wen *et al.*, 2014; Feng *et al.*, 2015; Gao *et al.*, 2015).

It is hypothesized that ice sheets at the maxima could cover approximately one-third of the land surface of the Northern Hemisphere (Lomolino *et al.*, 2005). In Eurasia, the ice sheets in the Pleistocene could reach the temperate zone and Central Asia at approximately 45°N during the maximal extent period (Lomolino *et al.*, 2005). During that period, the ice sheets were massive and could reach 3 km in thickness, and in China, glaciation may have reached Western and Central China (von Wissmann, 1937). However, the ice sheets did not reach most of the southern and southwestern parts of the country. Moreover, because of the mountainous ranges and the precipitation caused by monsoon circulation (windblown warm and humid oceanic air), Southern and Southwestern China (Oriental Realm) became ideal refuge areas for amphibians and other vertebrates, allowing these organisms to survive and differentiate (Fang *et al.*, 2013; Yue & Sun, 2013; Meng *et al.*, 2015). Mountain ranges also became important biogeographic barriers that facilitated the allopatric speciation and ecological radiation of amphibians. In summary, the geologic history and biogeographic vicariance largely contributed to the high diversity and endemism of amphibians in the mountain ranges of Southern and Southwestern China.

Continental drift and the corresponding tectonic collision can explain why so many areas in China within the Oriental Realm have numerous mountain ranges.

During prehistoric times, the Indian Plate was separated from Gondwana during the early Jurassic period (~120 Mya) and moved northward, colliding with Asia (which separated from Laurasia) at approximately 40 Mya (Lomolino *et al.*, 2005). This collision led to the uplifting of the Himalayan Mountains and adjacent mountain ranges (e.g., the Hengduan Mountains) (Zhong & Ding, 1996; Chaplin, 2005). The uplift of these mountains could have directly or indirectly affected the climatic variability in the southern and southwestern parts of the country, leading to a high level of topological complexity and climate heterogeneity in the Oriental Realm within China. All these factors have contributed to the high diversification of amphibians in China.

Finally, the high amphibian diversity and endemism in the islands of Hainan and Taiwan are largely attributed to the repeated exposure of the continental shelf, which connected these islands to the mainland during the glacial-interglacial cycles of the Pleistocene period (Zhang & Liu, 1991; Chen, 2013). During the Last Maximal Glacial period, the sea level was much lower than that observed in contemporary times (Davis, 1986). The global sea level could have been up to 160 meters lower than to its current level (Lomolino *et al.*, 2005). Consequently, the continental shelf in East Asia and Southeast Asia was completely exposed and served as a land bridge to allow animals and plants to migrate to adjacent oceanic islands (Heaney, 1985; Rickart *et al.*, 1991; Fernandez-Palacios *et al.*, 2015). The fluctuation of the sea level and the submergence and reemergence of the continental shelf could largely explain the high diversity and endemism of vertebrates in the islands of Hainan and Taiwan.

In comparison, the observation of the low amphibian distribution in areas inside the Palaearctic Realm (e.g., northern and western parts) of the country can be attributed to the emigration and local extinction events that occurred during the strong glacial periods and the re-colonization events that occurred during the final interglacial period, during which the climate began to warm and the ice sheets receded.

Amphibian extinction risks and correlating factors in China

The current amphibian diversity and distribution in China are determined by prehistoric biogeographic processes, but their future diversity and distribution are predominantly influenced by modern human activities. At the beginning of the Anthropocene epoch, amphibians worldwide became increasingly threatened by extinction resulting from human-induced climate change, habitat alterations and environmental pollution. As China is a representative of the megadiverse countries of the world, it is important to evaluate the current and potential conservation status of amphibians in this country.

According to the conservation biology textbook by Primack (2014), regarding global amphibians, habitat loss threatens 77% of the species, followed by overexploitation (19%) and the introduction of invasive species (14%). In China, habitat destruction, fragmentation and pollution are also primary factors driving the decline of amphibians (Fei, 1999; Fei *et al.*, 2012). A few amphibians in China have

been recorded as already extinct. For example, the Yunnan Lake Newt, *Cynops wolterstorffi*, which was historically distributed in the Kunming Lake in Yunnan Province (24.48°N, 102.40°E) with an elevation of approximately 1800 m (Feng *et al.*, 2007), is already extinct.

Narrow range sizes are a severe factor driving the global extinctions of species (Thomas *et al.*, 2004; Harris & Pimm, 2008; Pearson *et al.*, 2014). As mentioned in the introduction, approximately 70% of amphibians in China are endemic and typically possess very narrow ranges in very specialized habitats (e.g., only in mountainous lakes, streams or rivers at specific elevation ranges). Moreover, these amphibians are typically recorded with one or a few populations in a single location. For example, the Jingdong lazy toad (*Oreolalax jingdongensis*) is found only in the Ailao Mountains in Yunnan Province (elevational range: 1500-2450 m), whereas the Medog spadefoot toad (*Xenophrys medogensis*) has been recorded only in Medog County in Tibet (elevational range: 850-1350 m). The population sizes of these species are often much smaller than those of other species with wider distributional ranges. Thus, the compounding effects of narrow range sizes, specialized habitat requirements, small population sizes and habitat loss would definitely exacerbate the extinction of amphibians in China and worldwide.

As mentioned above, human overexploitation is another leading problem driving the global extinction of amphibians. This problem is particularly relevant to amphibians in China. For example, in addition to being threatened by habitat

degradation (Wang, 2000), the Chinese Giant Salamander (*Andrias davidianus*), which is the longest amphibian in the world, is hunted or cultivated by local people for commercial purposes (usually as food in restaurants). Though commercial cultivation may reduce the extinction risk of wild *A. davidianus* in its natural habitat, this strategy leads to the potential reduction of the genetic diversity of the species, particularly when captive populations are released and hybridized with wild populations. Furthermore, the captive individuals are difficult to breed, and, thus, more wild individuals of *A. davidianus* are likely to be hunted, increasing the risk of extinction.

Environmental pollution, particularly the pollution of shallow water bodies, seriously threatens amphibian survival in China. For example, one of the main factors driving the extinction of the species *C. wolterstorffi* mentioned above was the pollution of Kunming Lake, which was caused by the disposal of industrial waste and domestic sewage (Fei *et al.*, 2012).

Infectious diseases are another potential factor driving the extinction of amphibians in China and worldwide. For example, the fungus disease Chytridiomycosis, which is caused by *Batrachochytrium dendrobatidis*, is a highly epidemic disease that causes the mortality of amphibians in many regions and countries worldwide, although its prevalence in China is not currently a problem (Wei *et al.*, 2010; Bai *et al.*, 2012; Zhu *et al.*, 2014). Climate change is another factor that is widely recognized to be responsible for the global amphibian decline (Araujo *et al.*,

2006; Wake, 2007; Hof *et al.*, 2011; Loyola *et al.*, 2014). When the climate is warming, the outbreak risk of the infectious disease caused by *B. dendrobatidis* is expected to increase, resulting in a higher probability of amphibian extinction (Pounds *et al.*, 2006).

Alien species could be a potential factor influencing the survival of amphibians. For example, the American bullfrog (*Rana catesbeiana*) is one invasive amphibian currently found in China (Fei, 1999). *R. catesbeiana* can predate upon other small native frog species in their invaded ranges (Fei *et al.*, 2012) and has been suspected to be responsible for the extinction of *C. wolterstorffi* in the Kunming Lake, where *R. catesbeiana* was introduced (Fei *et al.*, 2012).

Aims and structure of this thesis

This thesis contains three research chapters. Chapter 2 assesses the shift in the diversity and distribution of amphibians in China resulting from future climate change and land use alterations. The purpose is to evaluate the effectiveness of the current network of protected areas in China in representing suitable ranges, climates and habitats for amphibians, including the effects of future climate change and habitat loss.

Chapter 3 evaluates the directional range shift patterns of suitable amphibian habitats using circular statistics to better understand how climate-driven factors will

shift not only the distance of the species' ranges but also their direction. Circular statistics provide a powerful tool for evaluating both the shift distance and direction and quantifying the correlations between the range shift of the species and possible explanatory environmental factors. A full understanding of the ecological mechanisms underpinning the range shifts of amphibians can provide conservation insights for the design of reserve networks and conservation corridors.

Finally, in Chapter 4, I develop novel models of metapopulation dynamics to predict the magnitude and relaxation time of extinction debt for forest-dwelling endemic amphibians in China. The metapopulation models developed here can explicitly incorporate the effects of weak and strong Allee effects on the extinction time (delay time) of species. Moreover, the future dynamics of forest cover are allowed to vary such that different outcomes, which range from optimistic (with a minimal loss of forest cover) to pessimistic (with a high-degree loss of forest cover), can be obtained.

In summary, the research presented in my thesis contributes to a better understanding of the potential changes in the ranges and extinction patterns of amphibians in China due to the combined effects of climate change and habitat loss. The combination of different statistical methods, including species distribution modeling, climatic velocity, and circular statistics, are valuable tools for analyzing the species range shifts, extinction debt and, accordingly, the effectiveness of protected areas in conserving amphibians.

Literature cited

- Alroy J (2015) Current extinction rates of reptiles and amphibians. *PNAS*, **112**, 13003–13008.
- Araujo M, Thuiller W, Pearson R (2006) Climate warming and the decline of amphibians and reptiles in Europe. *Journal of Biogeography*, **33**, 1712–1728.
- Bai C, Liu X, Fisher M, Garner T, Li Y (2012) Global and endemic Asian lineages of the emerging pathogenic fungus Batrachochytrium dendrobatidis widely infect amphibians in China. *Diversity and Distributions*, **18**, 307–318.
- Bartlett R, Bartlett P (2006) *Guide and reference to the amphibians of eastern and central North America*. University Press of Florida, Gainesville, FL, USA, 312 pp.
- Chaplin G (2005) Physical geography of the Gaoligong Shan Area of southwest China in relation to biodiversity. *Proceedings of the California Academy of Sciences*, **56**, 527–556.
- Chen L (2004) The precise biogeographic division of Palearctic and Oriental Realm in the East of China: based on data of amphibians. *Zoological Research*, **25**, 369–377.

- Chen Y (2013) Biotic element analysis of reptiles of China: a test of vicariance model. *Current Zoology*, **59**, 447–455.
- Chen Y, Bi J (2007) Biogeography and hotspots of amphibian species of China: Implications to reserve selection and conservation. *Current Science*, **92**, 480–489.
- Chen Y, Srivastava D (2015) Latitudinal concordance between biogeographic regionalization, community structure and richness patterns: a study on the reptiles of China. *The Science of Nature*, **102**, 1253.
- Davis M (1986) Climatic stability, time lags and community disequilibrium. In: *Community Ecology* (eds Diamond J, Case T), pp. 269–284. Harper & Row, New York.
- Dong B, Che J, Ding L, Huang S, Murphy R, Zhao E, Zhang Y (2012) Testing hypotheses of Pleistocene population history using coalescent simulations: refugial isolation and secondary contact in *Pseudepidalea raddei* (Amphibia: Bufonidae). *Asian Herpetological Research*, **3**, 103–113.
- Fang F, Sun H, Zhao Q et al. (2013) Patterns of diversity, areas of endemism, and multiple glacial refuges for freshwater crabs of the genus *Sinopotamon* in China (Decapoda: Brachyura: Potamidae). *PLoS ONE*, **8**, e53143.
- Fei L (1999) *Atlas of amphibians of China*. Henan Science and Technology Press, Zhengzhou, China.

- Fei L, Ye C, Jiang J (2012) *Colored atlas of Chinese amphibians and their distributions*. Sichuan Science & Technology Press, Chengdu, China, 1-619 pp.
- Feng X, Lau M, Stuart S, Chanson J, Cox N, Fischman D (2007) Conservation needs of amphibians in China: a review. *Science in China Series C: Life Sciences*, **50**, 265.
- Feng G, Mao L, Sandel B, Swenson N, Svenning J (2015) High plant endemism in China is partially linked to reduced glacial-interglacial climate change. *Journal of Biogeography*, DOI: 10.1111/jbi.12613.
- Fernandez-Palacios J, Rijsdijk K, Norder S et al. (2015) Towards a glacial-sensitive model of island biogeography. *Global Ecology and Biogeography*, DOI: 10.1111/geb.12320.
- Gao Y, Zhang Y, Gao X, Zhu Z (2015) Pleistocene glaciations, demographic expansion and subsequent isolation promoted morphological heterogeneity: a phylogeographic study of the alpine Rosa sericea complex (Rosaceae). *Scientific Reports*, **5**, 11698.
- Goin C, Goin O, Zug G (1978) *Introduction to Herpetology*, 3rd ed. WH Freeman and Company, San Francisco.
- Gong W, Chen C, Dobes C, Fu C, Koch M (2008) Phylogeography of a living fossil: pleistocene glaciations forced Ginkgo biloba L. (Ginkgoaceae) into two refuge

areas in China with limited subsequent postglacial expansion. *Molecular Phylogenetics and Evolution*, **48**, 1094–1105.

Harris G, Pimm S (2008) Range size and extinction risk in forest birds. *Conservation Biology*, **22**, 163–171.

Heaney L (1985) Zoogeographic evidence for middle and late Pleistocene land bridges to Philippine islands. *Modern Quaternary Research in Southeast Asia*, **9**, 127–143.

Hof C, Araujo M, Jetz W, Rahbek C (2011) Additive threats from pathogens, climate and land-use change for global amphibian diversity. *Nature*, **480**, 516–519.

Lomolino M, Riddle B, Brown J (2005) *Biogeography*. Sinauer Associates, Sunderland, Massachusetts, 845 pp.

Loyola R, Lemes P, Brum F, Provete D, Duarte L (2014) Clade-specific consequences of climate change to amphibians in Atlantic forest protected areas. *Ecography*, **37**, 65–72.

Meng L, Chen G, Li Z, Yang Y, Wang Z, Wang L (2015) Refugial isolation and range expansions drive the genetic structure of Oxyria sinensis (Polygonaceae) in the Himalaya-Hengduan Mountains. *Scientific Reports*, **5**, 10396.

Pearson R, Stanton J, Shoemaker K et al. (2014) Life history and spatial traits predict extinction risk due to climate change. *Nature Climate Change*, **4**, 217.

Pounds J, Bustamante M, Coloma L et al. (2006) Widespread amphibian extinctions from epidemic disease driven by global warming. *Nature*, **439**, 161–167.

Primack R (2014) *Essentials of conservation biology*, 6th edn. Sinauer Associates, Sunderland, Massachusetts, USA, 1-603 pp.

Rickart E, Heaney L, Utzurum R (1991) Distribution and ecology of small mammals along an elevational transect in southeastern Luzon, Philippines. *Journal of Mammalogy*, **72**, 458–469.

Smith M, Green D (2005) Dispersal and the metapopulation paradigm in amphibian ecology and conservation: are all amphibian populations metapopulations? *Ecography*, **28**, 110–128.

Thomas C, Cameron A, Green R et al. (2004) Extinction risk from climate change. *Nature*, **427**, 145–148.

Wake D (1991) Declining amphibian populations. *Science*, **253**, 860.

Wake D (2007) Climate change implicated in amphibian and lizard declines. *Proceedings of the National Academy of Science of the United States of America*, **104**, 8201–8202.

Wang P (2000) Protection of the habitat of giant salamanders should be realized. *Sichuan Journal of Zoology*, **19**, 164.

Wei Y, Xu K, Zhu D, Chen X, Wang X (2010) Early-spring survey for Batrachochytrium dendrobatidis in wild *Rana dybowskii* in Heilongjiang Province, China. *Diseases of Aquatic Organisms*, **92**, 241–244.

Wen J, Zhang J, Nie Z, Zhong Y, Sun H (2014) Evolutionary diversifications of plants on the Qinghai-Tibetan Plateau. *Frontiers in Genetics*, **5**, 4.

von Wissmann H (1937) The Pleistocene glaciation in China. *Bulletin of the Geological Society of China*, **17**, 145–168.

You Y, Sun K, Xu L et al. (2010) Pleistocene glacial cycle effects on the phylogeography of the Chinese endemic bat species, *Myotis davidii*. *BMC Evolutionary Biology*, **10**, 208.

Yue L, Sun H (2013) Montane refugia isolation and plateau population expansion: phylogeography of Sino-Himalayan endemic *Spenceria ramalana* (Rosaceae). *Journal of Systematics and Evolution*, **52**, 326–340.

Zhang R (2004) Relict distribution of land vertebrates and Quaternary glaciation in China. *Acta Zoologica Sinica*, **50**, 841–851.

Zhang Z, Liu R (1991) The Holocene along the coast of Hainan Island, China. *Chinese Geographical Science*, **1**, 188–196.

Zhong D, Ding L (1996) Rising process of the Qinghai-Xizang (Tibet) Plateau and its mechanism. *Science in China (Series D)*, **39**, 369–379.

Zhu W, Bai C, Wang S, Soto-Azat C, Li X, Liu X, Li Y (2014) Retrospective survey
of museum specimens reveals historically widespread presence of
Batrachochytrium dendrobatidis in China. *EcoHealth*, **11**, 241–250.

Chapter 2 Assessing the effectiveness of China's protected areas to conserve current and future amphibian diversity¹

Summary

Protected areas are an important tool for conserving species. In this study, I assessed the effectiveness of protected areas to conserve amphibian biodiversity in response to future changes in climate and land use. Both range maps and occurrence records of amphibian species in China were analyzed separately using ensemble species distribution modeling across three spatial scales (for checking scale dependence of the results and conclusions). Climate velocity and corresponding residence time in protected areas and species' ranges were calculated. A variety of other indices for assessing protected area effectiveness were also calculated. The results showed that, future declines in amphibian richness, endemism, phylogenetic diversity, phylogenetic endemism and suitable habitat were significantly lower in protected areas than in unprotected, complementary-priority or richness-hotspot areas. However, less-disturbed amphibian habitat, calculated from current and future projected land use data, in both protected and unprotected areas were consistently lost over time although this reduction was lower in protected areas. Furthermore, although residence time of precipitation was longer in both protected areas and in species' ranges within protected areas, resident time of temperature was significantly shorter in

¹ A version of this chapter has been published in *Diversity and Distributions*, 2017, 23, 146–157.

both. These results were consistent regardless of data sources and spatial scales. Therefore, current protected areas of China can maintain future amphibian distribution and diversity, but are insufficient in preventing the loss of suitable climate and less-disturbed habitat. I identified the locations of the top 10% of future conservation gaps for amphibians that performed the best over all the effectiveness indices. Two largest gap zones, including the southern parts of Tibet and the Hengduan Mountains, were recommended to be included in future conservation network design.

Introduction

Although protected areas represent the most common approach to conserving species and ecosystems, they are vulnerable to climate change (Araujo *et al.*, 2011) and sensitive to habitat loss (Brooks *et al.*, 2002). Protected areas are not effective to cover current biodiversity (Joppa *et al.* 2013), but it is still poorly known whether they will become worse at conserving future biodiversity, particularly given the anthropogenic alterations of natural habitat and climate change.

Amphibians are widely considered to be the most threatened vertebrate group (Alroy, 2015), with nearly 40% of global species being classified at risk of extinction

(Primack, 2014). Conservation of amphibians at global and regional scales is therefore a high priority. If protected areas are effective at preventing amphibians from extinction under future environmental change, then protected areas might also be effective in protecting other at-risk plants and animals (Rodrigues & Brooks, 2007; Xu *et al.*, 2008).

Gap analyses of the effectiveness of the current protected area network has mostly been assessed using the current representativeness of biodiversity and ecosystems within protected areas (Soutullo *et al.*, 2008; Jenkins & Joppa, 2009). However, as climate changes, species will shift their distribution and abundance (Pavon-Jordan *et al.*, 2015; Zhang *et al.*, 2015). It is therefore necessary to assess the effectiveness of protected areas in terms of both the current coverage of biodiversity and the adaptive ability of species within protected areas to future change (Alagador *et al.*, 2014; Pouzols *et al.*, 2014). In some studies, protected areas maintained suitable climates, reduced historical habitat loss, and facilitated the colonization and range expansion of species (Araújo *et al.*, 2011; Geldmann *et al.*, 2013; Hiley *et al.*, 2013; Thomas *et al.*, 2012).

A number of simple criteria have been used to evaluate protected area effectiveness (Pressey *et al.*, 2007). For example, species richness and rarity are often used to identify areas of conservation gaps (Williams *et al.*, 1996). Other indices, such as functional and phylogenetic diversity, are also becoming more recognized and used in protected area assessments (Faith, 1992; Thuiller *et al.*, 2015). In addition,

statistical methods that project species' potential distribution and measure species' exposure to a changing climate are helpful in assessing species' responses to climate change in protected areas.

Species distribution modeling (SDM) has long been applied to the assessment of protected area effectiveness (Araujo *et al.*, 2011; Meller *et al.*, 2014). SDMs can project suitable ranges of species over different time periods and thus provide insights into future range shifts of species (Zhang *et al.*, 2015). Another relevant measure, climate velocity (Loaire *et al.*, 2009), is increasingly used to assess the vulnerabilities (or exposures) of biodiversity to climate change (Sandel *et al.*, 2011; VanDerWal *et al.*, 2013; Burrows *et al.*, 2014). Climate velocity predicts how long suitable climate can be maintained and how fast species must shift their ranges to maintain climatic equilibrium conditions (Hamann *et al.*, 2015). By quantifying exposures and responses of species to climate change, SDMs and climate velocity are important methods that can be used to assess the future effectiveness of protected areas in conserving, as in this study, amphibian diversity and suitable climate.

Amount of suitable habitat in protected areas is a crucial factor affecting species diversity and distribution (Fahrig, 2001). Understanding potential changes in habitat in protected areas informs their status of effectiveness since it is less likely that species will go extinct in protected areas when their natural habitat is sufficiently preserved. Although protected areas have been found to be effective in preserving

historical and current habitats (Geldmann *et al.*, 2013), it is less clear whether they will be effective in preventing future habitat loss.

China is one of the most biodiverse countries. Protected areas cover ~15% of the land surface (He, 2009). China is also rich in amphibian diversity, having over 400 amphibian species with nearly 70% being endemic and many are range-limited and information-missing (Fei *et al.*, 2012). China's southern and southwestern mountainous regions have been well recognized as a global hotspot of amphibian diversity, but also a global hotspot of high extinction risk (Stuart *et al.*, 2004; Fritz & Rahbek, 2012). Therefore, evaluation of the effectiveness of China's protected areas at preventing amphibian decline under future climate change and anthropogenically-caused habitat loss can help guide regional amphibian conservation. I clarify here again, the effectiveness that is assessed in the present study is restricted to the coverage of species' ranges and spatial diversity patterns over time.

Materials and Methods

Distributional data

In this study, 182 native amphibians (ranges being restricted to China or at least 50% of the global range within China) were used to model future range shifts of species and subsequently used to assess protected area effectiveness. A list of these species was provided as Table S1 in Supporting Information. These species were

selected because of sufficient museum occurrence records by combining and checking distributional data from different sources (≥ 5 georeferenced records per species) and available digital range maps from the IUCN spatial database (<http://www.iucnredlist.org/technical-documents/spatial-data>). The museum distribution records of these species were extensively collected, visually checked and combined from numerous sources over the past ten years including published literature and online databases (including but not limited to: Atlas of Chinese amphibians and their distributions (Fei, 1999; Fei *et al.*, 2012); GBIF: <http://www.gbif.org/> and Chinese Animal Scientific Database: <http://www.zoology.csdb.cn/page/showTreeMap.vpage?uri=cnAmpRep.tableTaxa>).

The list of species used for the present study is presented as Table 2-S1. Moreover, a list of data-deficit species that are not analyzed in the present study is also presented in Table 2-S2. In general, species with occurrence records less than 10 (34 amphibians in a total in my study) may not have reliable prediction of species' potential distribution. However, five records are shown to be reasonable for modeling the suitable ranges of narrow-ranged species (Stockwell & Peterson, 2002; van Proosdij *et al.*, 2015; Zhang *et al.*, 2015).

Three grid cell networks with sizes of $0.1^\circ \times 0.1^\circ$, $0.25^\circ \times 0.25^\circ$, and $0.5^\circ \times 0.5^\circ$ were applied to the land surface of China (including Taiwan and Hainan Islands) for checking modeling consistency and scale dependency of the results. For each amphibian species, its presence/absence within each grid cell at each of the three spatial scales was determined. A cell was only identified to have the species' presence

if $\geq 50\%$ of the cell area was covered by the species' range-map polygon. For occurrence records of each species, the presence in each grid cell was determined by the location of occurrence records at each spatial scale. A species was classified as present in a cell if at least one occurrence record of the species was recorded in that cell.

Distribution of China's protected areas was based on the World Database on Protected Areas (WDPA; <http://www.protectedplanet.net>), which contained six classes (I-VI) of protected areas categorized by the World Conservation Union (Dudley *et al.*, 2013). WDPA regularly updates the conservation areas at a global scale, but the addition of new protected areas in China over the past 10 years have almost become steady and no large areas have been brought into current protected area network recently (Cao *et al.*, 2015). At each of the three spatial resolutions, a grid cell was identified as being part of a protected area if $\geq 50\%$ of its area was covered by protected area polygons. Using this criterion, 11945, 1788, and 402 grid cells were identified to represent current protected areas at resolutions $0.1^\circ \times 0.1^\circ$, $0.25^\circ \times 0.25^\circ$, and $0.5^\circ \times 0.5^\circ$, respectively, for checking consistency of the analyses and results.

Bioclimatic and land use data

Bioclimatic variables, derived from the WorldClim database (Hijmans *et al.*, 2005), for three general circulation models using two extreme emission scenarios

(representative concentration pathways: RCPs 2.6 and 8.5) were used to parameterize SDMs. Climate data between the years of 1950 and 2000 were used to represent the current climate. Three general circulation models (GCMs), HadGEM2-ES (Jones *et al.*, 2011), CCSM (Otto-Bliesner *et al.*, 2006) and MIROC (Yokohata *et al.*, 2007) were used to represent different outcomes of future climate by the 2070s. For each GCM model, two extreme representative climate emission scenarios (RCP 2.6 and RCP 8.5) were compared (we did not use other emission scenarios in this study since we have sufficient climatic data sets combined from different GCM and two RCPs for comparison). To simplify discussion of results from the species distribution modeling (SDM) outputs, I focused on the MIROC+RCP2.6 results since the results from GCMs with alternative RCPs were similar. All bioclimatic data were downloaded from the WorldClim database (<http://www.worldclim.org/>).

Here, RCP8.5 represented a high-emission but low-mitigation future (Rogelj *et al.*, 2012). The temperature under RCP8.5 was predicted to increase by 4°C to 6°C around by the year of 2100 (Rogelj *et al.*, 2012). In contrast, the RCP2.6 scenario represented a low-emission future with a lower projected future increase in temperature around 2°C or lower (van Vuuren *et al.*, 2011). Both scenarios (coupled with MIROC model) were compared because they represented two extreme outcomes in the future that allowed ones to explore the responses of amphibians to different potential situations of future climate change.

To control potential multi-collinearity among the 19 bioclimatic variables, a variance inflation factor (VIF) was used to identify and remove highly correlated bioclimatic variables using a threshold value of 5 (those covariates that are strongly collinear with others would have VIF values larger than this threshold). This resulted in the use of the following 5 independent variables for constructing SDMs: bio3 (isothermality), bio8 (mean temperature of the wettest quarter), bio14 (precipitation of the driest month), bio15 (precipitation seasonality), and bio18 (precipitation of the warmest quarter). Additionally, bio1 (annual mean temperature) and bio12 (annual total precipitation) were retained to calculate velocity and residence time. These bioclimatic variables reflect the water requirement and thermal limit of amphibians and thus are critical to determine their diversity and distribution (Chen, 2013). Values at each grid cell at the three spatial resolutions were the averages of those within the grid at the original resolution (2.5 minute, ~5 km).

For measuring future change of amphibian suitable habitat in protected areas, selected land use variables were collected from the Globio3 land use dataset (Alkemade *et al.*, 2009; Bellard *et al.*, 2013) at $0.5^\circ \times 0.5^\circ$ resolution under A2 high-emission scenario. These coarse-resolution land use data were downscaled to higher resolutions $0.1^\circ \times 0.1^\circ$ and $0.25^\circ \times 0.25^\circ$ using bilinear interpolation. As similar to previous studies (Bellard *et al.*, 2013), I reclassified the original 30 land use classes into 12 variables/classes (LU1-LU12) because some original classes occurred in too few grid cells or were highly correlated (Bellard *et al.*, 2013). Names for these land use variables are presented in Table 2-S3. Each land use variable was calculated as

the occupied area fraction of a grid cell. I had considered alternative emission scenarios, including A1B and B1, but the results habitat changes in protected areas were similar and therefore not further considered. The proportion of less-disturbed natural habitat suitable for amphibians was calculated as the sum of fractioned area of wetlands, water bodies, forest cover and grassland, in each grid cell at the current time (representing the average climatic condition from the baseline period of 1950-2000) and in the 2070s (representing the average climatic condition of the years of 2061-2080), respectively.

Species distribution modeling (SDM)

The selected five bioclimatic variables (bio3, bio8, bio14, bio15 and bio18) were used to model current and future distribution of amphibians of China using two separate data sets (range maps and museum distributional points) at three spatial scales ($0.1^\circ \times 0.1^\circ$, $0.25^\circ \times 0.25^\circ$ and $0.5^\circ \times 0.5^\circ$). Ensemble SDMs, assuming the equilibrium of species distribution with neighboring environment while ignoring biotic interactions among species, were constructed using three statistical algorithms in the BIOMOD2 package (Thuiller *et al.*, 2009) using the R platform (R Development Core Team, 2013). These included Generalized additive model (GAM) (Hastie & Tibshirani, 1990; Wood, 2006), Random Forest (RF) (Culter *et al.*, 2007) and Maximum entropy (MAXENT) (Phillips & Dudik, 2008; Elith *et al.*, 2011). To estimate the final distribution of species, a consensus method was used where

locations were predicted where all three methods agreed. All models used observed presences as input with a 70% random sample for model development and the remaining 30% sample for model evaluation. Absences were defined as all other cells with no presence information. Ten replicates of each model (training and evaluation) were performed. Equal weightings were assumed for both presence and absence data (Bellard *et al.*, 2013).

I also incorporated land use variables into SDMs. Specifically, I utilized VIF to choose the least correlated land use covariates from the re-classified 12 land use variables. After VIF selection, seven land use classes (LU1, LU2, LU3, LU5, LU7, LU9 and LU12) were retained for SDM modeling with the selected five bioclimatic variables. However, I observed that the results with the addition of land use information across different spatial resolutions were similar to the SDM outputs using the selected five bioclimatic variables only and therefore only the SDM outputs based on the five bioclimatic variables were interpreted.

Two metrics were used to evaluate model performance: true skill statistic (TSS) and the receiver operating characteristic area under the curve (AUC) (Bellard *et al.*, 2013). The TSS ranges from -1 to 1 with values of ≤ 0 indicating the model performs no better than random. The AUC ranges from 0.5 to 1. A model performs better if it is evaluated to have a higher AUC value (e.g., an ideally perfect model is expected to have an AUC of 1). A rule of thumb is that a model performs reasonably well if its AUC value is larger than 0.8. To convert probability maps to binary distributional ranges for species with high statistical confidence, a threshold criterion that maximized the sum of sensitivity (or true positive rate: the proportion of positives that

were correctly identified) and specificity (or true negative rate: the proportion of negatives that were correctly identified) values was used (Liu *et al.*, 2005, 2011). In all the analyses, both AUC and TSS values were very high: mean AUC was 0.9104 with 95% confidence interval (0.9023, 0.9185), and mean TSS was 0.8012 with 95% confidence interval (0.7864, 0.8160). This result confirmed that the SDM models built for the present analyses were statistically reliable.

Because SDMs ignored biotic interactions and dispersal limitation of species, the prediction of species' potential ranges may not be realistic since species can disperse anywhere in the original SDM outputs. I used a dispersal limitation rule to limit distributions. Final binary presence-absence maps therefore assumed each amphibian species could migrate at most ~100 km from its current observed range to adjacent areas in 2070s. This dispersal assumption is reasonable as some amphibians could disperse away 30 km per year, for example, juvenile *Anaxyrus fowleri* could disperse over 30 km within 15 months (Smith & Green, 2006; Sinsch, 2014). Centered at a focused cell, this distance is equal to ~ 2 square grid cells away at $0.5^\circ \times 0.5^\circ$ spatial scale, ~4 grid cells away at $0.25^\circ \times 0.25^\circ$ spatial scale and ~10 cells away at $0.1^\circ \times 0.1^\circ$ spatial scale, respectively. The predicted range of a species was then compared to a convex hull constructed from the currently observed range map (or distributional points depending on the data sets used) of species with an extended buffer zone whereby the distance from the inner boundary to the outer boundary was ~100 km. The purpose of doing this was to implement the dispersal limitation rule. The final projected range of a species included only the part inside the geometry combining the

convex hull and its buffer zone. I considered alternative universal dispersal distances (50 km and 200 km), but the results were similar.

Climate velocity and residence time of climate

Climate velocity was computed for annual mean temperature and annual total precipitation, reflecting the thermal limit and water requirement for amphibians (VanDerWal *et al.*, 2013). A new velocity computational algorithm (Hamann *et al.*, 2015), which was shown to effectively avoid infinite velocity, could be calculated as a mathematical formula as follows (Chen, 2015):

$$V_A(N) = \frac{\min_{B \in N} \{ dist(AB) \times \frac{1}{I(d(A_{current}, B_{future}) \leq t)} \}}{Time_{|future-current|}}$$

(2-1)

where $V_A(N)$ is the velocity in a site A using the whole area N as the search background. $Time_{|future-current|}$ is the year number by subtracting the future-time period to the current-time period. $I(\bullet)$ is an indicator function and returns 1 when the condition inside the parenthesis is satisfied; otherwise returns 0. $dist(AB)$ is the geographic distance between sites A and B . $d(A_{current}, B_{future})$ is the climatic distance between sites A and B at current and future times ($A_{current}$ and B_{future}), respectively. The climatic distance is measured as the absolute difference of current and future climatic

values in sites A and B . t is the threshold of measuring climatic analogy between two sites. A low t indicates high similarity of climate between sites and it remains an open question to define an optimal threshold t . I used a threshold of $t=0.5$ in this study. I also tried other thresholds of 0.05, 0.1 and 1, but these returned similar results and therefore not used further. Climate velocity measures the changing rate of climatic variables that are usually assumed to be independent from species' distributions, even though its calculation procedure (equation 2-1) is akin to some SDM algorithms that project species' suitable distributions (Chen, 2015).

The corresponding residence time of climate (i.e., how long similar climatic condition can stay in the same site) was computed as follows (Loaire *et al.*, 2009):

$$RT(i) = \left| \frac{r_i}{V_i} \right| \approx \left| \frac{\sqrt{A_i / \pi}}{V_i} \right|$$

(2-2)

where r_i is the diameter of the grid cell i , which is approximated by $\sqrt{A_i / \pi}$, where A_i is the areal size of the grid cell and π is the circular constant. V_i is the velocity of the relevant climatic variable measured at cell i using equation (2-1).

Computation of phylogenetic diversity and phylogenetic endemism

A previously published global amphibian tree (Isaac *et al.*, 2012) was used as the backbone when constructing the tree for amphibians of China. In detail, a sub-tree

with 152 amphibians found in China from the backbone tree was extracted. I then imputed the missing species into the sub-tree that contained species belonging to the same genus.

For each grid cell, I computed phylogenetic diversity for the species assemblage found in the cell at both current and future times respectively as,

$$PD = \sum_{c \in C} L_c \quad (2-3)$$

Where C is the set of the branches that connect all the focused species in the tips to the root; c is one of the branches in the set C . L_c is the branch length for the branch c .

For each grid cell, I computed phylogenetic endemism for the species assemblage found in the cell at both present and future times respectively as (Rosauer *et al.*, 2009; Rosauer & Jetz, 2015),

$$PE = \sum_{c \in C} \frac{L_c}{R_c} \quad (2-4)$$

where R_c is the area size for the combined range which merges the projected ranges for all the living descendants for branch c .

Reference sites and indices of protected area effectiveness

Three kinds of ‘reference’ sites were identified for comparison with protected areas: (1) unprotected reference sites were those grid cells that have no current protected area status; (2) richness hotspot reference sites contained grid cells with the

highest number of amphibian species while keeping the total number of protected area grid cells the same; and (3) complementary reference sites that included those grid cells identified as high biodiversity value based on the complementarity principle with again keeping the same number of cells as the current protected areas. These complementary sites typically had unique species that were rarely found in other sites so they are not necessarily areas of high biodiversity (Pressey *et al.*, 1993; Margules & Pressey, 2000).

To identify complementary reference sites for amphibians of China, I used the projected distribution of species at the current time for each spatial scale ($0.1^\circ \times 0.1^\circ$, $0.25^\circ \times 0.25^\circ$ and $0.5^\circ \times 0.5^\circ$) to compute the priority rank of all grid cells using the Zonation version 4.0 (Lehtomaki & Moilanen, 2013). The following settings were applied in Zonation: warp factor of 2 was used for edge removal and the removal rule followed the additive benefit function. All species were equally weighted and a smoothing factor of 2 was used. I did not mask current protected areas thereby allowing all grid cells to be freely selected during the prioritization process. This resulted in a complementary-site reference network that was independent of the distribution of current protected areas.

To evaluate the effectiveness of protected areas with respect to reference sites, I calculated a set of diversity indices related to amphibian distribution and diversity (including potential changes of species richness, corrected weighted species endemism, phylogenetic diversity and phylogenetic endemism between current time

and 2070s), residence time of climate, and land use change (potential change of proportion of less-disturbed habitat between the current time and 2070s). All these indices were calculated in both the grid cells representing current protected areas and in other reference sites, respectively. For each amphibian species, both residence time of climate and potential change of less-disturbed natural habitat were also compared in grid cells representing species' partial ranges covered by protected versus unprotected areas, respectively. Details of descriptions and calculations of the effectiveness indices are presented as follows.

- 1) Change of species richness: measured as $Richness_{2070s}(i) - Richness_{current}(i)$.

Where $Richness_{2070s}(i)$ and $Richness_{current}(i)$ indicate the projected species richness at the current time and 2070s respectively at a grid cell i .

- 2) Change of corrected weighted endemism: measured as $I_{2070s}(i) - I_{current}(i)$.

Where $I_{2070s}(i)$ and $I_{current}(i)$ indicate the corrected weighted species endemism (Crisp *et al.*, 2001; Linder, 2002) calculated at the current time and 2070s respectively at a grid cell i . For a grid cell, the corrected weighted species

$$\text{endemism was calculated as } WE(i) = \frac{\sum_j \frac{P_{ji}}{R_j}}{\sum_j P_{ji}}.$$

Where R_j is the projected range size of species j based on SDM outputs and P_{ji} is the projected presence (=1) or absence (=0) status of species j at the grid cell i .

Corrected weighted species endemism was used because it was independent of species richness (Linder, 2000, 2002; Crisp *et al.*, 2001).

- 3) Change of phylogenetic diversity (Faith, 1992): measured as $PD_{2070s}(i) - PD_{current}(i)$. Where $PD_{2070s}(i)$ and $PD_{current}(i)$ indicate the phylogenetic diversity calculated at the current time and 2070s respectively at a grid cell i using equation (2-3) above.
- 4) Change of phylogenetic endemism (Rosauer *et al.*, 2009): measured as $PE_{2070s}(i) - PE_{current}(i)$. Where $PE_{2070s}(i)$ and $PE_{current}(i)$ indicate the phylogenetic endemism calculated at the current time and 2070s respectively at a grid cell i using equation (2-4) above.
- 5) Residence time of climate: measured as $RT_{prec}(i)$ and $RT_{temp}(i)$ for annual total precipitation and annual mean temperature respectively using equation (2-2).
- 6) Change of proportion of total available habitat: measured as $PH_{2070s}(i) - PH_{current}(i)$. Where $PH_{2070s}(i)$ and $PH_{current}(i)$ indicate the proportion of total available undisturbed habitat calculated at the current time and 2070s respectively at a grid cell i . Fractions of forest cover, water bodies, wetlands and pasture/grassland (including LU1-LU6, LU9 and LU12 in Table 2-S3) in a cell were summed to measure total suitable less-disturbed natural habitat for amphibians. These habitats were commonly found to present amphibians of China based on previous literature (Fei, 1999; Fei *et al.*, 2012). Bare, managed, artificial and non-habitat of ice (including LU7, LU8, LU10 and LU11) were excluded as they are frequently disturbed or altered by humans.

Additionally, the following species-range-related indices were calculated in grid cells where each amphibian species was projected to occur at the current time. In

other words, these indices were related to each single species and its range. Two-sample t-test was used to compare the index values in grid cells jointly covered by species' projected range and protected areas and in the cells jointly covered by species' range and unprotected areas:

- 7) Mean residence time of climate in species' partial ranges covered by protected versus unprotected areas: measured as $RT_{prec}(i)$ and $RT_{temp}(i)$ for annual total precipitation and annual mean temperature respectively using equation (2-2). Here i is a grid cell where a species was projected to occupy the current time. This cell can be covered by either protected or unprotected areas.
- 8) Change of proportion of total available habitat in species' partial ranges covered by protected versus unprotected areas: similar to the above index (6), this range-related index was measured as $PH_{2070s}(i) - PH_{current}(i)$. Where $PH_{2070s}(i)$ and $PH_{current}(i)$ indicate the proportion of suitable undisturbed habitat calculated at the current time and 2070s respectively at a grid cell i . Here i is a grid cell where a species was projected to occupy at the current time. This cell can be covered by either protected or unprotected areas.

Each of the three kinds of reference sites was compared to protected areas using a two-sample *t*-test for each of the above indices to determine whether protected areas were significantly more effective in protecting amphibian diversity than reference sites. For example, if the future losses of species were significantly lower in protected areas than those in other reference sites, then the current protected areas were determined to be more effective than other reference areas in conserving China's

amphibian diversity (i.e., an index of potential change of amphibian richness over time).

Here, unprotected reference sites reflected a null model involving no conservation efforts, while richness hotspots and complementary reference sites reflected two hypothetical conservation scenarios that represent two simple but important conservation strategies (Pressey *et al.*, 1993; Williams *et al.*, 1996; Margules & Pressey, 2000). Richness hotspots identify a set of sites with the highest number of species, while ignoring the coverage of individual species. In contrast, complementary sites selected a set of sites that best covers all the species while minimizing the number of selected sites (i.e. the minimum coverage problem in conservation) (Kirkpatrick, 1983).

Identifying conservation gaps

If current protected areas and reference sites are not sufficiently effective in conserving biodiversity, I proposed a score-based ranking method to identify locations of potential future protected areas (i.e. conservation gaps). Similar types of ranking methods have been used elsewhere for conservation prioritization studies (Alagador *et al.*, 2014; Braid & Nielsen, 2015; Yap *et al.*, 2015). My method integrates and balances the values of all effectiveness indices that measure different aspects of diversity and the performance of a site in conserving the diversity. The

method selects the top 10% of sites that are not yet covered by the current protected areas. Specifically, the prioritization score of a site i is calculated as

$$S_i = \sum_k \log(r_{ik})$$

(2-5)

where r_{ik} is the rank of the site i in the k -th effectiveness index. A site has a larger rank if it performs better in an effectiveness index. Thus, using this equation (2-5), those sites with the top 10% highest scores are identified as areas of conservation gaps. I also selected the top 5% and 20% of conservation gaps, but the results were similar and therefore not shown here.

Results

Here I presented an assessment of China's protected area effectiveness at the $0.25^\circ \times 0.25^\circ$ scale; results were very similar at other two spatial scales and between different data sets (range maps versus museum records). Thus, for simplicity, all the other results were reported as a whole in Figs. 2-S1 to 2-S14. Based on the 50% area coverage criterion, most moderate- to large-sized protected areas were well represented by the grid cells at the $0.25^\circ \times 0.25^\circ$ scale and located mostly in the western, central and northeastern parts of the country (Fig. 2-1A). By comparison, regardless of the species data sets used, grid cells representing hotspots of richness

were concentrated in the southern and southwestern parts of China (Figs. 2-1B to 2-1C), while grid cells representing complementary sites were more widely distributed across the country (Figs. 2-1D to 2-1E).

Amphibian diversity (as measured by richness, corrected weighted species endemism, phylogenetic diversity and phylogenetic endemism) showed a consistent loss between the current conditions and 2070s at reference sites compared to the protected sites (Fig. 2-2). Decreases were all statistically significant, except change in endemism in non-protected areas (Fig. 2-2B). In contrast, diversity values showed little if any change or even positive changes within current protected areas (Fig. 2-2). For example, future amphibian richness did not change in protected areas while there was a projected significant loss in reference sites (Fig. 2-2A). Amphibian phylogenetic diversity and endemism were projected to increase in protected areas but declined significantly in hotspots of richness and complementary reference sites (Figs. 2-2C to 2-2D).

Residence time of annual total precipitation was significantly longer in both protected areas (Fig. 2-3B) and the part of species' ranges within them (Fig. 2-3C). However, residence time of mean annual temperature was significantly shorter overall (Figs. 2-3A and 2-3C). Furthermore, although the loss of suitable habitat was significantly lower in protected areas and species' partial ranges covered by them than reference sites (Figs. 2-4A to 2-4B), the magnitude of loss in less-disturbed natural habitat in protected areas or species' partial ranges within protected areas was

substantial. For example, the future reduction of less-disturbed habitat could average nearly 4% in amphibian ranges within the protected areas (Fig. 2-4B). Analyses of occurrence records or at other two spatial resolutions ($0.1^\circ \times 0.1^\circ$ and $0.5^\circ \times 0.5^\circ$) showed similar results, although some variations were observed (Figs. 2-S1 to 2-S7).

Discussion

I evaluated the effectiveness of China's protected areas in preventing future loss of native amphibian diversity and habitat due to projected changes in climate and land use. These results, derived from different sources of data (range maps versus occurrence records), consistently demonstrated that current protected area network in China positively contributed towards maintaining amphibian diversity in the future. For example, loss in amphibian biodiversity, as measured by indices related to amphibian distribution and diversity, was higher in reference sites compared to those in protected areas at different spatial resolutions (Fig. 2-2 and panels A-D in Figs. 2-S3 to 2-S7). SDM results suggested that protected areas in China will help slow potential amphibian loss by preserving their distribution and diversity under future environmental change.

However, performance of protected areas varies among indices and across spatial scales. For example, residence time of annual precipitation was typically longer in protected than unprotected areas (Fig. 2-3B and panel F in Figs. 2-S3 to 2-S7), while residence time of annual mean temperature was always significantly shorter in

protected areas than other reference sites (Fig. 2-3A and panel E in Figs. 2-S3 to 2-S7). Climatic residence time in species' partial ranges covered by protected areas compared with unprotected areas was similar (Fig. 2-3C and panel H in Figs. 2-S3 to 2-S7). These results suggest that protected areas will better maintain water conditions than thermal conditions. A more serious challenge to China's current protected area network is that suitable less-disturbed habitat within protected areas are predicted to decline (up to 4%) over the next few decades, although these losses are projected to be less severe than in unprotected areas (Fig. 2-4B and panel I in Figs. 2-S3 to 2-S7). These climate velocity and land use results suggest that current IUCN-level protected areas of China are not sufficient in size to maintain suitable climate and less-disturbed habitat so as to prevent future amphibian loss.

It is therefore necessary to identify potential conservation gaps and the locations that most effectively conserve amphibians in order to prioritize future IUCN-level protected areas. By using the score-ranking method, the top 10% of conservation gaps not covered by the current protected areas were located mainly in the southwestern part of the country (Fig. 2-5). In particular, the southern parts of both the Tibet and the Hengduan Mountains were consistently identified as the two largest and top-ranked conservation gap areas across different data sets (range maps and museum records) and spatial scales (Figs. 2-5 and 2-S8), even though the locations of other top-ranked conservation gap areas can vary. These conservation priority areas are characterized by a tropical monsoonal climate with ample annual rainfall (Lin & Zhao, 1996; Ning *et al.*, 2012). Both areas were shown to be effective in conserving amphibians under

environmental change, as they always performed better than the current protected areas across all examined indices and across all spatial scales (Fig. 2-6 and Figs. 2-S9 to 2-S13).

Currently, the southern part of Tibet is not covered by any IUCN-level protected areas of China (Figs. 5 and S8), although the southern part of the Hengduan Mountains (Figs. 2-5 and 2-S8) does have some small-size protected sites (Fig. 2-1 and Figs. 2-S1 to 2-S2). However, these small-size protected areas do not sufficiently represent the larger area of the southern Hengduan Mountains (Figs. 2-5 and 2-S8).

Given that the goal of the 2011-2020 Biodiversity Strategic Plan (<https://www.cbd.int/sp/>) is to expand the global network of protected areas to cover at least 17% of the worldwide land surface, I suggest that these two large areas be designated as protected areas, which will benefit the conservation of other species, such as endangered fern species (Wang *et al.*, 2016).

My results also support the importance of using complementarity principles to design protected areas (Brown *et al.*, 2015). The two top-ranked large gap areas based on the score-ranking method (equation 2-5) were also identified in the complementarity analysis (Figs. 2-5 versus 2-1D to 2-1E). One of the main merits of using a complementarity analysis is that it does not require *a priori* information from climate velocity- and land-use information (of course, they can be integrated into the complementarity analysis if needed) but simply the distribution of species over the studied area. Thus, complementarity analysis is a powerful tool in conservation

reserve design planning (Tulloch *et al.*, 2013; Chades *et al.*, 2015) by using distribution or habitat information as minimal inputs (Watts *et al.*, 2009; Lehtomaki & Moilanen, 2013).

It is worth noting that not all the top-ranked gap areas identified by equation 2-5 could be identified using complementarity analysis. For example, when comparing Fig. 2-1D with Fig. 2-5, one can see some top 10% sites (in red color of Fig. 2-5) in northern part of China (in particular, the north-eastern part) could not be covered by complementary sites (in green color of Fig. 2-1D). There is much ongoing debate on whether simple scoring or ranking methods are effective and sufficient in guiding conservation planning. Some researchers prefer simple scoring methods (Jenkins *et al.*, 2015; Li & Pimm, 2016), while others recommend more complex optimization algorithms like complementarity analysis (Nicholson & Possingham, 2006; Wintle *et al.*, 2011; Brown *et al.*, 2015). I took a hybrid approach by combining and comparing both methods as some previous studies (Williams *et al.*, 1996; Yip *et al.*, 2006).

Finally, the conservation of amphibians in China still faces many challenges and uncertainties, which could further worsen the effectiveness of current protected areas. First, prioritization of conservation areas using a fine-filter (species) approach requires high quality species distribution data. In this study, I projected the distribution of amphibian species using best available data from different sources and the SDM projection results at the community level were very similar (Fig. 2-S14). The exclusion of narrow-range and data-deficit species (because they do not have

sufficient distributional information to build SDMs) may influence the results (Howard and Bickford, 2014; Jetz and Freckleton, 2015). Second, habitat fragmentation and human disturbance in or around protected areas and those top-ranked sites identified as conservation gaps still exist and pose threats to local species and ecosystems (Ren *et al.*, 2015). Third, although future projected species richness and endemism of amphibians were well represented in protected areas and the prioritized future conservation gaps (Figs. 2-2 and 2-6), their abundance may be substantially altered by climate change (Pavon-Jordan *et al.*, 2015). Therefore, monitoring in current protected areas and establishment of IUCN-level conservation reserves across China are needed to better deal with future environmental change.

Literature cited

- Alagador D, Cerdeira J, Araujo M (2014) Shifting protected areas: scheduling spatial priorities under climate change. *Journal of Applied Ecology*, **51**, 703–713.
- Alkemade R, Oorschot M, Miles L, Nelleman C, Bakkenes M, ten Brink B (2009) GLOBIO3: a framework to investigate options for reducing global terrestrial biodiversity loss. *Ecosystems*, **12**, 374–390.
- Alroy J (2015) Current extinction rates of reptiles and amphibians. *PNAS*, **112**, 13003–13008.

- Araujo M, Alagador D, Cabeza M, Nogues-Bravo D, Thuiller W (2011) Climate change threatens European conservation areas. *Ecology Letters*, **14**, 484–492.
- Bellard C, Thuiller W, Leroy B, Genovesi P, Bakkenes M, Courchamp F (2013) Will climate change promote future invasions? *Global Change Biology*, **19**, 3740–3748.
- Braid A, Nielsen S (2015) Prioritizing sites for protection and restoration for Grizzly Bears (*Ursus arctos*) in Southwestern Alberta, Canada. *PLoS ONE*, **10**, e0132501.
- Brooks T, Mittermeier R, Mittermeier C et al. (2002) Habitat loss and extinction in the hotspots of biodiversity. *Conservation Biology*, **16**, 909–923.
- Brown C, Bode M, Venter O et al. (2015) Effective conservation requires clear objectives and prioritizing actions, not places or species. *Proceedings of the National Academy of Sciences of the United States of America*, **112**, E4342.
- Burrows M, Schoeman D, Richardson A et al. (2014) Geographical limits to species-range shifts are suggested by climate velocity. *Nature*, **507**, 492–495.
- Cao M, Peng L, Liu S (2015) Analysis of the network of protected areas in China based on a geographic perspective: current status, issues and integration. *Sustainability*, **7**, 15617–15631.

- Chades I, Nicol S, van Leeuwen S et al. (2015) Benefits of integrating complementarity into priority threat management. *Conservation Biology*, **29**, 525–536.
- Chen Y (2013) Habitat suitability modeling of amphibian species in southern and central China: environmental correlates and potential richness mapping. *Science China Life Sciences*, **56**, 476-484.
- Chen Y (2015) New climate velocity algorithm is nearly equivalent to simple species distribution modeling methods. *Global Change Biology*, **21**, 2832–2833.
- Crisp M, Laffan S, Linder H, Monro A (2001) Endemism in the Australian flora. *Journal of Biogeography*, **28**, 183–198.
- Culter D, Edwards T, Beard K, Culter A, Hess K, Gibson J, Lawler J (2007) Random forests for classification in ecology. *Ecology*, **88**, 2783–2792.
- Dudley N, Shadie P, Stolton S (2013) *Guidelines for applying protected area management categories including IUCN WCPA best practice guidance on recognising protected areas and assigning management categories and governance types*. IUCN, 1-86 pp.
- Elith J, Phillips S, Hastie T, Dudik M, Chee Y, Yates C (2011) A statistical explanation of MaxEnt for ecologists. *Diversity and Distributions*, **17**, 43–57.
- Fahrig L (2001) How much habitat is enough? *Biological Conservation*, **100**, 65–74.

- Faith D (1992) Conservation evaluation and phylogenetic diversity. *Biological Conservation*, **61**, 1–10.
- Fei L (1999) *Atlas of amphibians of China*. Henan Science and Technology Press, Zhengzhou, China.
- Fei L, Ye C, Jiang J (2012) *Colored atlas of Chinese amphibians and their distributions*. Sichuan Science & Technology Press, Chengdu, China, 1-619 pp.
- Fritz S, Rahbek C (2012) Global patterns of amphibian phylogenetic diversity. *Journal of Biogeography*, **39**, 1373–1382.
- Geldmann J, Barnes M, Coad L, Craigie I, Hockings M, Burgess N (2013) Effectiveness of terrestrial protected areas in reducing habitat loss and population declines. *Biological Conservation*, **161**, 230–238.
- Hamann A, Roberts D, Barber Q, Carroll C, Nielsen S (2015) Velocity of climate change algorithms for guiding conservation and management. *Global Change Biology*, **21**, 997–1004.
- Hastie T, Tibshirani R (1990) *Generalized additive models*. Chapman and Hall/CRC.
- He F (2009) Price of prosperity: economic development and biological conservation in China. *Journal of Applied Ecology*, **46**, 511–515.

Hijmans R, Cameron S, Parra J, Jones P, Jarvise A (2005) Very high resolution interpolated climate surfaces for global land areas. *International Journal of Climatology*, **25**, 1965–1978.

Hiley J, Bradbury R, Holling M, Thomas C (2013) Protected areas act as establishment centres for species colonizing the UK. *PRSB*, **280**, 20122310.

Howard S, Bickford D (2014) Amphibians over the edge: silent extinction risk of Data Deficient species. *Diversity and Distributions*, **20**, 837–846.

Isaac N, Redding D, Meredith H, Safi K (2012) Phylogenetically-informed priorities for amphibian conservation. *Plos One*, **7**, e43912.

Jenkins C, Joppa L (2009) Expansion of the global terrestrial protected area system. *Biological Conservation*, **142**, 2166–2174.

Jenkins C, van Houtan K, Pimm S, Sexton J (2015) US protected lands mismatch biodiversity priorities. *Proceedings of the National Academy of Sciences of the United States of America*, **112**, 5081–5086.

Jetz W, Freckleton R (2015) Toward a general framework for predicting threat status of data-deficient species from phylogenetic, spatial and environmental information. *Philosophical Transactions of the Royal Society B*, **370**, 20140016.

Jones C, Hughes J, Bellouin N et al. (2011) The HadGEM2-ES implementation of CMIP5 centennial simulations. *Geoscientific Model Development*, **4**, 543–570.

Kirkpatrick J (1983) An iterative method for establishing priorities for the selection of nature reserves: an example from Tasmania. *Biological Conservation*, **25**, 127–134.

Lehtomaki J, Moilanen A (2013) Methods and workflow for spatial conservation prioritization using Zonation. *Environmental Modelling & Software*, **47**, 128–137.

Li B, Pimm S (2016) China's endemic vertebrates sheltering under the protective umbrella of the giant panda. *Conservation Biology*, **30**, 329–339.

Lin Z, Zhao X (1996) Spatial characteristics of changes in temperature and precipitation of the Qinghai-Xizang (Tibet) Plateau. *Science in China (Series D)*, **39**, 442–448.

Linder H (2000) Plant diversity and endemism in sub-Saharan tropical Africa. *Journal of Biogeography*, **28**, 169–182.

Linder H (2002) Plant diversity and endemism in sub-Saharan tropical Africa. *Journal of Biogeography*, **28**, 169–182.

Liu C, Berry P, Dawson T, Pearson R (2005) Selecting thresholds of occurrence in the prediction of species distributions. *Ecography*, **28**, 385–393.

Liu C, White M, Newell G (2011) Measuring and comparing the accuracy of species distribution models with presence-absence data. *Ecography*, **34**, 232–243.

Loarie S, Duffy P, Hamilton H, Asner G, Field C, Ackerly D (2009) The velocity of climate change. *Nature*, **462**, 1052–1057.

Margules C, Pressey R (2000) Systematic conservation planning. *Nature*, **405**, 243–253.

Meller L, Cabeza M, Pironon S, Barbet-Massin M, Maiorano L, Georges D, Thuiller W (2014) Ensemble distribution models in conservation prioritization: from consensus predictions to consensus reserve networks. *Diversity and Distributions*, **20**, 309–321.

Nicholson E, Possingham H (2006) Objectives for multiple-species conservation planning. *Conservation Biology*, **20**, 871–881.

Ning B, Yang X, Chang L (2012) Changes of temperature and precipitation extremes in Hengduan Mountains, Qinghai-Tibet Plateau in 1961-2008. *Chinese Geographical Science*, **22**, 422–436.

Otto-Btiesner B, Brady E, Clauzet G, Tomas R, Levis S, Kothavala Z (2006) Last glacial maximum and Holocene climate in CCSM3. *Journal of Climate*, **19**, 2526–2544.

Pavon-Jordan D, Fox A, Clausen P et al. (2015) Climate-driven changes in winter abundances of a migratory waterbird in relation to EU protected areas. *Diversity and Distributions*, **21**, 571–582.

- Phillips S, Dudik M (2008) Modeling of species distributions with Maxent: new extensions and a comprehensive evaluation. *Ecography*, **31**, 161–175.
- Pouzols F, Toivonen T, Minin E et al. (2014) Global protected area expansion is compromised by projected land-use and parochialism. *Nature*, **516**, 383–386.
- Pressey R, Humphries C, Margules C, Vane-Wright R, Williams P (1993) Beyond opportunism: key principles for systematic reserve selection. *Trends in Ecology and Evolution*, **8**, 124–128.
- Pressey R, Cabeza M, Watts M, Cowling R, Wilson K (2007) Conservation planning in a changing world. *Trends in Ecology and Evolution*, **22**, 583–592.
- Primack R (2014) *Essentials of conservation biology*, 6th edn. Sinauer Associates, Sunderland, Massachusetts, USA, 1-603 pp.
- van Proosdij A, Sosef M, Wieringa J, Raes N (2015) Minimum required number of specimen records to develop accurate species distribution models. *Ecography*, **38**, 1–11.
- R Development Core Team (2013) R: A Language and Environment for Statistical Computing, Vienna, Austria. ISBN 3-900051-07-0, URL <http://www.R-project.org>.
- Ren G, Young S, Wang L et al. (2015) Effectiveness of China's national forest protection program and nature reserves. *Conservation Biology*, **29**, 1368–1377.

Rodrigues A, Brooks T (2007) Shortcuts for biodiversity conservation planning: the effectiveness of surrogates. *Annual Review of Ecology, Evolution and Systematics*, **38**, 713–737.

Rogelj J, Meinsahusen M, Knutti R (2012) Global warming under old and new scenarios using IPCC climate sensitivity range estimates. *Nature Climate Change*, **2**, 248–253.

Rosauer D, Jetz W (2015) Phylogenetic endemism in terrestrial mammals. *Global Ecology and Biogeography*, **24**, 168–179.

Rosauer D, Laffan S, Crisp M, Donnellan S, Cook L (2009) Phylogenetic endemism: a new approach for identifying geographical concentrations of evolutionary history. *Molecular Ecology*, **18**, 4061–4072.

Sandel B, Arge L, Dalsgaard B, Davies R, Gaston K, Sutherland W, Svenning J (2011) The influence of late Quaternary climate-change velocity on species endemism. *Science*, **334**, 660.

Sinsch U (2014) Movement ecology of amphibians: from individual migratory behaviour to spatially structured populations in heterogeneous landscapes. *Canadian Journal of Zoology*, **92**, 491-502.

Smith MA, Green DM (2006) Sex, isolation and fidelity: unbiased long-distance dispersal in a terrestrial amphibian. *Ecography*, **29**, 649-658.

- Soutullo A, De Castro M, Urios V (2008) Linking political and scientifically derived targets for global biodiversity conservation: implications for the expansion of the global network of protected areas. *Diversity and Distributions*, **14**, 604–613.
- Stockwell D, Peterson A (2002) Effects of sample size on accuracy of species distribution models. *Ecological Modelling*, **148**, 1–13.
- Stuart S, Chanson J, Cox N, Young B, Rodrigues A, Fischman D, Waller R (2004) Status and trends of amphibian declines and extinctions worldwide. *Science*, **306**, 1783–1786.
- Thomas C, Gillingham P, Bradbury R et al. (2012) Protected areas facilitate species' range expansions. *Proceedings of the National Academy of Sciences*, **109**, 14063–14068.
- Thuiller W, Lafourcade B, Engler R, Araujo M (2009) BIOMOD-a platform for ensemble forecasting of species distributions. *Ecography*, **32**, 369–373.
- Thuiller W, Maiorano L, Mazel F et al. (2015) Conserving the functional and phylogenetic trees of life of European tetrapods. *Philosophical Transactions of the Royal Society B*, **370**, 20140005.
- Tulloch A, Chades I, Possingham H (2013) Accounting for complementarity to maximize monitoring power for species management. *Conservation Biology*, **27**, 988–999.

VanDerWal J, Murphy H, Kutt A, Perkins G, Bateman B, Perry J, Reside A (2013)

Focus on poleward shifts in species' distribution underestimates the fingerprint of climate change. *Nature Climate Change*, **3**, 239–243.

van Vuuren D, Stehfest E, den Elzen M et al. (2011) RCP2.6: exploring the possibility to keep global mean temperature increase below 2 Celsius degree. *Climatic Change*, **109**, 95–116.

Wang C, Wan J, Zhang Z, Zhang G (2016) Identifying appropriate protected areas for endangered fern species under climate change. *SpringerPlus*, **5**, 904.

Watts M, Bal I, Stewart R et al. (2009) Marxan with zones: software for optimal conservation based land- and sea-use zoning. *Environmental Modelling & Software*, 1513–1521.

Williams P, Gibbons D, Margules C, Rebelo A, Humphries C, Pressey R (1996) A comparison of richness hotspots, rarity hotspots, and complementary areas for conserving diversity of British birds. *Conservation Biology*, **10**, 155–174.

Wintle B, Bekessy S, Keith D et al. (2011) Ecological-economic optimization of biodiversity conservation under climate change. *Nature Climate Change*, **1**, 355–359.

Wood S (2006) *Generalized additive models: an introduction with R*. Chapman and Hall/CRC.

Xu H, Wu J, Liu Y et al. (2008) Biodiversity congruence and conservation strategies: a national test. *BioScience*, **58**, 632–639.

Yap T, Koo M, Ambrose R, Wake D, Vredenburg V (2015) Averting a North American biodiversity crisis. *Science*, **349**, 481–482.

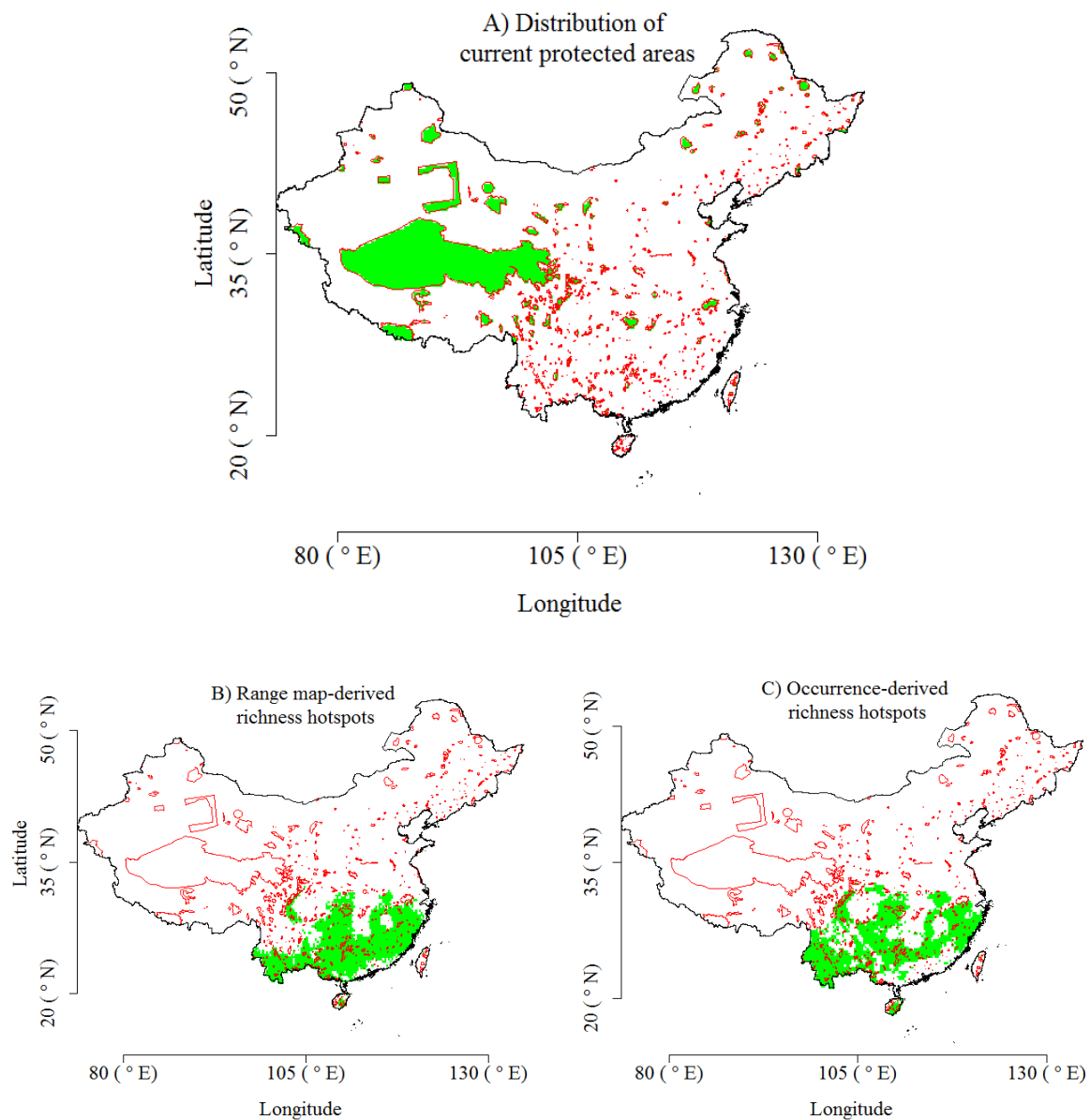
Yip J, Corlett R, Dudgeon D (2006) Selecting small reserves in a human-dominated landscape: a case study of Hong Kong, China. *Journal of Environmental Management*, **78**, 86–96.

Yokohata T, Emori S, Nozawa T et al. (2007) Different transient climate responses of two versions of an atmosphere-ocean coupled general circulation model. *Geophysical Research Letters*, **34**, L02707.

Zhang J, Nielsen S, Stolar J, Chen Y, Thuiller W (2015) Gains and losses of plant species and phylogenetic diversity for a northern high-latitude region. *Diversity and Distributions*, **21**, 1441–1454.

Figures

Fig. 2-1. Distribution of grid cells (in green color) that are used to represent current protected areas of China (A), range map-derived hotspots of richness (B), occurrence-derived hotspots of richness (C), range map-derived complementary sites (D) and occurrence-derived complementary sites (E) at $0.25^{\circ} \times 0.25^{\circ}$ spatial resolution. Grid cells are identified as protected areas when at least 50% of their area is currently protected (in red color), which are superimposed in the maps.



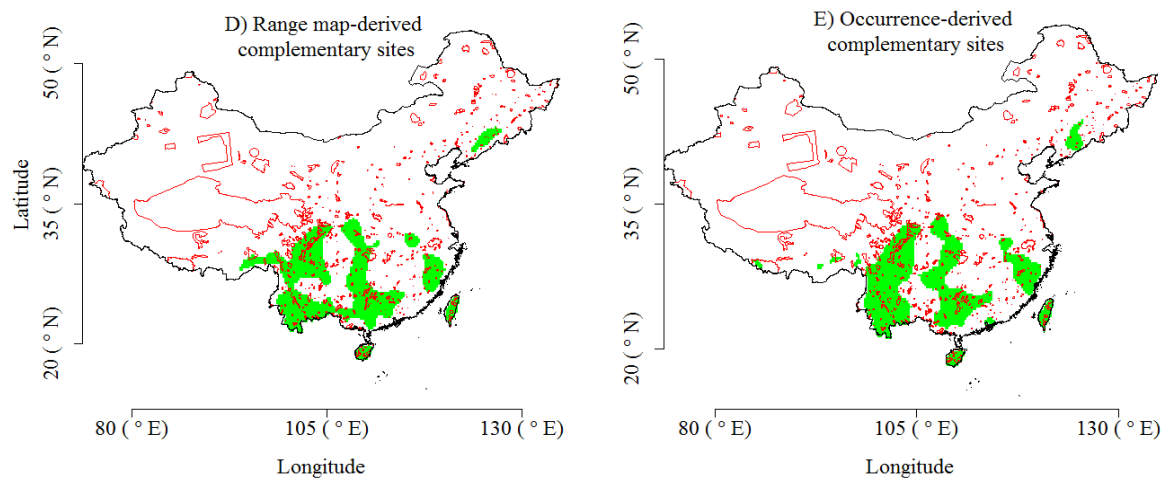


Fig. 2-2. Predicted change using range maps at the $0.25^\circ \times 0.25^\circ$ spatial resolution of species richness (A), corrected weighted endemism (B), phylogenetic diversity (C) and phylogenetic endemism (D) between current and 2070s in protected areas (PAs) versus reference sites (unprotected areas: non-PAs; richness hotspots: RH; complementary sites: CS). Error bars indicate the 95% confidence interval. “*” and “NS” above each histogram for reference sites indicates that the comparison between PAs and reference sites is significant ($P < 0.05$) or non-significant ($P > 0.05$), respectively based on a *t* test.

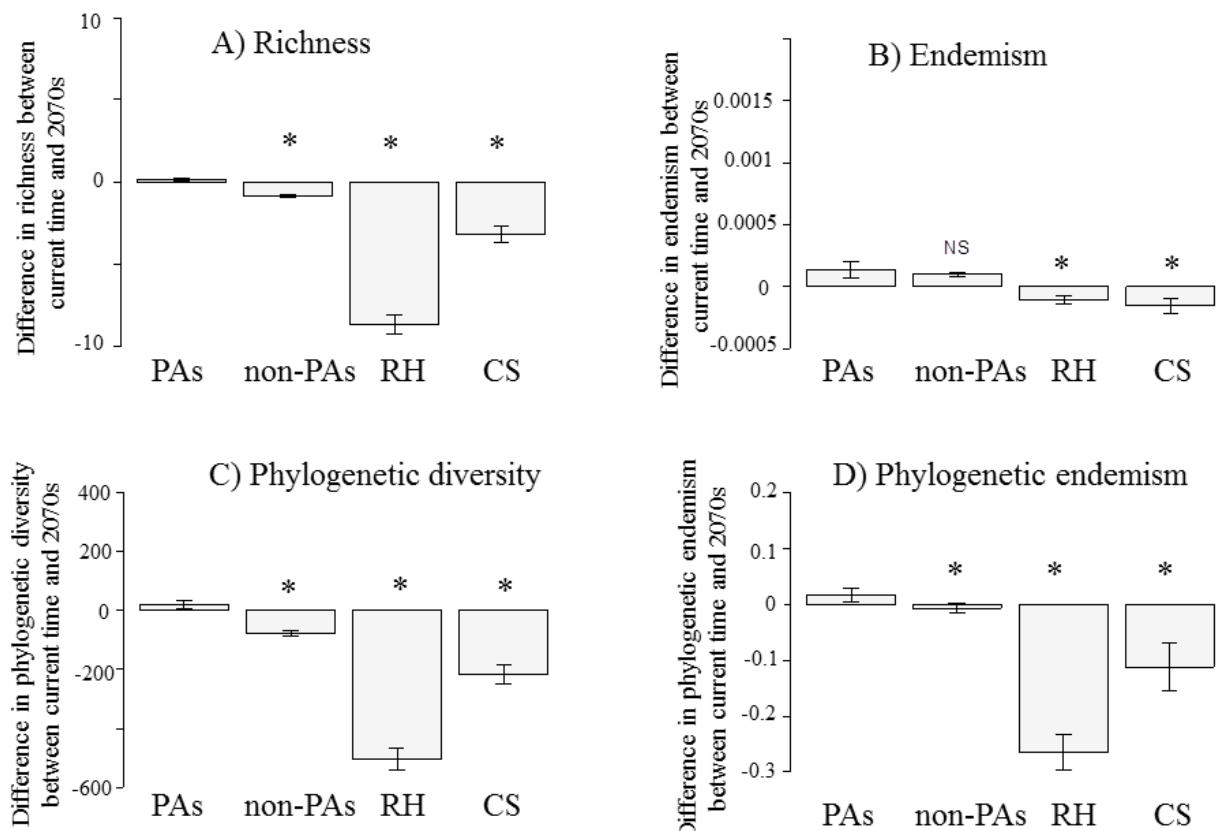


Fig. 2-3. Residence time of climate using range maps at the $0.25^\circ \times 0.25^\circ$ spatial resolution in protected areas (PAs) versus reference sites (unprotected areas: non-PAs; richness hotspots: RH; complementary sites: CS) and in species' partial ranges within protected versus unprotected areas. Error bars indicate the 95% confidence interval. In A and B, “*” indicates that the comparison between PAs and each reference site is significant ($P < 0.05$) using a *t* test. In C, “*” indicates the comparison of residence time of climate in species' partial ranges covered by protected areas versus unprotected areas is significant ($P < 0.05$).

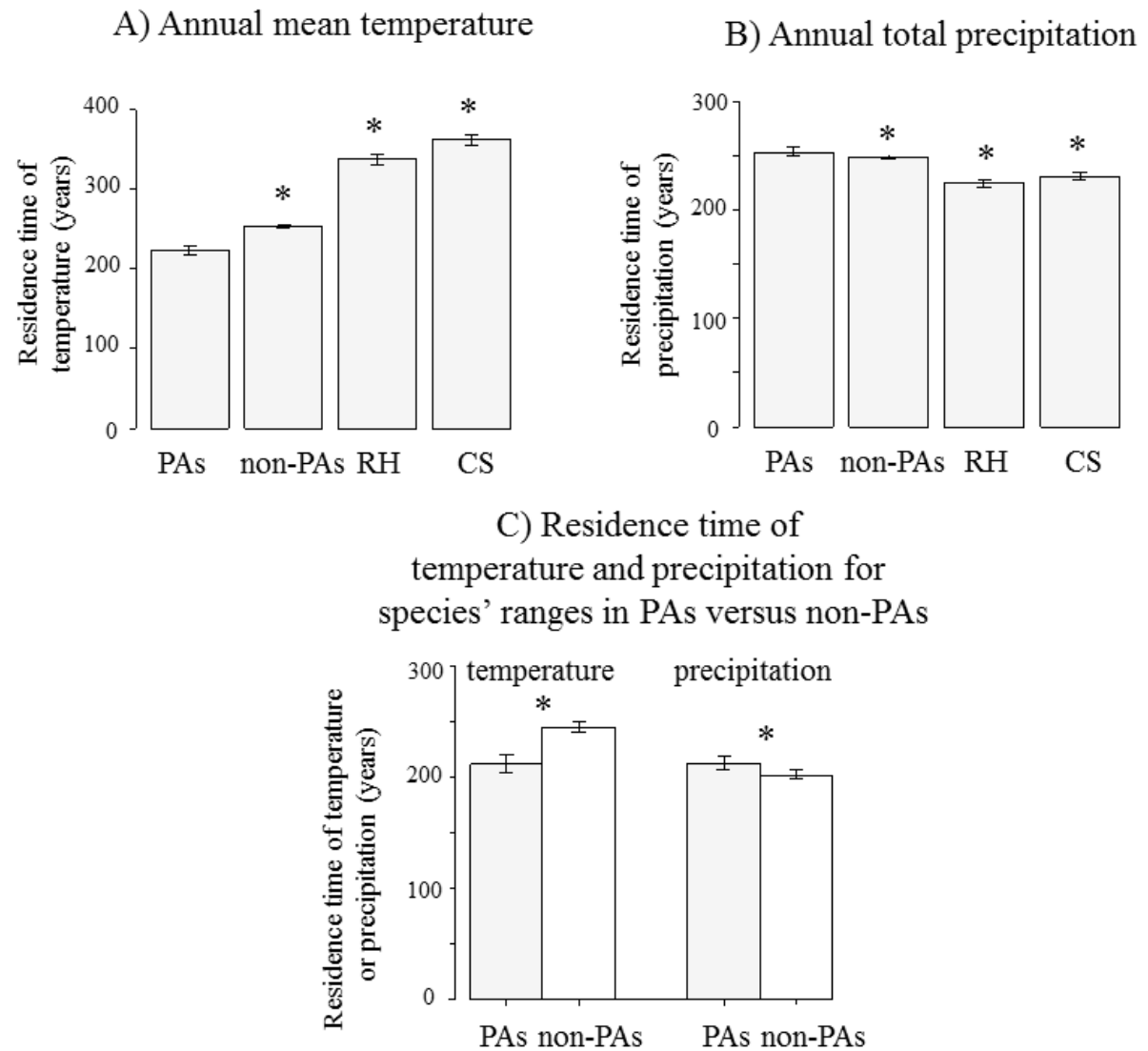


Fig. 2-4. Predicted change using range maps at the $0.25^\circ \times 0.25^\circ$ spatial resolution between the current time and the 2070s, in proportion of natural habitat in protected areas (PAs) versus reference sites (unprotected areas: non-PAs; richness hotspots: RH; complementary sites: CS) and in species' partial ranges covered by protected versus unprotected areas. Error bars indicate the 95% confidence interval. In A, “*” indicates that the comparison between PAs and each reference site is significant ($P < 0.05$) through a *t* test. In B, “**” indicates the comparison of potential change of proportion of natural habitat in species' partial ranges covered by protected areas versus unprotected areas is significant ($P < 0.05$).

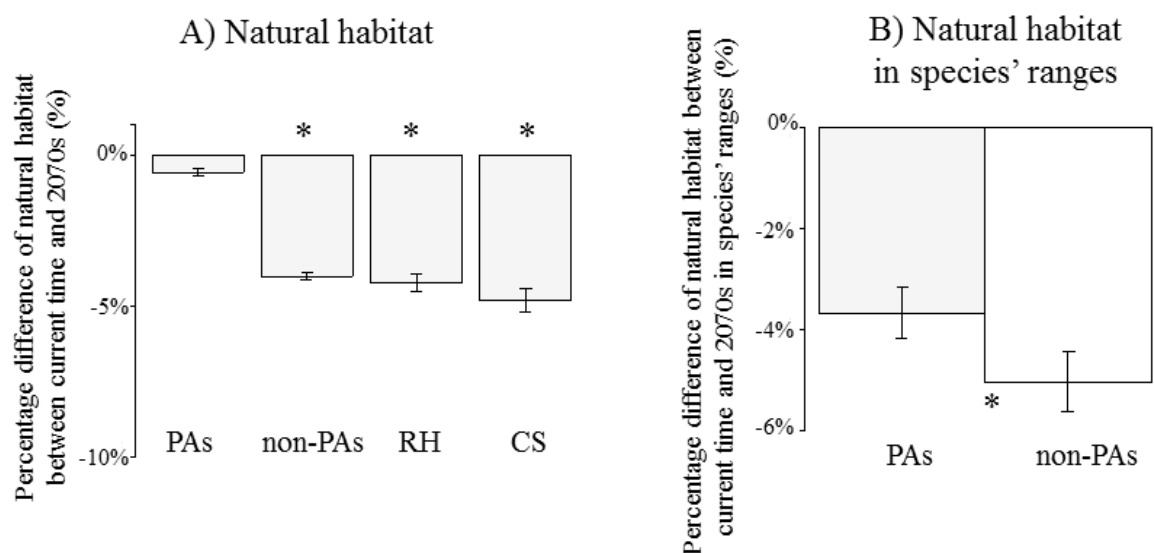


Fig. 2-5. Distribution of the top 10% of conservation gaps (in red color) that are not covered by the current distribution of protected areas (in green color) using a $0.25^\circ \times 0.25^\circ$ spatial resolution and range map data. Two blue rectangles indicate the two large recommended conservation areas discussed in the text.

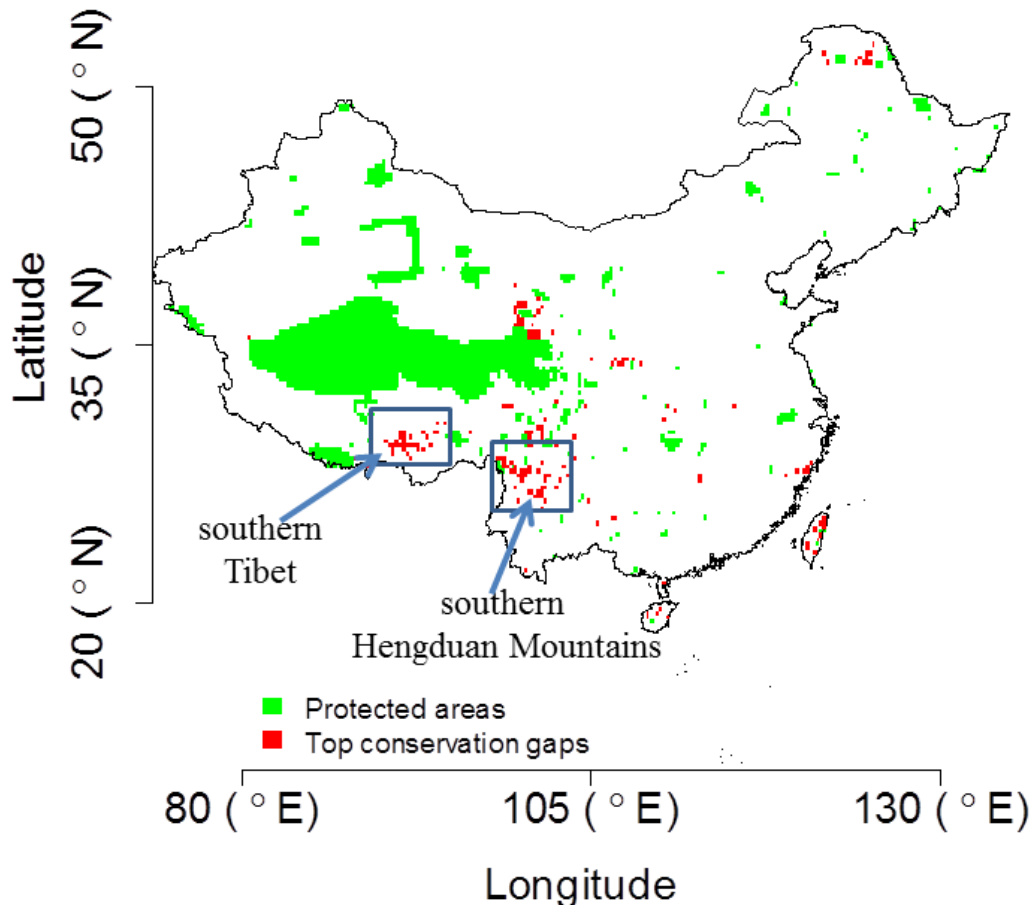
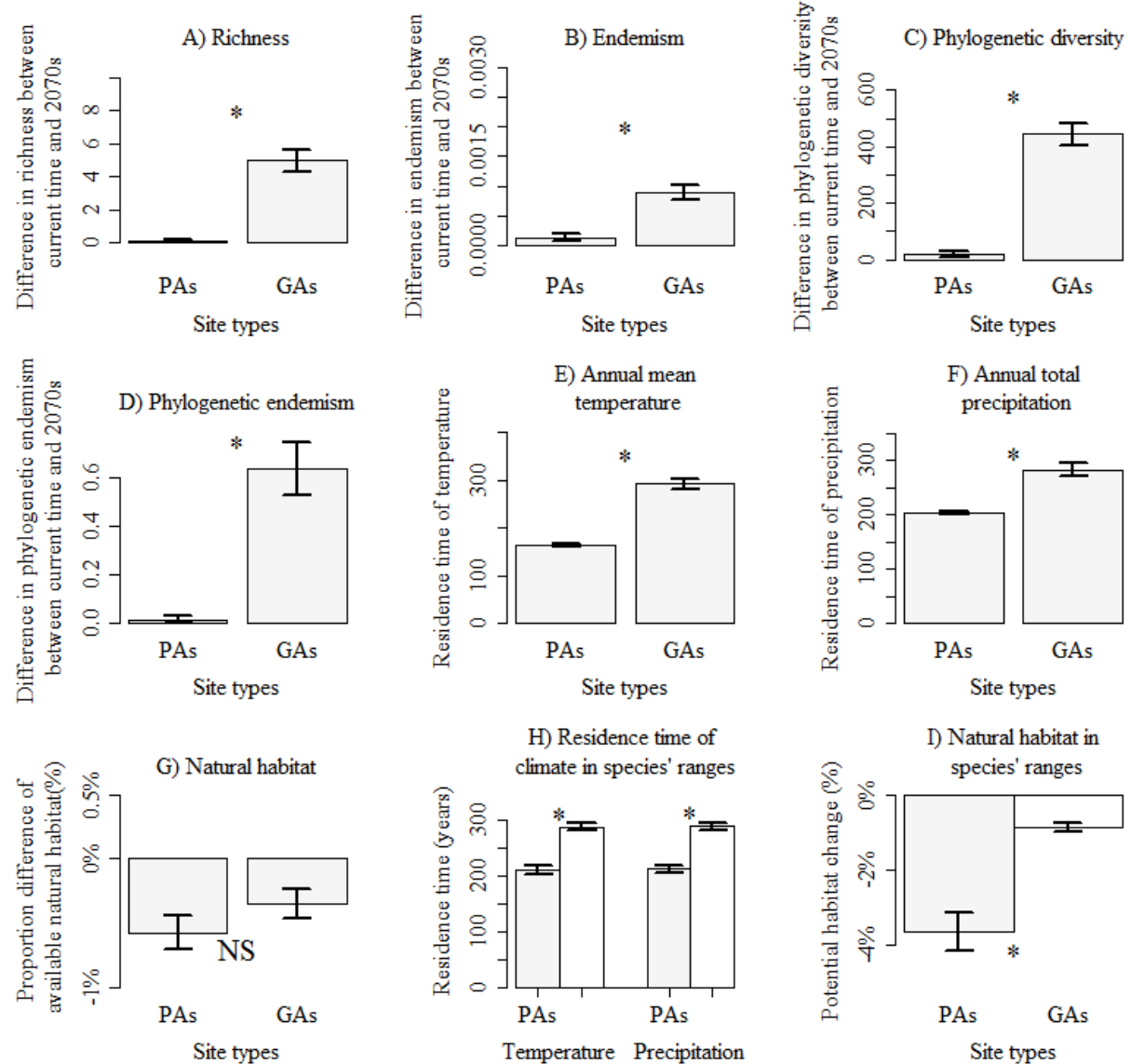


Fig. 2-6. Comparison of the top 10% of conservation gaps (GAs) versus current protected areas (PAs) of China, as measured by different effectiveness indices.



Supporting Information

Table 2-S1. A list of amphibian species of China used for the present study.

<i>Amolops chunganensis</i>	<i>Nanorana quadranus</i>
<i>Amolops granulosus</i>	<i>Nanorana unculuanus</i>
<i>Amolops kangtingensis</i>	<i>Nanorana ventripunctata</i>
<i>Amolops lisanensis</i>	<i>Nanorana yunnanensis</i>
<i>Amolops mantzorum</i>	<i>Occidozyga lima</i>
<i>Amolops marmoratus</i>	<i>Occidozyga martensii</i>
<i>Amolops monticola</i>	<i>Odorrana andersonii</i>
<i>Amolops ricketti</i>	<i>Odorrana grahami</i>
<i>Amolops viridimaculatus</i>	<i>Odorrana hainanensis</i>
<i>Amolops wuyiensis</i>	<i>Odorrana jingdongensis</i>
<i>Andrias davidianus</i>	<i>Odorrana lungshengensis</i>
<i>Babina adenopleura</i>	<i>Odorrana margaretae</i>
<i>Babina daunchina</i>	<i>Odorrana schmackeri</i>
<i>Babina lini</i>	<i>Odorrana swinhoana</i>
<i>Babina pleuraden</i>	<i>Odorrana tiannanensis</i>
<i>Batrachuperus karlschmidti</i>	<i>Odorrana versabilis</i>
<i>Batrachuperus londongensis</i>	<i>Onychodactylus fischeri</i>
<i>Batrachuperus pinchonii</i>	<i>Ophryophryne microstoma</i>
<i>Batrachuperus tibetanus</i>	<i>Oreolalax jingdongensis</i>
<i>Batrachuperus yenyuanensis</i>	<i>Oreolalax lichuanensis</i>
<i>Bombina orientalis</i>	<i>Oreolalax major</i>
<i>Brachytarsophrys feae</i>	<i>Oreolalax multipunctatus</i>
<i>Brachytarsophrys platyparietus</i>	<i>Oreolalax popei</i>
<i>Buergeria japonica</i>	<i>Oreolalax puxiongensis</i>
<i>Buergeria oxycephala</i>	<i>Oreolalax rhodostigmatus</i>
<i>Buergeria robusta</i>	<i>Oreolalax rugosus</i>

<i>Bufo ailaoanus</i>	<i>Oreolalax schmidti</i>
<i>Bufo bankorensis</i>	<i>Oreolalax xiangchengensis</i>
<i>Bufo gargarizans</i>	<i>Pachyhynobius shangchengensis</i>
<i>Bufo minshanicus</i>	<i>Pachytriton brevipes</i>
<i>Bufo stejnegeri</i>	<i>Pachytriton labiatus</i>
<i>Bufo tibetanus</i>	<i>Paramesotriton caudopunctatus</i>
<i>Bufo tuberculatus</i>	<i>Paramesotriton chinensis</i>
<i>Calluella yunnanensis</i>	<i>Paramesotriton hongkongensis</i>
<i>Chiromantis doriae</i>	<i>Pelophylax hubeiensis</i>
<i>Chiromantis vittatus</i>	<i>Pelophylax plancyi</i>
<i>Cynops cyanurus</i>	<i>Pelophylax tenggerensis</i>
<i>Cynops orientalis</i>	<i>Polypedates megacephalus</i>
<i>Duttaphrynus himalayanus</i>	<i>Polypedates mutus</i>
<i>Duttaphrynus melanostictus</i>	<i>Pseudepidalea raddei</i>
<i>Fejervarya cancrivora</i>	<i>Pseudorana sangzhiensis</i>
<i>Fejervarya limnocharis</i>	<i>Pseudorana weiningensis</i>
<i>Glandirana emeljanovi</i>	<i>Quasipaa boulengeri</i>
<i>Glandirana minima</i>	<i>Quasipaa exilispinosa</i>
<i>Glandirana tientaiensis</i>	<i>Quasipaa jiulongensis</i>
<i>Hoplobatrachus rugulosus</i>	<i>Quasipaa shini</i>
<i>Hyla annectans</i>	<i>Quasipaa spinosa</i>
<i>Hyla chinensis</i>	<i>Rana amurensis</i>
<i>Hyla immaculata</i>	<i>Rana chaochiaoensis</i>
<i>Hyla japonica</i>	<i>Rana chensinensis</i>
<i>Hyla sanchiangensis</i>	<i>Rana omeimontis</i>
<i>Hyla simplex</i>	<i>Rana shuchinae</i>
<i>Hyla tsinlingensis</i>	<i>Rhacophorus chenfui</i>

<i>Hylarana guentheri</i>	<i>Rhacophorus dennysi</i>
<i>Hylarana latouchii</i>	<i>Rhacophorus dugritei</i>
<i>Hylarana macrodactyla</i>	<i>Rhacophorus feae</i>
<i>Hylarana nigrovittata</i>	<i>Rhacophorus hungfuensis</i>
<i>Hylarana spinulosa</i>	<i>Rhacophorus maximus</i>
<i>Hylarana taipehensis</i>	<i>Rhacophorus moltrechti</i>
<i>Hynobius chinensis</i>	<i>Rhacophorus omeimontis</i>
<i>Hynobius leechii</i>	<i>Rhacophorus rhodopus</i>
<i>Ingerana liui</i>	<i>Rhacophorus taipeianus</i>
<i>Ingerana medogensis</i>	<i>Rhacophorus translineatus</i>
<i>Kalophrynum interlineatus</i>	<i>Rhacophorus tuberculatus</i>
<i>Kaloula borealis</i>	<i>Rhacophorus yaoshanensis</i>
<i>Kaloula pulchra</i>	<i>Salamandrella keyserlingii</i>
<i>Kaloula rugifera</i>	<i>Scutiger boulengeri</i>
<i>Kaloula verrucosa</i>	<i>Scutiger glandulatus</i>
<i>Kurixalus eiffingeri</i>	<i>Scutiger maculatus</i>
<i>Kurixalus idiootocus</i>	<i>Scutiger mammatus</i>
<i>Kurixalus odontotarsus</i>	<i>Scutiger muliensis</i>
<i>Leptobrachium boringii</i>	<i>Scutiger ningshanensis</i>
<i>Leptobrachium chapaense</i>	<i>Scutiger nyungchiensis</i>
<i>Leptobrachium liui</i>	<i>Scutiger pingwuensis</i>
<i>Leptolalax liui</i>	<i>Scutiger tuberculatus</i>
<i>Leptolalax oshanensis</i>	<i>Tylototriton asperrimus</i>
<i>Leptolalax pelodytoides</i>	<i>Tylototriton hainanensis</i>
<i>Limnonectes fragilis</i>	<i>Tylototriton kweichowensis</i>
<i>Limnonectes fujianensis</i>	<i>Tylototriton taliangensis</i>
<i>Limnonectes kuhlii</i>	<i>Tylototriton verrucosus</i>
<i>Liua shihii</i>	<i>Tylototriton wenxianensis</i>
<i>Liua tsinpaensis</i>	<i>Xenophrys boettgeri</i>

<i>Microhyla berdmorei</i>	<i>Xenophrys glandulosa</i>
<i>Microhyla butleri</i>	<i>Xenophrys mangshanensis</i>
<i>Microhyla heymonsi</i>	<i>Xenophrys medogensis</i>
<i>Microhyla mixtura</i>	<i>Xenophrys nankiangensis</i>
<i>Microhyla pulchra</i>	<i>Xenophrys pachyproctus</i>
<i>Nanorana liebigii</i>	<i>Xenophrys spinata</i>
<i>Nanorana maculosa</i>	<i>Microhyla fissipes</i>
<i>Nanorana parkeri</i>	<i>Rana kukunoris</i>
<i>Nanorana pleskei</i>	<i>Rana zhenhaiensis</i>

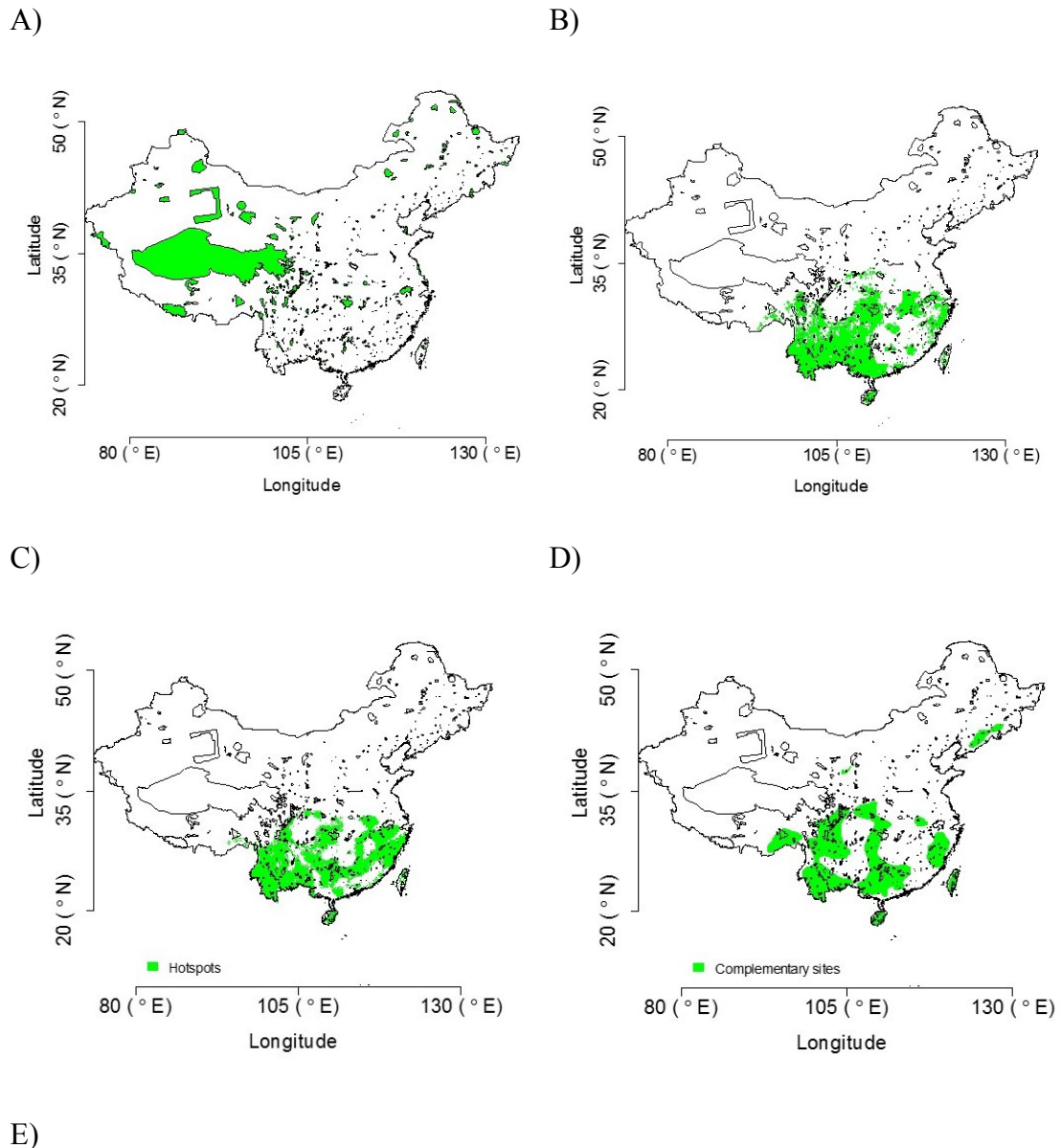
Table 2-S2. A list of data-deficit amphibian species of China those are not included for the present study.

<i>Amolops aniqiaoensis</i>	<i>Nanorana medogensis</i>
<i>Amolops bellulus</i>	<i>Nanorana taihangnica</i>
<i>Amolops caelumnoctis</i>	<i>Odorrana graminea</i>
<i>Amolops liangshanensis</i>	<i>Oreolalax nanjiangensis</i>
<i>Amolops medogensis</i>	<i>Pseudepidalea zamdaensis</i>
<i>Batrachuperus taibaiensis</i>	<i>Pseudohynobius kuankuoshuiensis</i>
<i>Brachytarsophrys chuannanensis</i>	<i>Quasipaa yei</i>
<i>Bufo aspinus</i>	<i>Rana hanluica</i>
<i>Bufo kabischi</i>	<i>Rana kunyuensis</i>
<i>Bufo wolongensis</i>	<i>Rana zhengi</i>
<i>Cynops chenggongensis</i>	<i>Rhacophorus duboisi</i>
<i>Fejervarya multistriata</i>	<i>Rhacophorus hui</i>
<i>Hyla zhaopingensis</i>	<i>Rhacophorus puerensis</i>
<i>Hynobius guabangshanensis</i>	<i>Rhacophorus taronensis</i>
<i>Hynobius maoershanensis</i>	<i>Rhacophorus verrucopus</i>
<i>Ingerana alpina</i>	<i>Scutiger brevipes</i>
<i>Ingerana reticulata</i>	<i>Scutiger jiulongensis</i>
<i>Ingerana xizangensis</i>	<i>Theloderma kwangsiense</i>
<i>Kalophryns menglianicus</i>	<i>Xenophryns dawemontis</i>
<i>Leptobrachium promustache</i>	<i>Xenophryns huangshanensis</i>
<i>Leptolalax ventripunctatus</i>	<i>Xenophryns wawuensis</i>
<i>Nanorana conaensis</i>	<i>Xenophryns wuliangshanensis</i>
<i>Nanorana feae</i>	<i>Xenophryns zhangi</i>

Table 2-S3. Twelve reclassified land use (LU) classes derived from Globio3 data set for the present study.

New classes	Land use types covered
LU1	Tree cover
LU2	Tree Cover, regularly flooded
LU3	Mosaic habitat
LU4	Tree cover, burnt
LU5	Shrub cover, closed-open
LU6	Herbaceous cover
LU7	Cultivated and managed areas
LU8	Bare areas
LU9	Water bodies
LU10	Snow and ice
LU11	Artificial surfaces and associated areas
LU12	Pasture/grassland

Fig. 2-S1. Distribution of grid cells (in green colors) that are used to represent current protected areas of China (A), range map data set-derived richness hotspots (B), occurrence data set-derived richness hotspots (C), range map-derived complementary sites (D) and occurrence-derived complementary sites (E) at $0.1^\circ \times 0.1^\circ$ spatial resolution. Grid cells are identified as protected areas when at least 50% of their areas are covered by the polygons of current protected areas, which are superimposed in the maps.



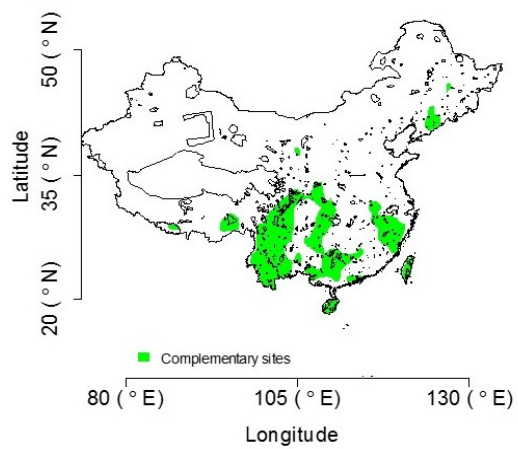
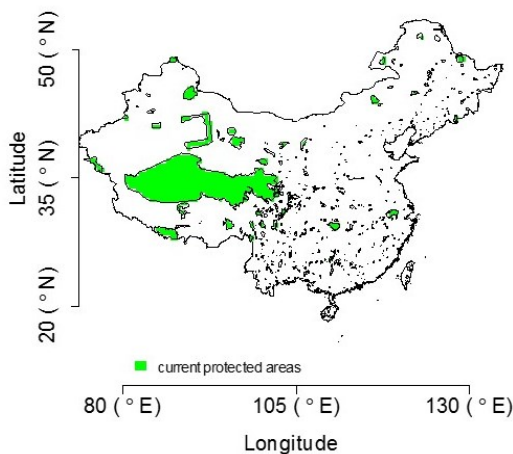
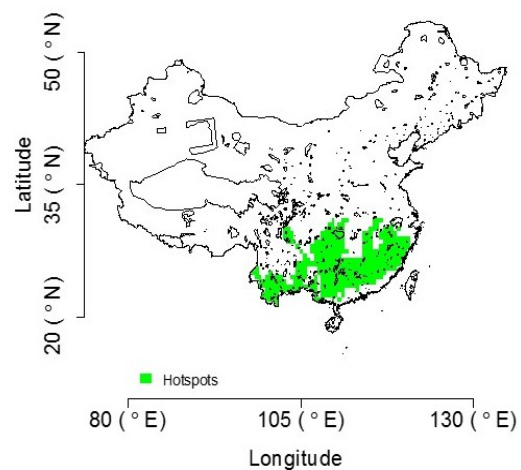


Fig. 2-S2. Distribution of grid cells (in green colors) that are used to represent current protected areas of China (A), range map-derived richness hotspots (B), occurrence-derived richness hotspots (C), range map-derived complementary sites (D) and occurrence-derived complementary sites (E) at $0.5^\circ \times 0.5^\circ$ spatial resolution. Grid cells are identified as protected areas only when at least 50% of their areas are covered by the polygons of current protected areas, which are superimposed in the maps.

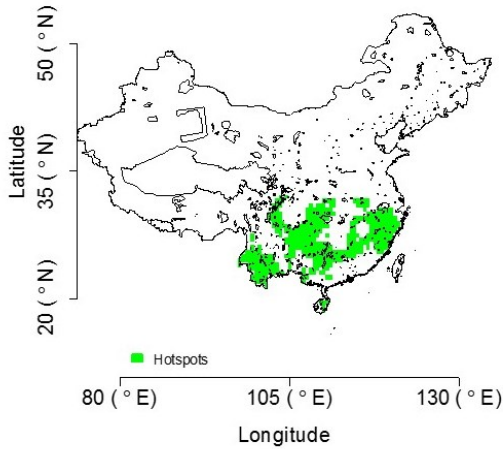
A)



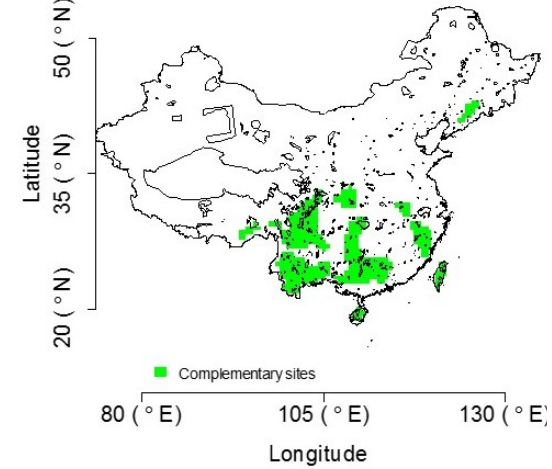
B)



C)



D)



E)

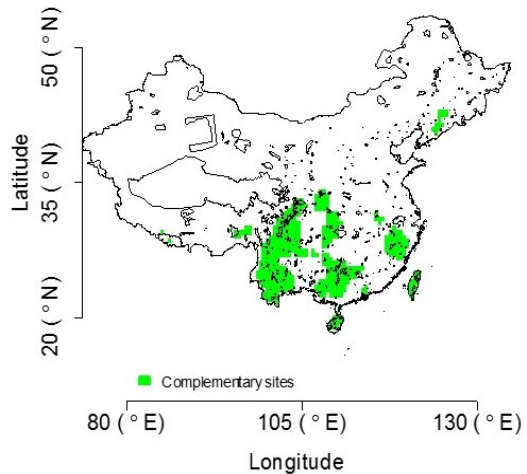
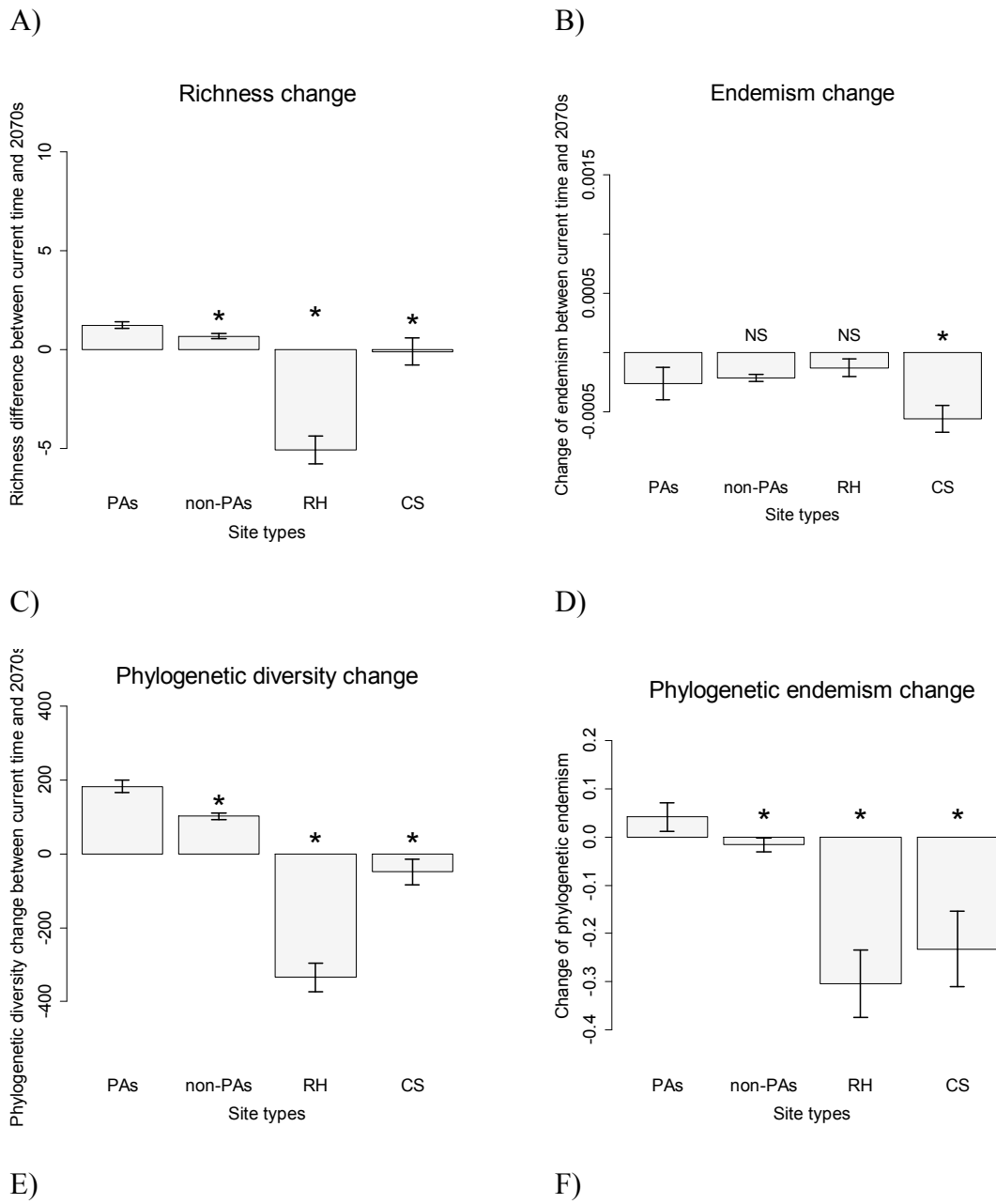
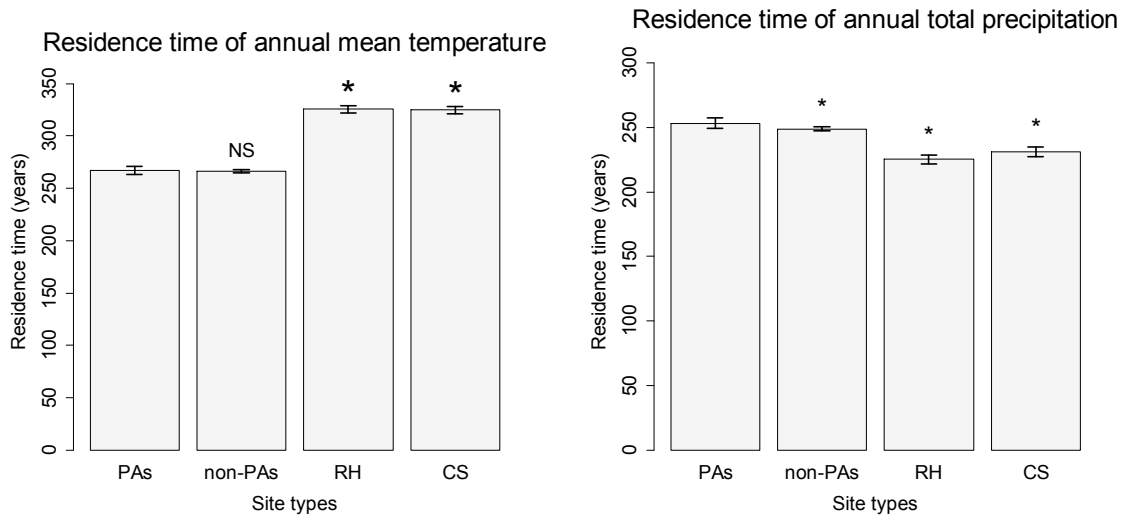


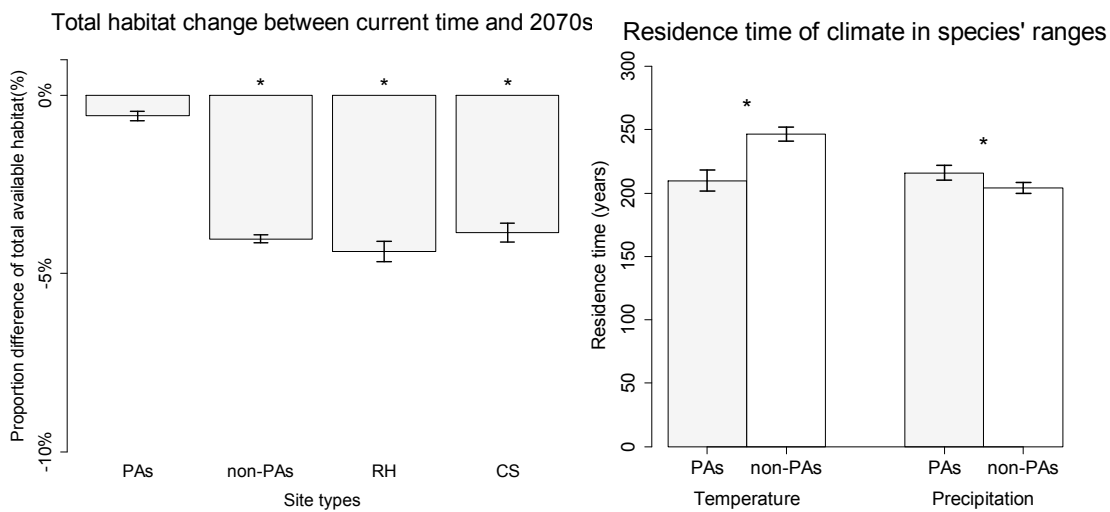
Fig. 2-S3. Comparison of effectiveness indices in protected areas (PAs), unprotected areas (non-PAs), richness hotspots (RH) and complementary sites (CS) at $0.25^\circ \times 0.25^\circ$ spatial resolution using occurrence data. These indices include: potential change in species richness (A), corrected weighted endemism (B), phylogenetic diversity (C), phylogenetic endemism (D), residence time of temperature (E), residence time of precipitation (F), and change of total suitable habitat over time (G). Additionally, comparisons of residence time of climate (H) and change of suitable habitat (I) in species' partial ranges covered by protected versus unprotected areas were provided. Error bars indicate the 95% confidence interval. “**” and “NS” indicate that the comparison between PAs and each kind of the reference sites through a *t*-test is significant ($P < 0.05$) and non-significant ($P > 0.05$) respectively.





G)

H)



I)

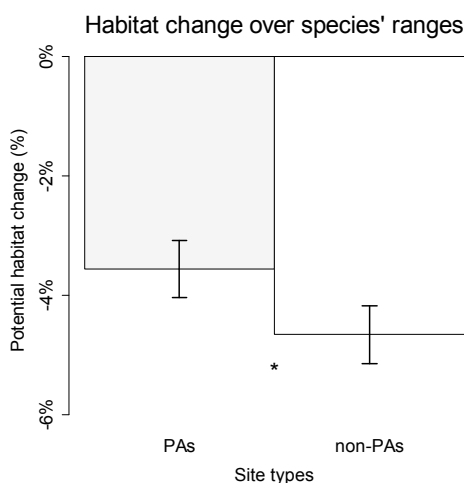
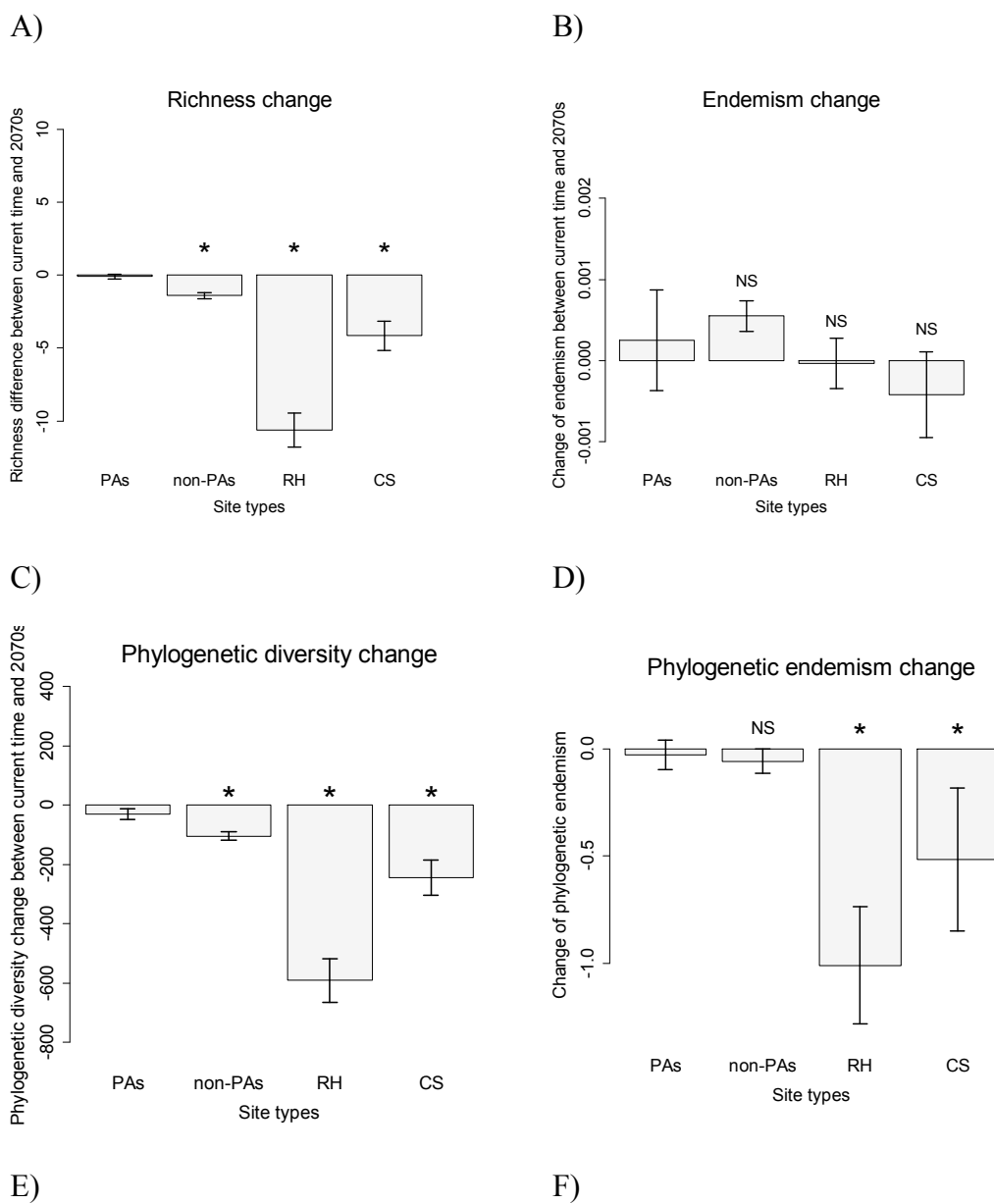
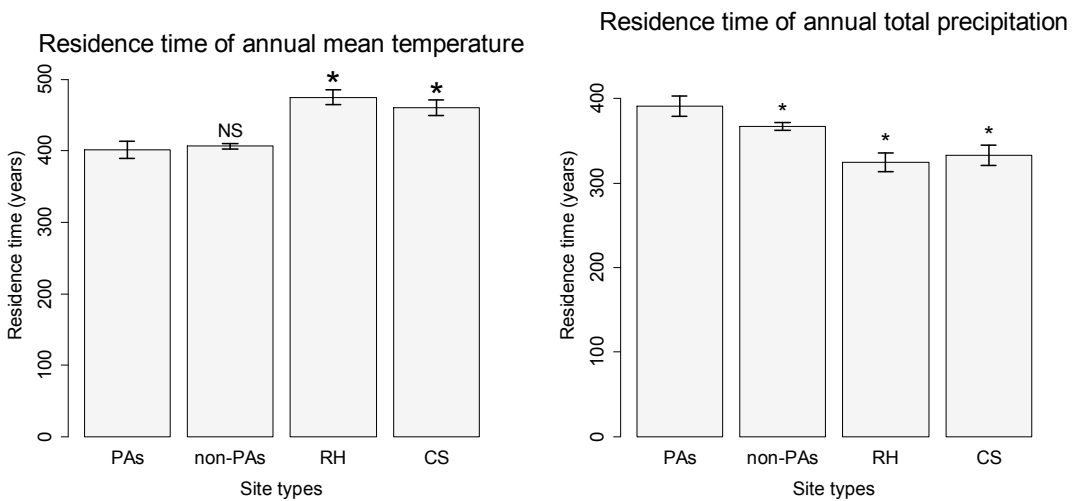


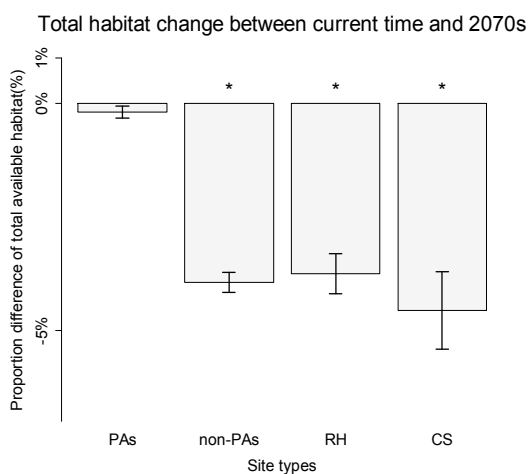
Fig. 2-S4. Comparison of effectiveness of diversity indices in protected areas (PAs), unprotected areas (non-PAs), richness hotspots (RH) and complementary sites (CS) at $0.5^\circ \times 0.5^\circ$ spatial resolution using range map data set. These indices include: potential change of species richness (A), corrected weighted endemism (B), phylogenetic diversity (C), phylogenetic endemism (D), residence time of temperature (E), residence time of precipitation (F), and change of total suitable habitat over time (G). Additionally, comparisons of residence time of climate (H) and change of suitable habitat (I) in species' partial ranges covered by protected versus unprotected areas are provided. Error bars indicate the 95% confidence interval. “*” and “NS” indicate that the comparison between PAs and each kind of the reference sites through a *t*-test is significant ($P < 0.05$) and non-significant ($P > 0.05$) respectively.



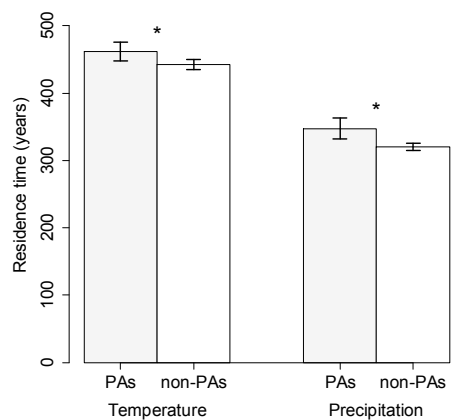


G)

H)



Residence time of climate in species' ranges



I)

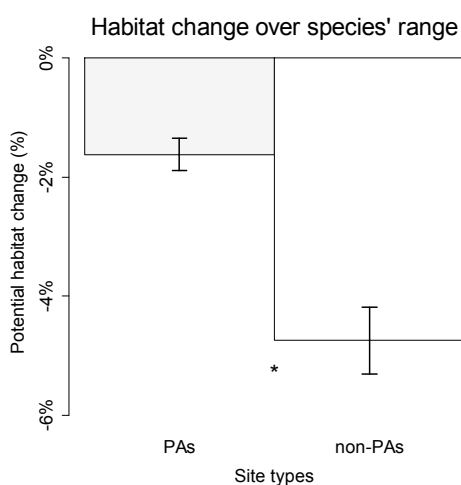
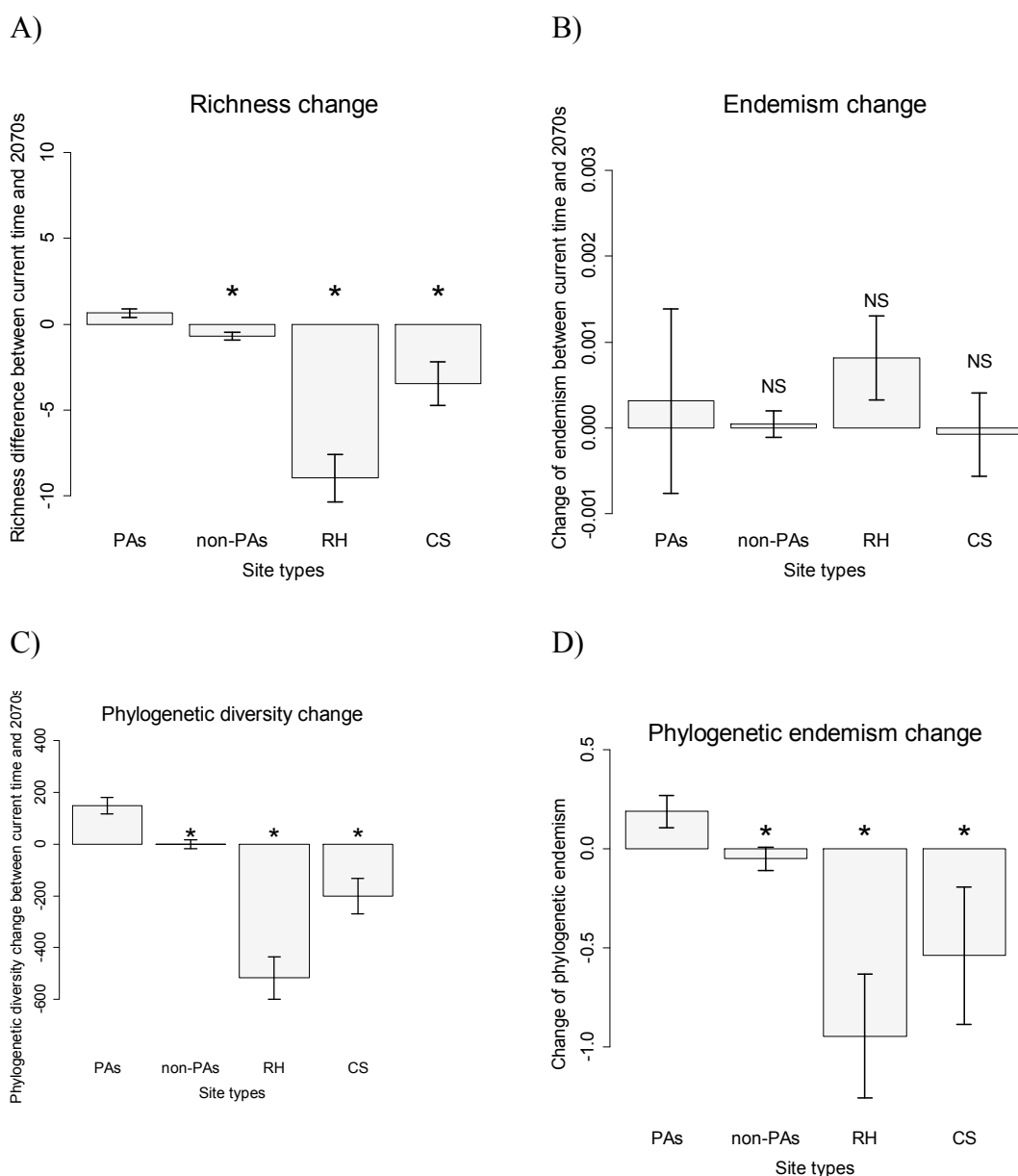
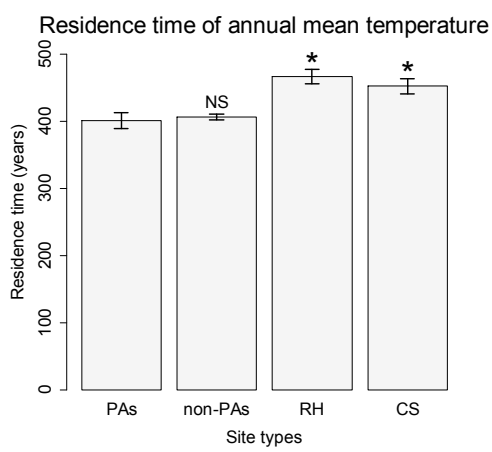


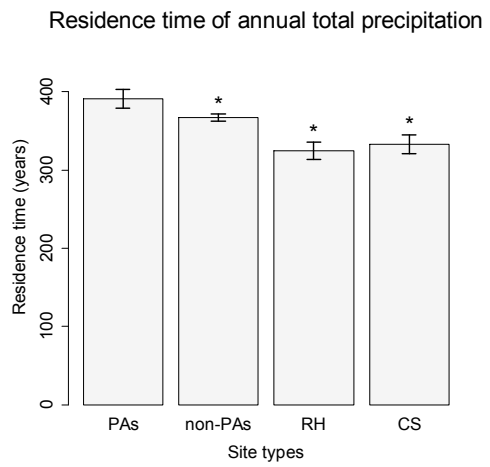
Fig. 2-S5. Comparison of effectiveness of diversity indices in protected areas (PAs), unprotected areas (non-PAs), richness hotspots (RH) and complementary sites (CS) at $0.5^\circ \times 0.5^\circ$ spatial resolution using occurrence data. These indices include: potential change of species richness (A), corrected weighted endemism (B), phylogenetic diversity (C), phylogenetic endemism (D), residence time of temperature (E), residence time of precipitation (F), and change of total suitable habitat over time (G). Additionally, comparisons of residence time of climate (H) and change of suitable habitat (I) in species' partial ranges covered by protected versus unprotected areas are provided. Error bars indicate the 95% confidence interval. “*” and “NS” indicate that the comparison between PAs and each kind of the reference sites through a *t*-test is significant ($P < 0.05$) and non-significant ($P > 0.05$) respectively.



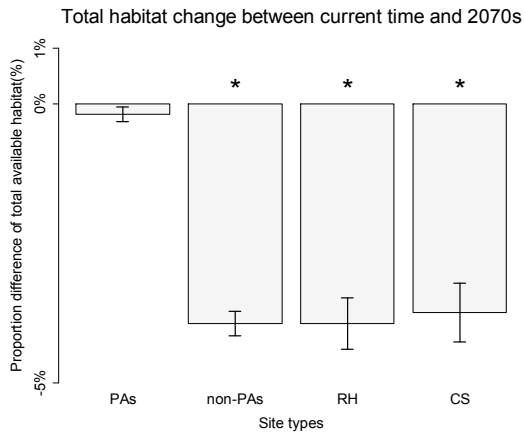
E)



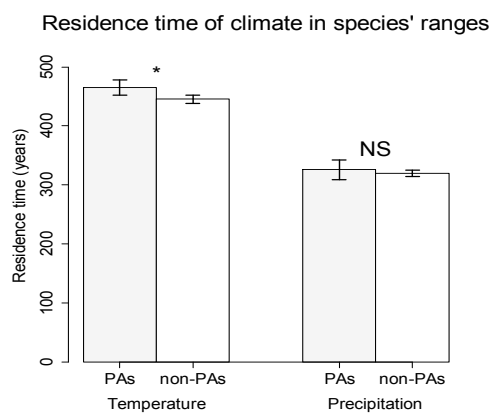
F)



G)



H)



I)

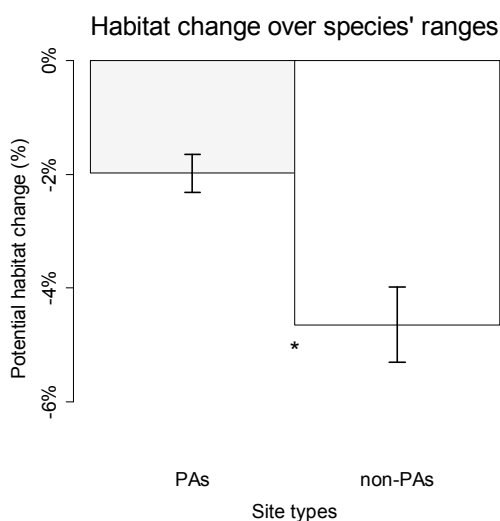
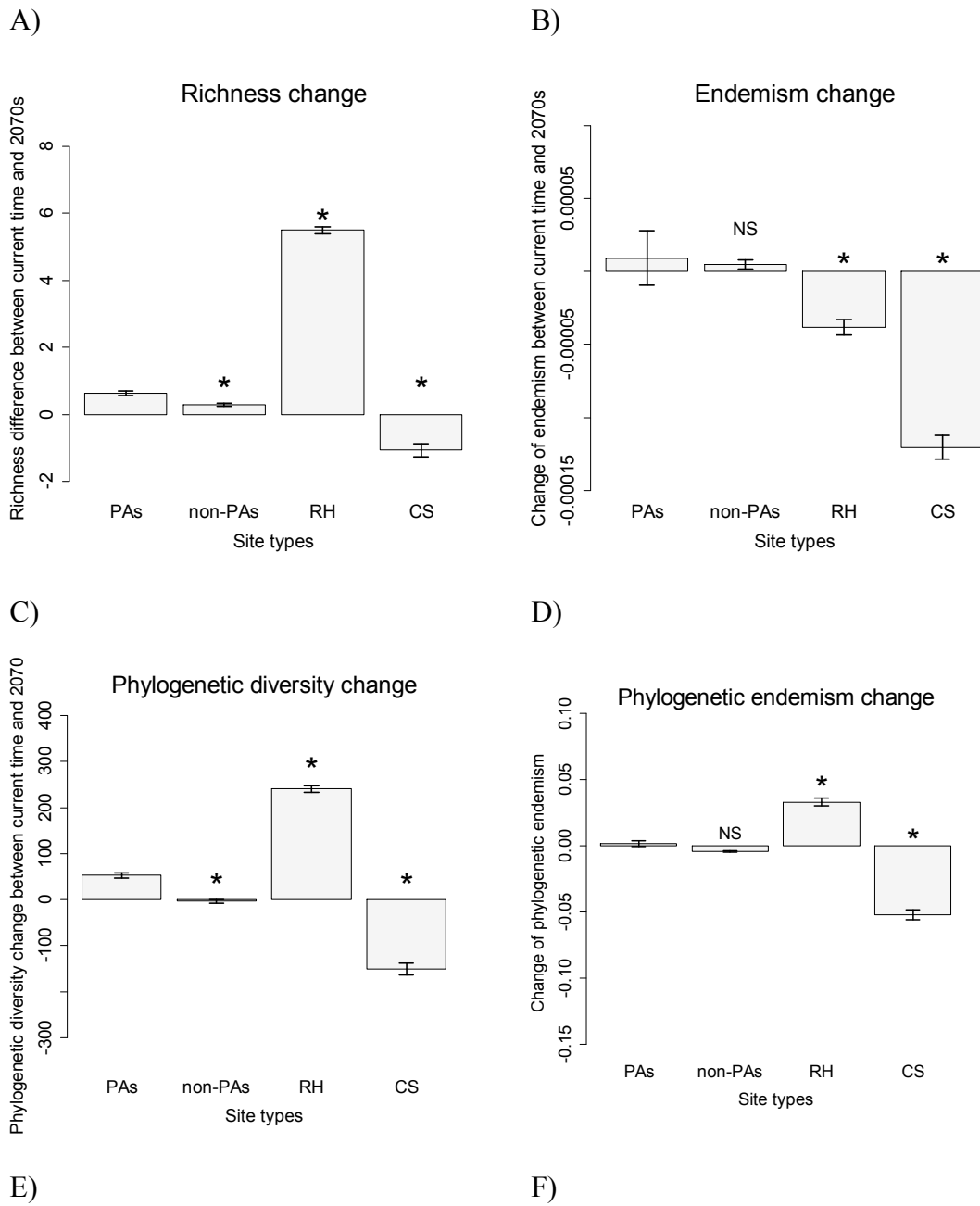
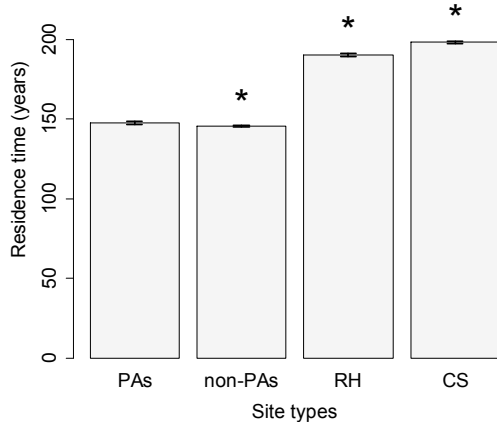


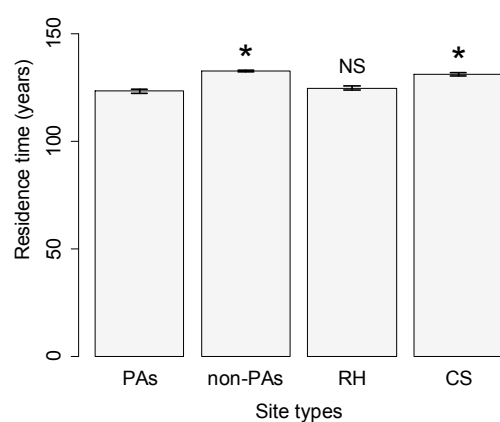
Fig. 2-S6. Comparison of effectiveness of diversity indices in protected areas (PAs), unprotected areas (non-PAs), richness hotspots (RH) and complementary sites (CS) at $0.1^\circ \times 0.1^\circ$ spatial resolution using range map data set. These indices include: potential change of species richness (A), corrected weighted endemism (B), phylogenetic diversity (C), phylogenetic endemism (D), residence time of temperature (E), residence time of precipitation (F), and change of total suitable habitat over time (G). Additionally, comparisons of residence time of climate (H) and change of suitable habitat (I) in species' partial ranges covered by protected versus unprotected areas are provided. Error bars indicate the 95% confidence interval. “*” and “NS” indicate that the comparison between PAs and each kind of the reference sites through a *t*-test is significant ($P < 0.05$) and non-significant ($P > 0.05$) respectively.



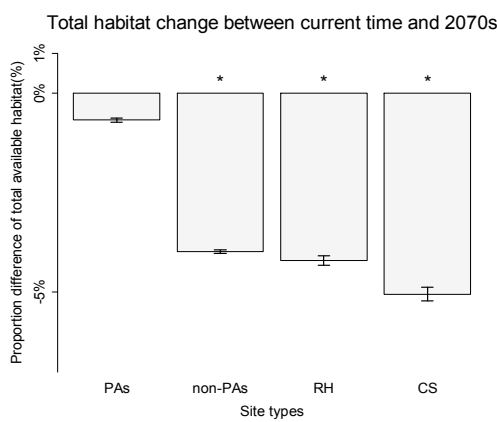
Residence time of annual mean temperature



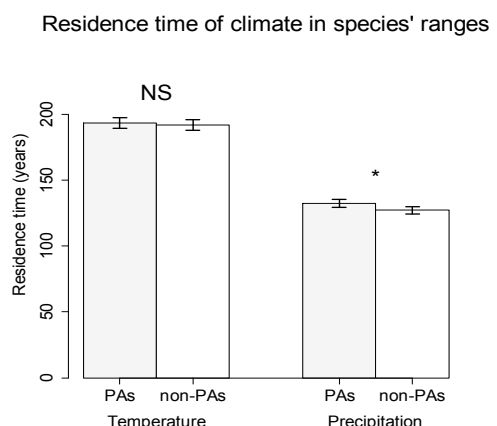
Residence time of annual total precipitation



G)



H)



I)

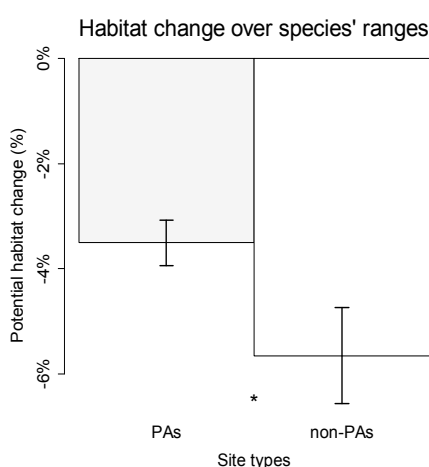
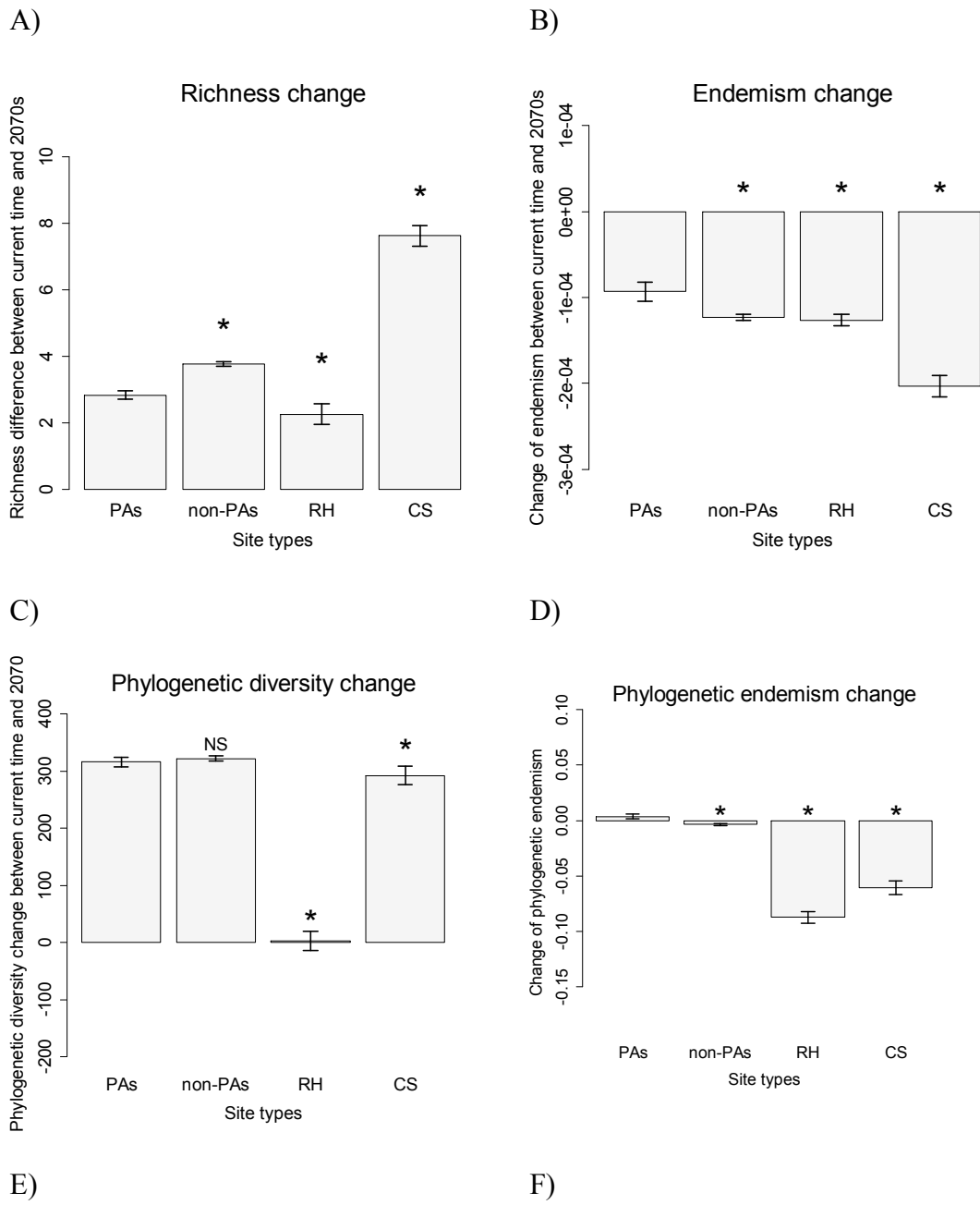
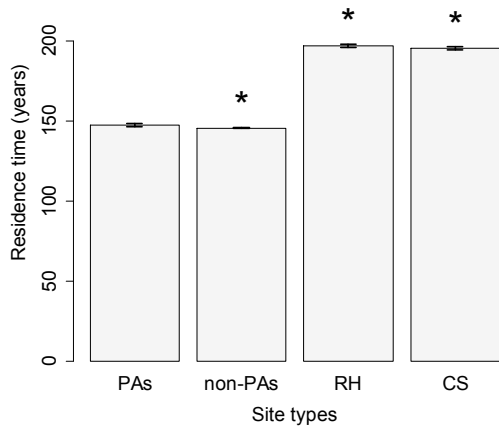


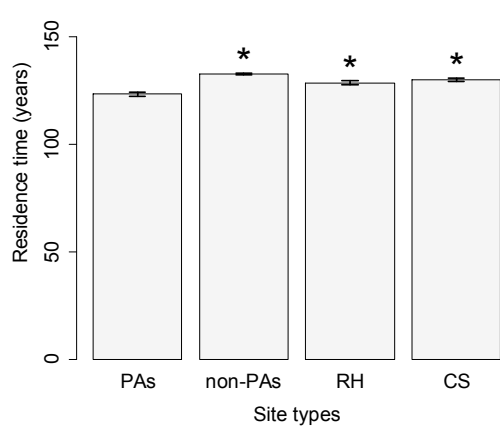
Fig. 2-S7. Comparison of effectiveness indices in protected areas (PAs), unprotected areas (non-PAs), richness hotspots (RH) and complementary sites (CS) at $0.1^\circ \times 0.1^\circ$ spatial resolution using occurrence data. These indices include: potential change of species richness (A), corrected weighted endemism (B), phylogenetic diversity (C), phylogenetic endemism (D), residence time of temperature (E), residence time of precipitation (F), and change of total suitable habitat over time (G). Additionally, comparisons of residence time of climate (H) and change of suitable habitat (I) in species' partial ranges covered by protected versus unprotected areas are provided. Error bars indicate the 95% confidence interval. “**” and “NS” indicate that the comparison between PAs and each kind of the reference sites through a *t*-test is significant ($P < 0.05$) and non-significant ($P > 0.05$) respectively.



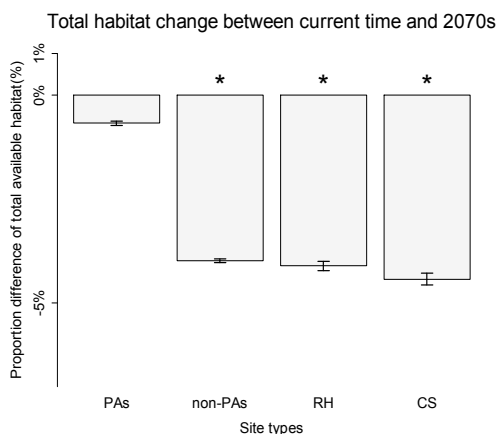
Residence time of annual mean temperature



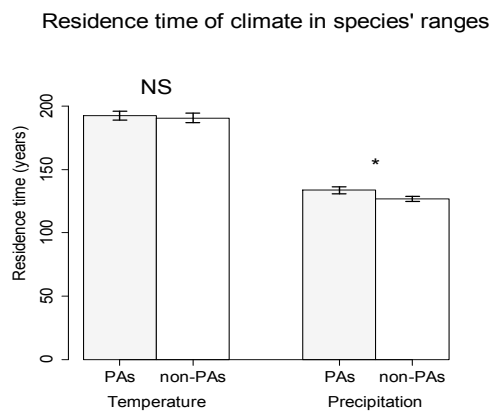
Residence time of annual total precipitation



G)



H)



I)

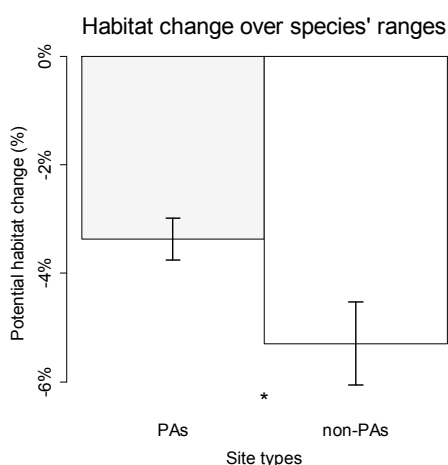
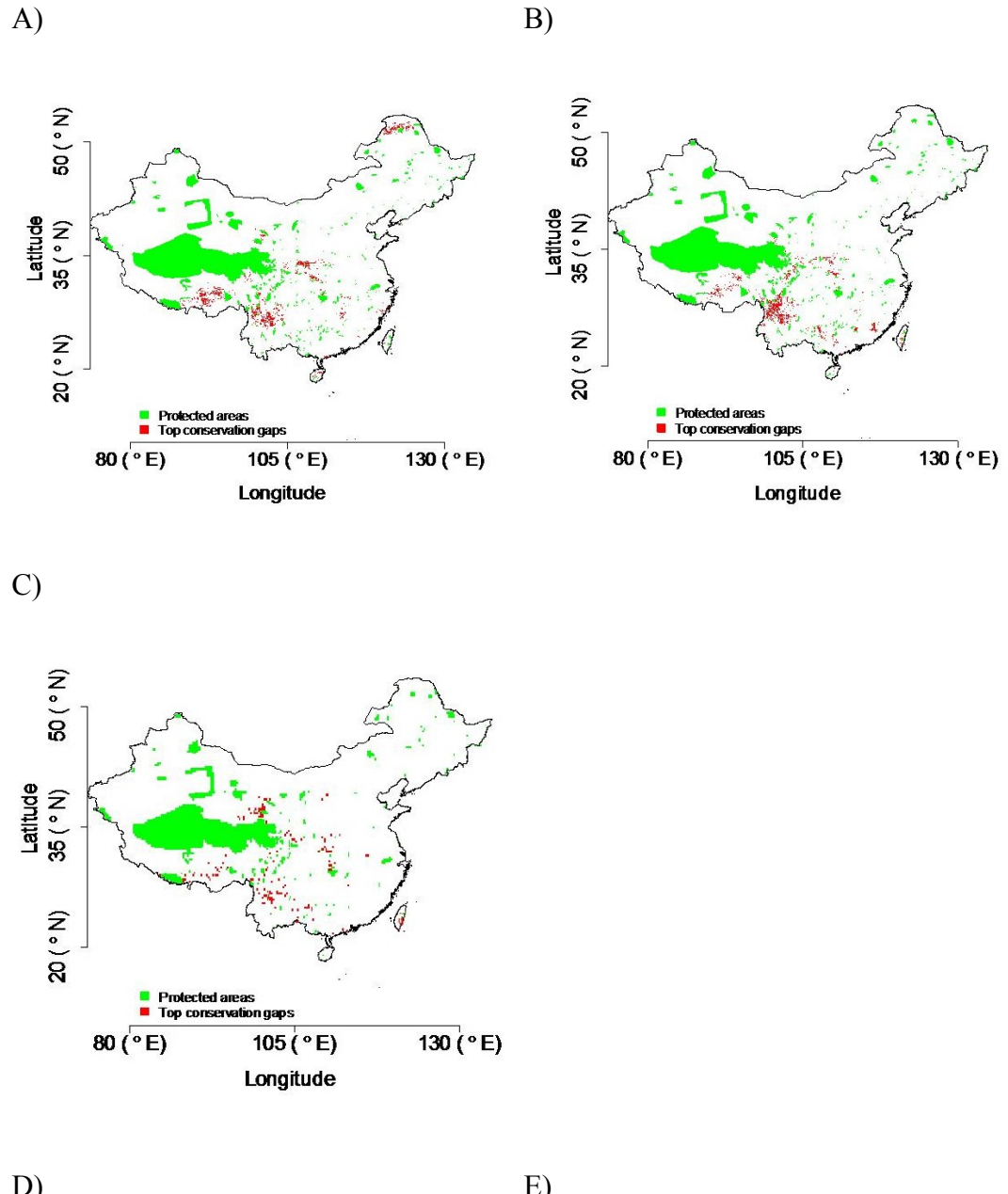


Fig. 2-S8. Top 10% of conservation gaps (in red color) identified using different distribution data and across three spatial scales. A) range map-derived conservation gaps at $0.1^\circ \times 0.1^\circ$ spatial scale; B) occurrence-derived conservation gaps at $0.1^\circ \times 0.1^\circ$ spatial scale; C) occurrence-derived conservation gaps at $0.25^\circ \times 0.25^\circ$ spatial scale; D) range map-derived conservation gaps at $0.5^\circ \times 0.5^\circ$ spatial scale; E) occurrence-derived conservation gap sat $0.5^\circ \times 0.5^\circ$ spatial scale.



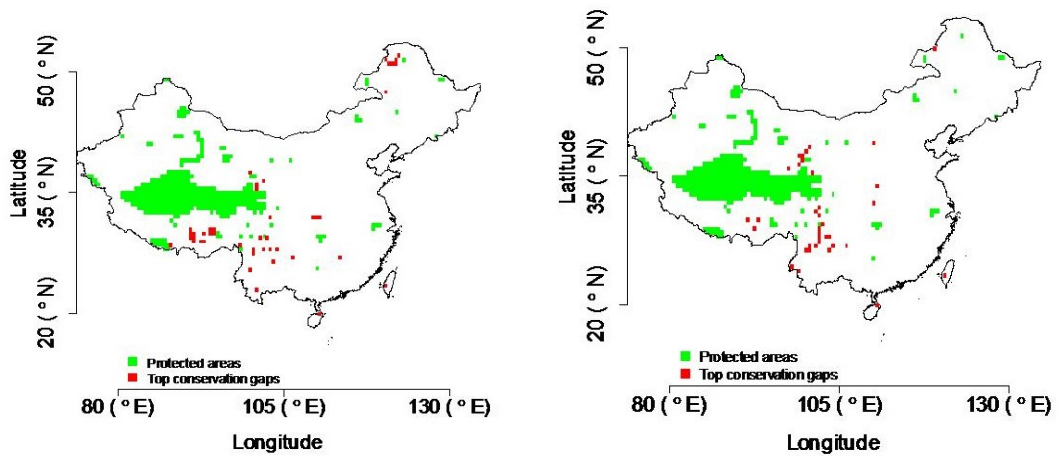
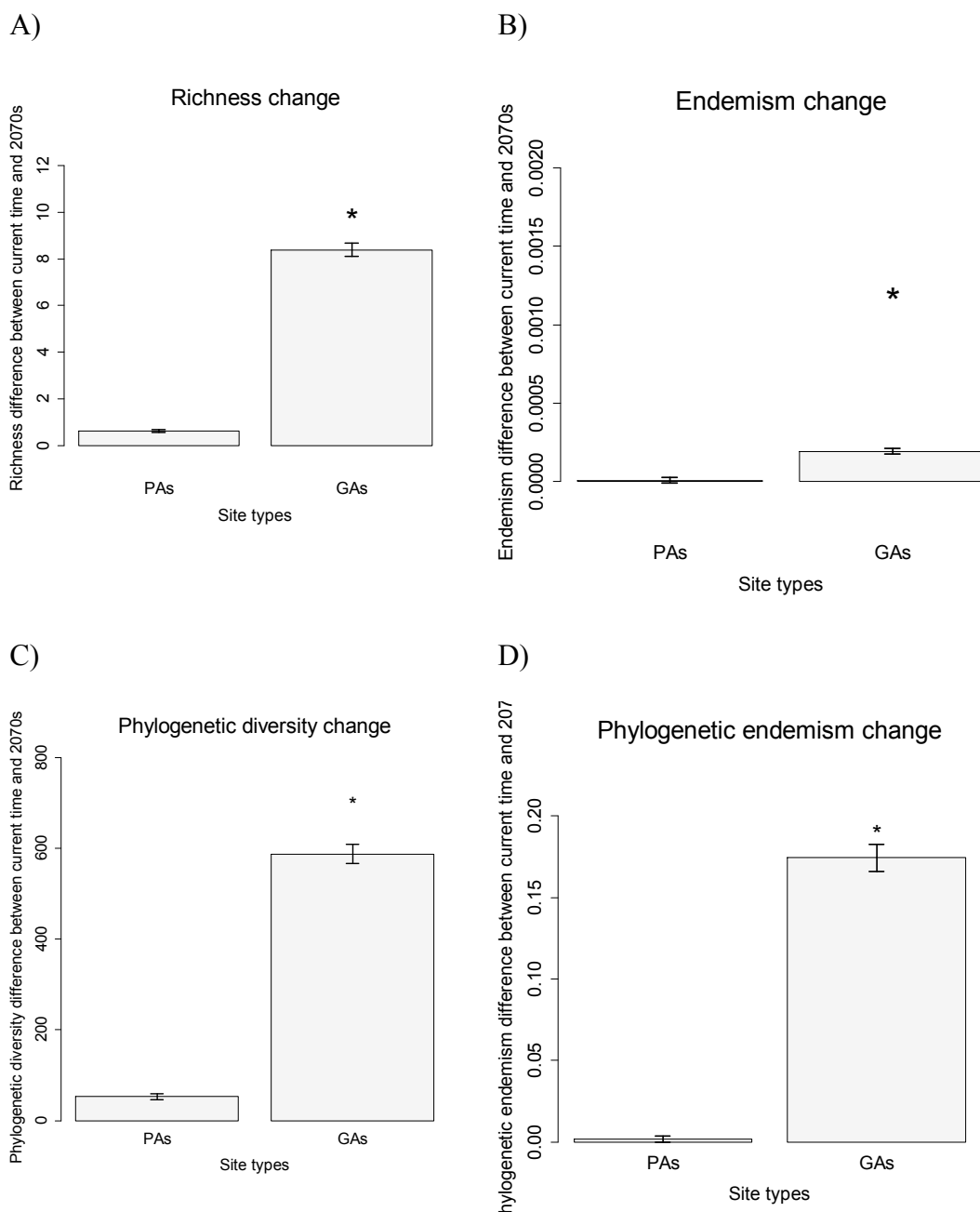
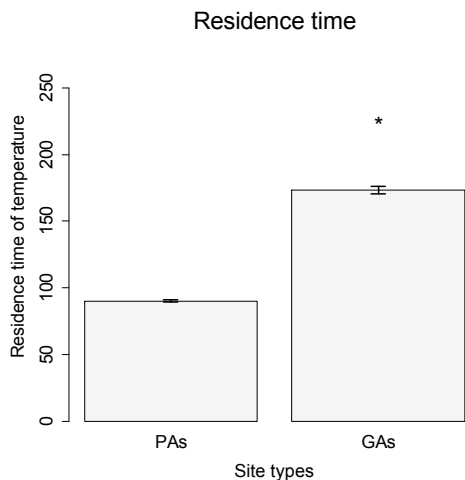


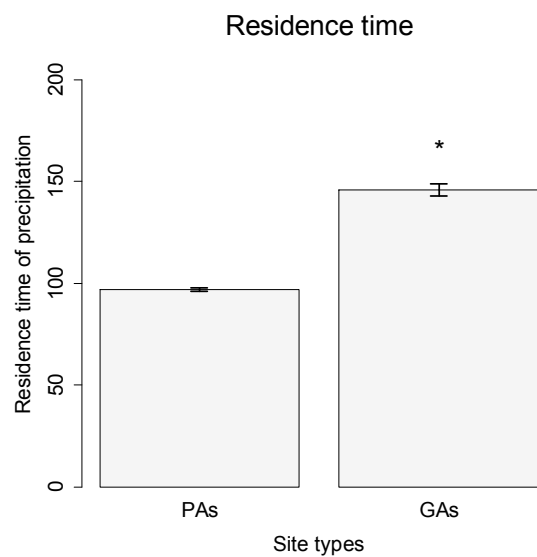
Fig. 2-S9. Comparison of effectiveness of diversity indices in protected areas (PAs) and top 10% of conservation gap areas (GA) at $0.1^\circ \times 0.1^\circ$ spatial resolution using range map data set. These indices include: potential change of species richness (A), corrected weighted endemism (B), phylogenetic diversity (C), phylogenetic endemism (D), residence time of temperature (E), residence time of precipitation (F), and change of total suitable habitat over time (G). Additionally, comparisons of residence time of climate (H) and change of suitable habitat (I) in species' partial ranges covered by protected versus unprotected areas are provided. Error bars indicate the 95% confidence interval. “*” and “NS” indicate that the comparison between PAs and GAs through a *t*-test is significant ($P < 0.05$) and non-significant ($P > 0.05$) respectively.



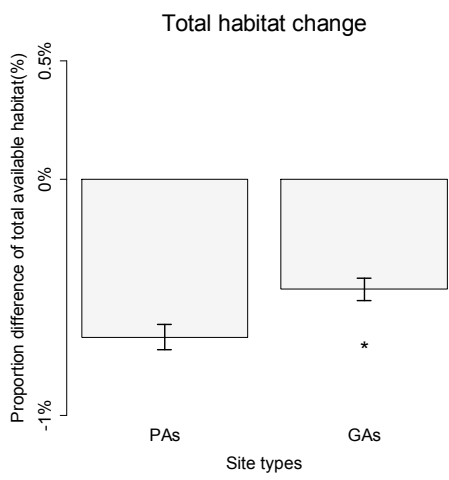
E)



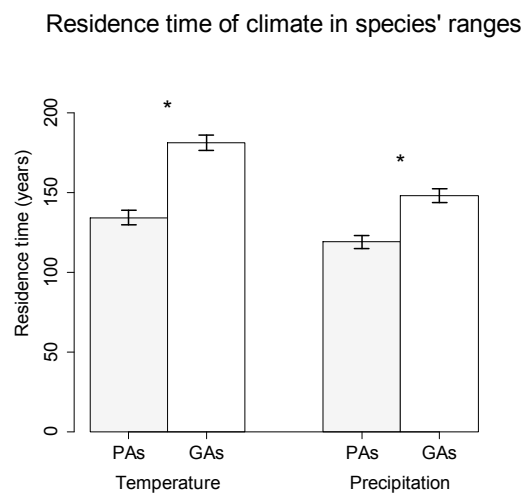
F)



G)



H)



I)

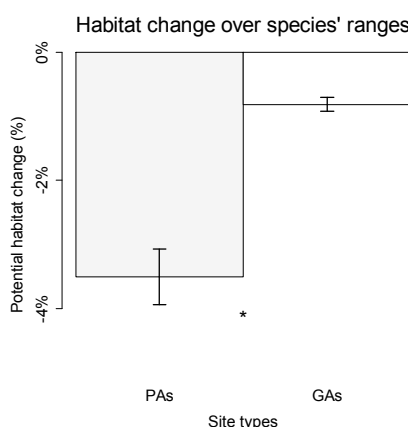
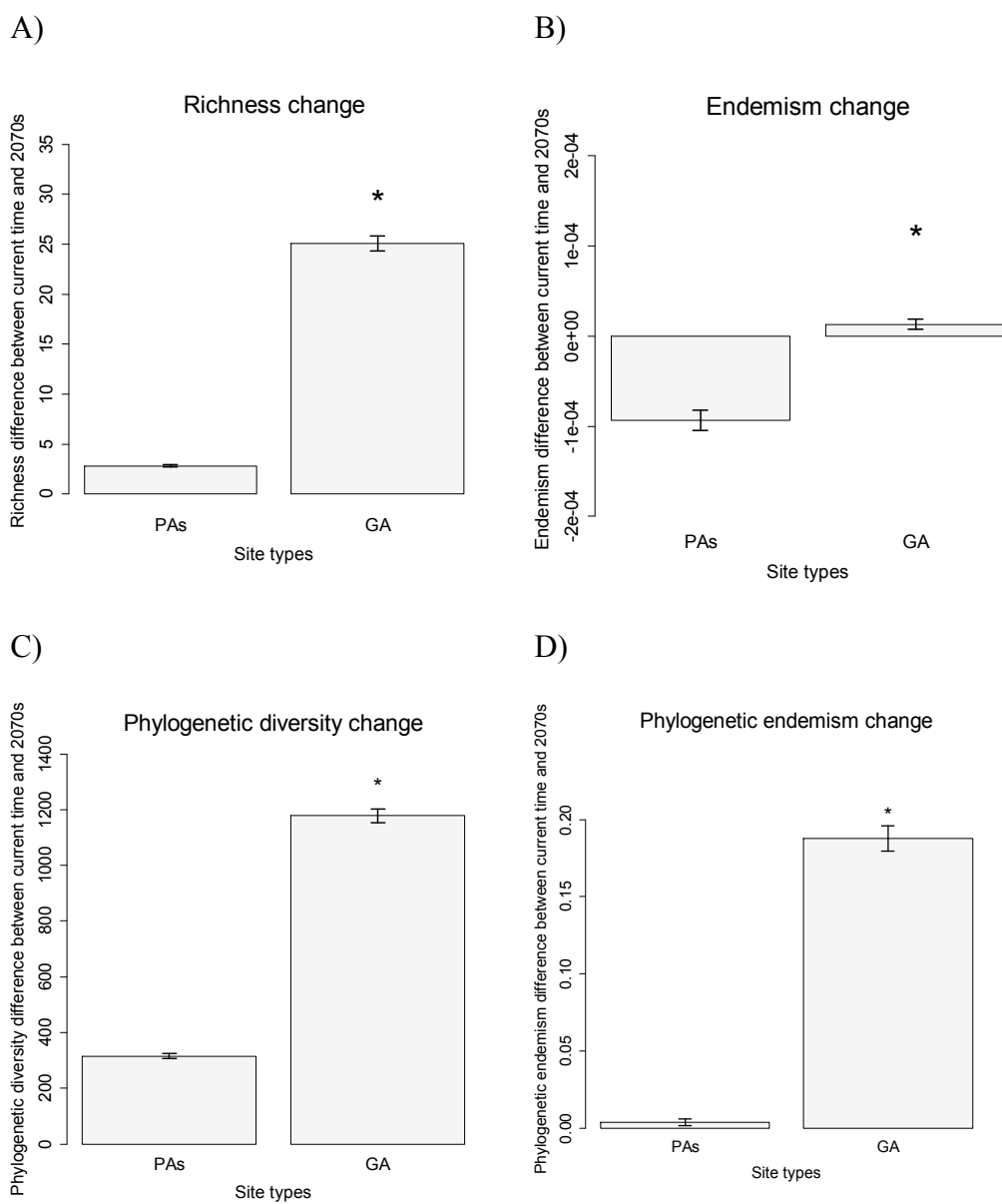
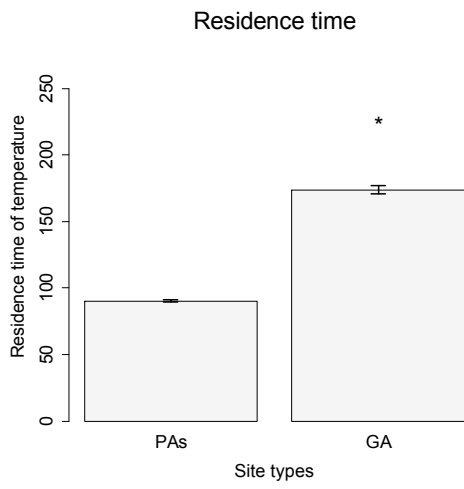


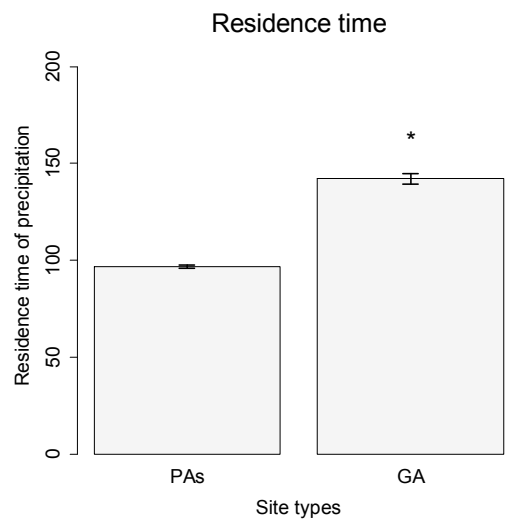
Fig. 2-S10. Comparison of effectiveness of diversity indices in protected areas (PAs) and top 10% conservation gap areas (GA) at $0.1^\circ \times 0.1^\circ$ spatial resolution using occurrence data set. These indices include: potential change of species richness (A), corrected weighted endemism (B), phylogenetic diversity (C), phylogenetic endemism (D), residence time of temperature (E), residence time of precipitation (F), and change of total suitable habitat over time (G). Additionally, comparisons of residence time of climate (H) and change of suitable habitat (I) in species' partial ranges covered by protected versus unprotected areas are provided. Error bars indicate the 95% confidence interval. “*” and “NS” indicate that the comparison between PAs and GAs through a *t*-test is significant ($P < 0.05$) and non-significant ($P > 0.05$) respectively.



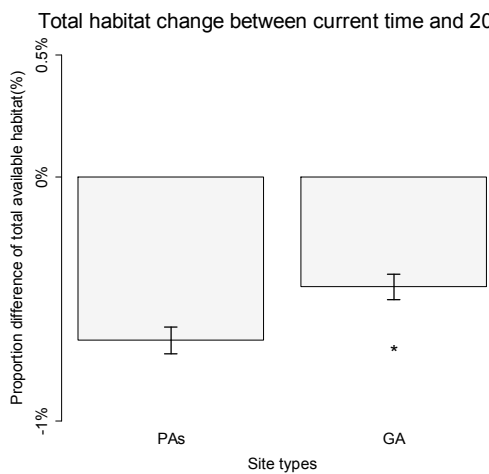
E)



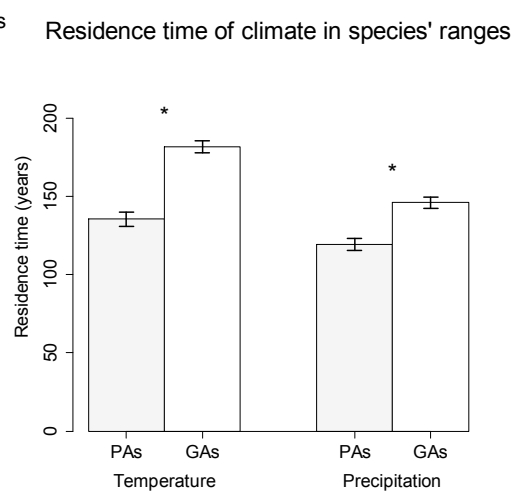
F)



G)



H)



I)

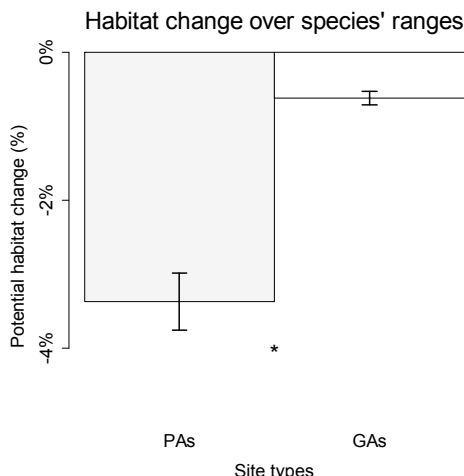
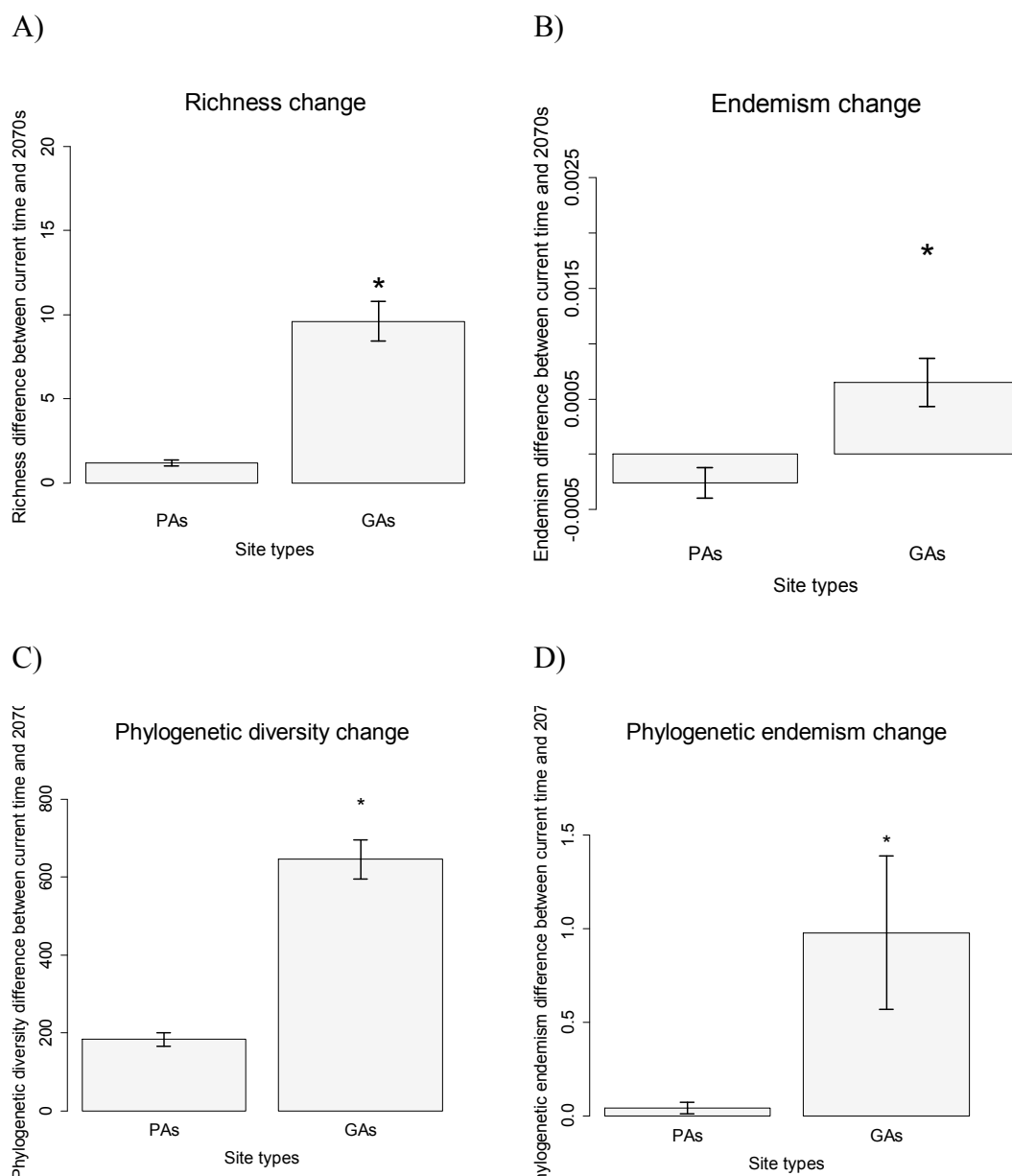
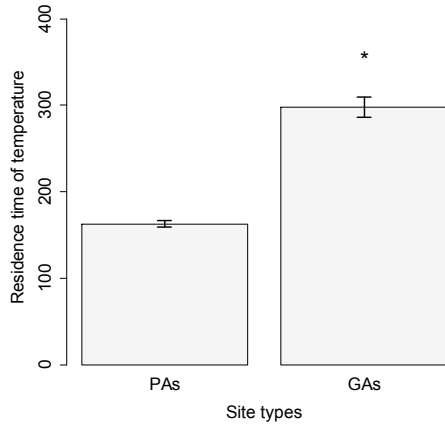


Fig. 2-S11. Comparison of effectiveness of diversity indices in protected areas (PAs) and top 10% conservation gap areas (GAs) at $0.25^\circ \times 0.25^\circ$ spatial resolution using occurrence data set. These indices include: potential change of species richness (A), corrected weighted endemism (B), phylogenetic diversity (C), phylogenetic endemism (D), residence time of temperature (E), residence time of precipitation (F), and change of total suitable habitat over time (G). Additionally, comparisons of residence time of climate (H) and change of suitable habitat (I) in species' partial ranges covered by protected versus unprotected areas are provided. Error bars indicate the 95% confidence interval. “*” and “NS” indicate that the comparison between PAs and GAs through a *t*-test is significant ($P < 0.05$) and non-significant ($P > 0.05$) respectively.



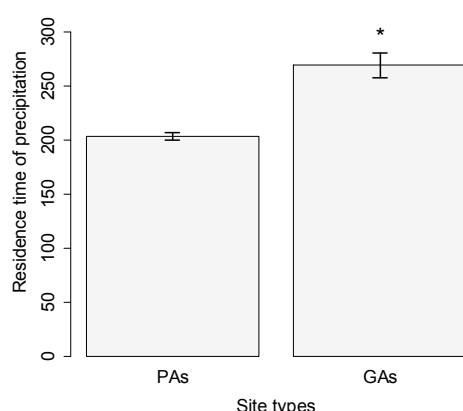
E)

Residence time



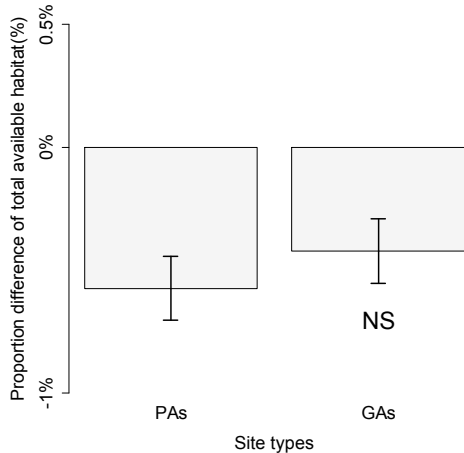
F)

Residence time



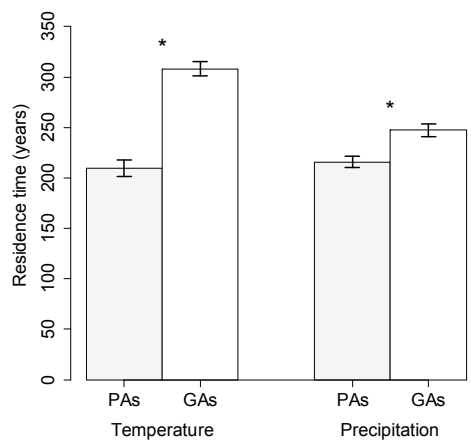
G)

Total habitat change



H)

Residence time of climate in species' ranges



I)

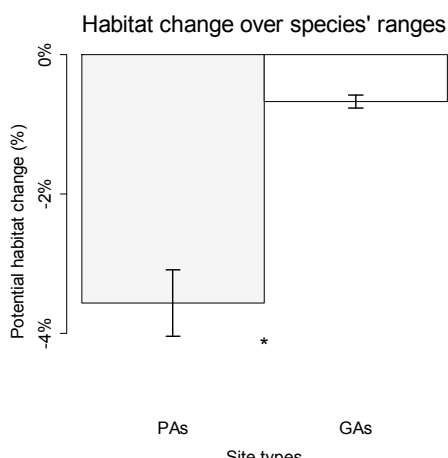
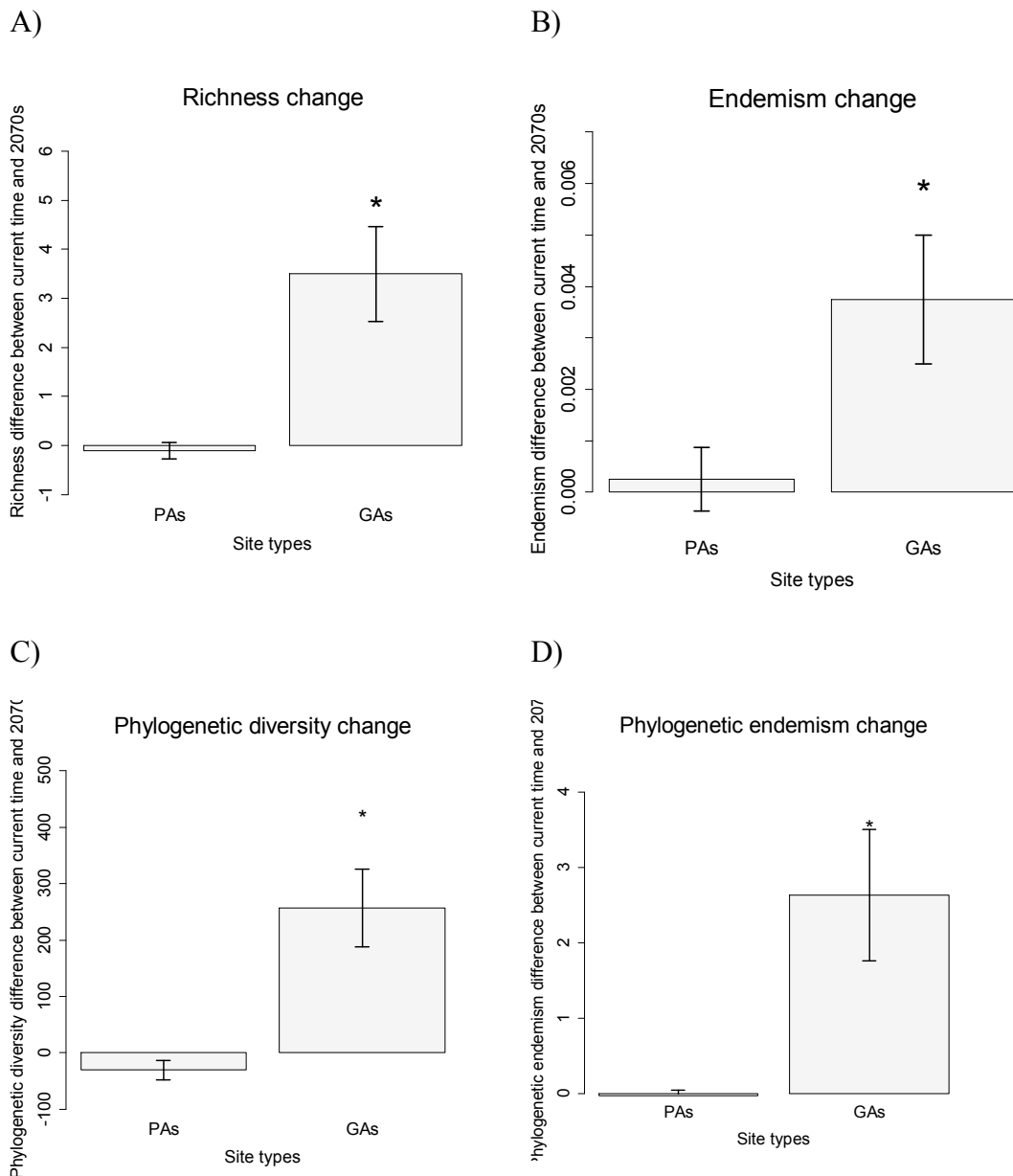
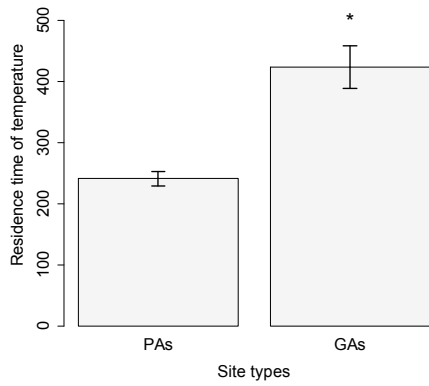


Fig. 2-S12. Comparison of effectiveness of diversity indices in protected areas (PAs) and top 10% conservation gap areas (GAs) at $0.5^\circ \times 0.5^\circ$ spatial resolution using range map data set. These indices include: potential change of species richness (A), corrected weighted endemism (B), phylogenetic diversity (C), phylogenetic endemism (D), residence time of temperature (E), residence time of precipitation (F), and change of total suitable habitat over time (G). Additionally, comparisons of residence time of climate (H) and change of suitable habitat (I) in species' partial ranges covered by protected versus unprotected areas are provided. Error bars indicate the 95% confidence interval. “*” and “NS” indicate that the comparison between PAs and GAs through a *t*-test is significant ($P < 0.05$) and non-significant ($P > 0.05$) respectively.



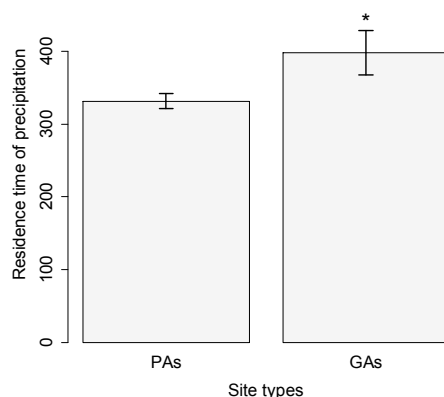
E)

Residence time



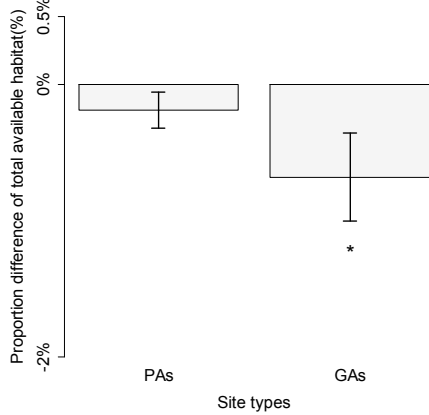
F)

Residence time



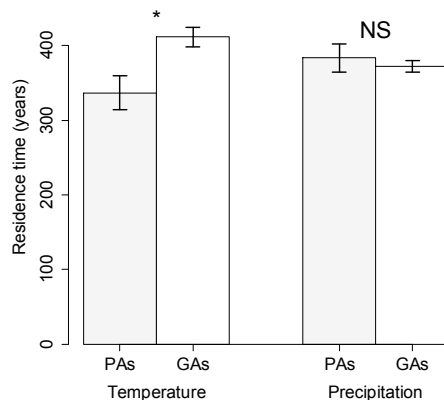
G)

Total habitat change



H)

Residence time of climate in species' ranges



I)

Habitat change over species' ranges

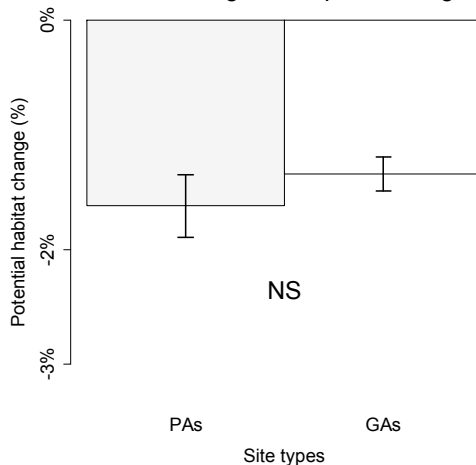
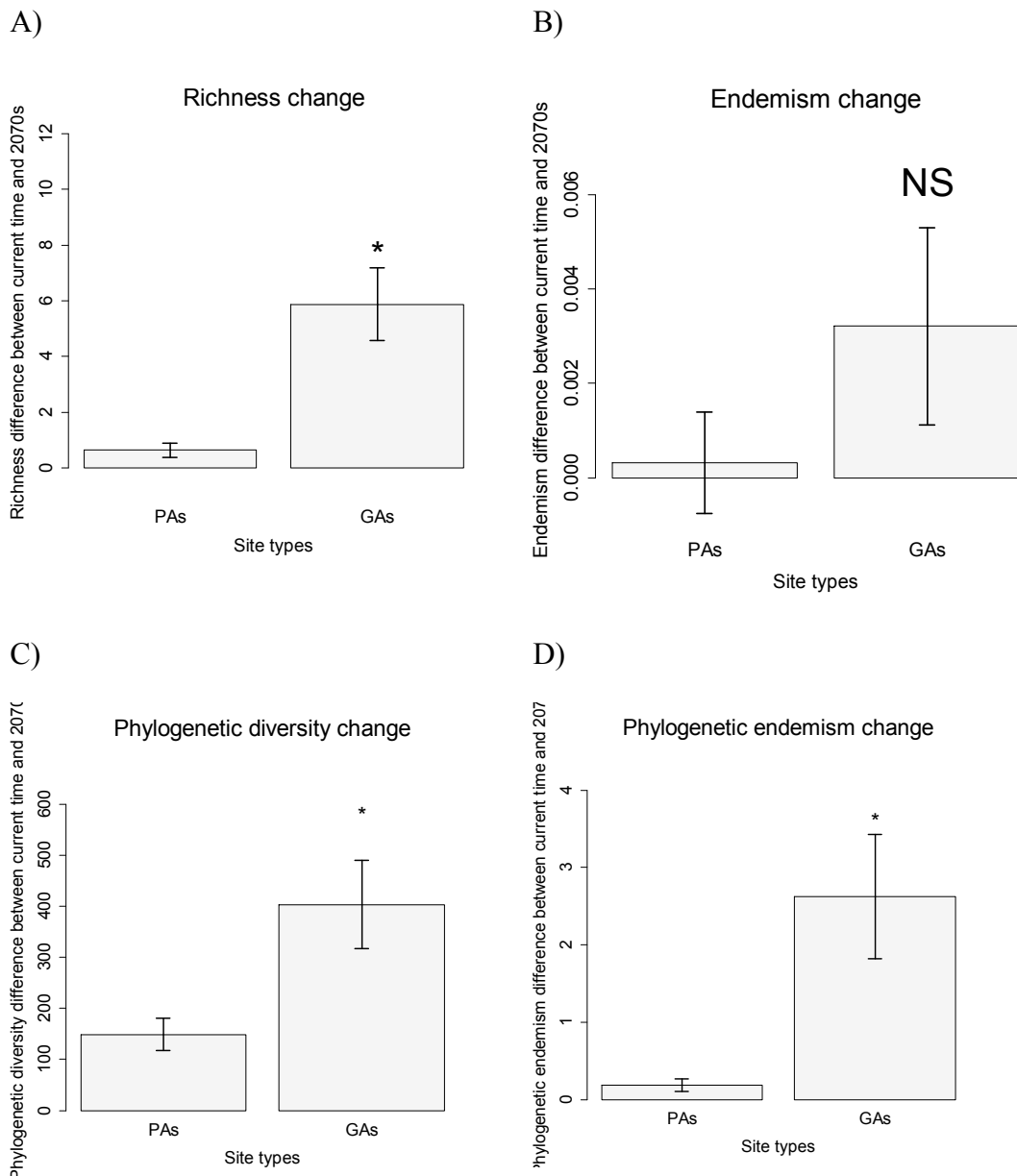
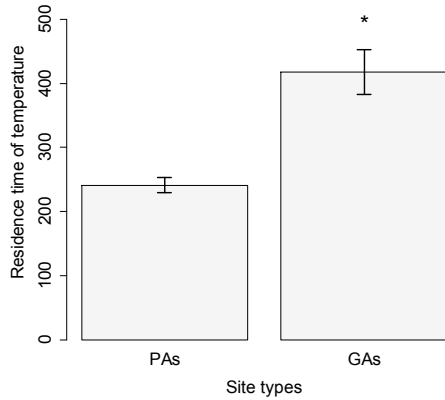


Fig. 2-S13. Comparison of effectiveness of diversity indices in protected areas (PAs) and top 10% conservation gap areas (GAs) at $0.5^\circ \times 0.5^\circ$ spatial resolution using occurrence data set. These indices include: potential change of species richness (A), corrected weighted endemism (B), phylogenetic diversity (C), phylogenetic endemism (D), residence time of temperature (E), residence time of precipitation (F), and change of total suitable habitat over time (G). Additionally, comparisons of residence time of climate (H) and change of suitable habitat (I) in species' partial ranges covered by protected versus unprotected areas are provided. Error bars indicate the 95% confidence interval. “*” and “NS” indicate that the comparison between PAs and GAs through a *t*-test is significant ($P < 0.05$) and non-significant ($P > 0.05$) respectively.



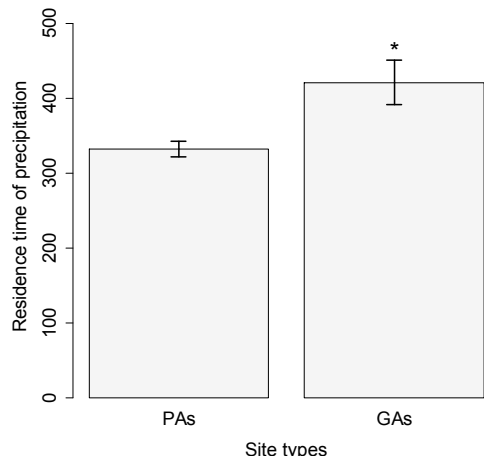
E)

Residence time



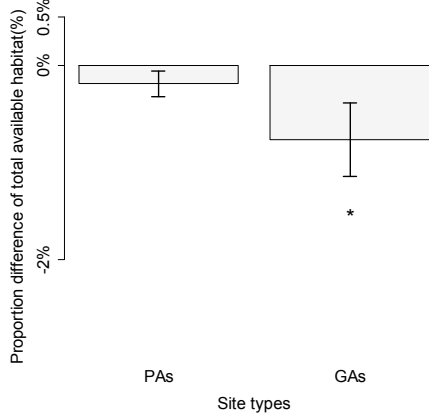
F)

Residence time



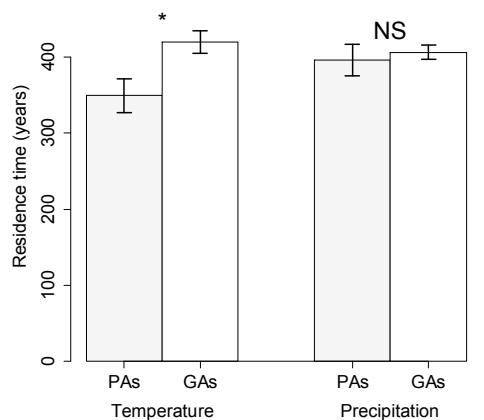
G)

Total habitat change



H)

Residence time of climate in species' ranges



I)

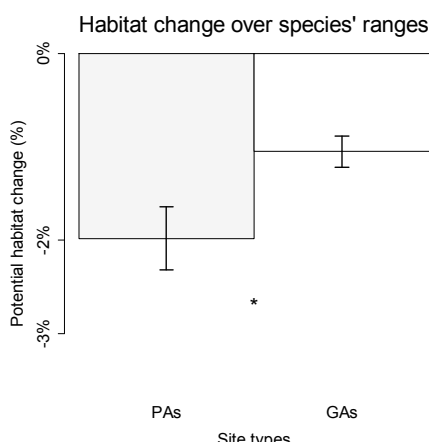
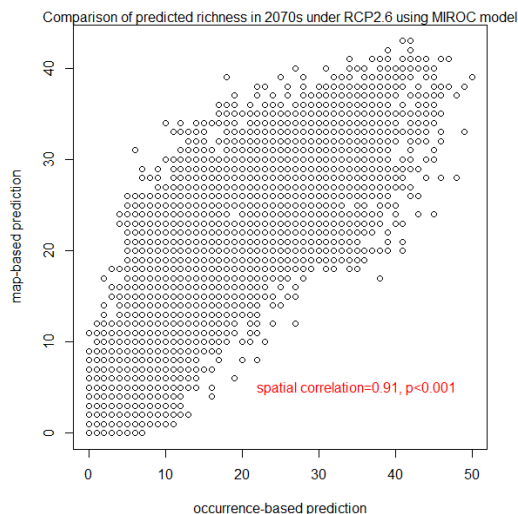
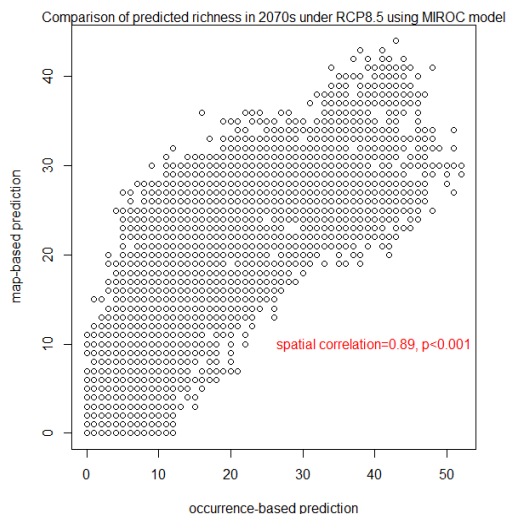


Fig. 2-S14. Comparison on the predicted richness derived from different data sets (range maps versus museum occurrence records) for climatic model MIROC and two RCPs at $0.25^\circ \times 0.25^\circ$ spatial resolution. Spatial correlation test is conducted by using Dutilleul's modified t-test. The comparisons are very similar at the other two spatial scales and all of them are significant and thus are omitted for simplicity.

A)



B)



Chapter 3 Directionality and spacing of climate-driven changes in amphibian ranges in China

Summary

Climate change will lead to shifts in species ranges, and one plausible pattern is a unidirectional poleward movement. Analyses of the range shift patterns (for both the magnitude and directionality) require methods that can measure the shifts in direction, which is a circular variable. In this study, I applied species distribution modeling (SDM) coupled with a post-SDM dispersal simulation to project the suitable ranges of amphibians in China over different time periods in the future. I then evaluated the range shifts of individual species by measuring both the distance and direction using changes in the geometric centroids of their ranges for both the current and the 2090s time periods. Circular statistics were used to determine whether the shifts were directional across the following three very different post-SDM dispersal scenarios: universal dispersal (or unlimited dispersal), deterministic limited dispersal and stochastic limited dispersal. Results showed that while each species had its own shift direction, on average, the range shifts of amphibians in China followed a bidirectional pattern. The amphibians shifted either toward northern or northeastern directions depending on the dispersal scenarios of the species and the climatic data. There was a significant and positive association between the shift distances and the latitudinal centers of the current ranges of amphibians, and the correlation between the shift

distance and the direction of the species was also significant. The shift direction versus the current direction and the magnitude of the climatic velocities in the species' current ranges were negatively correlated, while the shift distance versus the direction and the magnitude of the climate velocities were positively related. These results show that the ranges of amphibians in China will shift significantly in the future towards either northern or northeastern directions due to responses to global change. Furthermore, climate velocity and circular statistics are useful tools for studying the range shifts of species and their directionality.

Introduction

Environmental change, particularly climate change, has the potential to drive dramatic changes in the ranges of species in the form of contractions, expansions, or displacements. Because of the consistent spatial clines in the environment, these rearrangements of species ranges are unlikely to be random in directionality, but rather they follow predictable patterns that are related to geography and topography. Much evidence has shown a general tendency towards poleward movement in many species (Parmesan *et al.*, 1999; Thomas & Lennon, 1999; Hodgson *et al.*, 2015). However, the understanding and prediction of species range shifts, particularly the directional shift, remain limited largely because of the lack of appropriate methods (Dobrowski *et al.*, 2013). Due to this limitation, even the intuitive poleward-shift

hypothesis has recently been challenged in several species of birds (VanDerWal *et al.*, 2013; Gillings *et al.*, 2015).

Species range shifts consist of the following two coherent components: distance and direction. The shift distance, which is a linear variable, can be adequately quantified using conventional correlation and regression techniques and has been commonly studied in the previous literature (Chen *et al.*, 2011; Zhang *et al.*, 2015). However, the shift direction has received notably less attention (Dobrowski *et al.*, 2013; Chen, 2015; Gillings *et al.*, 2015). This is partially because the directional variables (with circular degrees from 0 to 360) require more advanced statistical approaches, as conventional correlation and regression techniques are unsuitable to analyze directional variables without a transformation.

Circular statistics are thus a useful tool: by transforming circular variables to linear variables, correlational and causal relations between linear and directional variables can be explored (Chen, 2015). Such approaches have been established (Upton & Fingleton, 1989; Jammalamadaka & SenGupta, 2001) and have been occasionally applied in some disciplines (Solow *et al.*, 1988; Jammalamadaka & Lund, 2006). Though these approaches might be well known to ecologists, only very recently, these approaches have begun to be used to explore macro-ecological questions in the context of climate change (Du *et al.*, 2015; Gillings *et al.*, 2015; Cunningham *et al.*, 2016).

The range shift of a species is largely confined by the climate velocity (Loaire *et al.*, 2009; VanDerWal *et al.*, 2013; Burrows *et al.*, 2014), which is a useful metric for quantifying the local spatiotemporal displacement rate of climate. This metric calculates the local rate of movement that is required to maintain a consistent climatic environment. Accordingly, populations of species that occur in high climate-velocity areas can be interpreted to be under a greater threat of extinction or subject to greater migration requirements (Roberts & Hamann, 2016) because of the quick disappearance of a suitable local climate. This greater threat could be particularly true for ecotherms (Cunningham *et al.*, 2016) due to the high dependence of their body heat on the ambient temperature. Therefore, the range shift of species, including both the distance and direction, should be correlated with and predicted by the climate velocity. Some studies have supported this hypothesis (Imbach *et al.*, 2013; Comte & Grenouillet, 2015), but the analysis of the relationship between the shift distance and the magnitude of the climate velocity has been limited to assessments of the distance without consideration of the direction. Because both climate velocity and species range shifts are vectors composed of magnitude and direction, circular statistics are required to investigate the associations between them (Chen, 2015).

The future range shift of a species is commonly forecasted using species distribution modeling (SDMs) (Elith & Leathwick, 2009; Franklin, 2009), which require both statistical algorithms and projected climate data. One problem associated with SDMs is that the quality of the climatic data and the different features of the statistical models could influence the predictive consensus of the future range of the

species (Lawler *et al.*, 2006). While many studies have extensively evaluated the uncertainties of climate data (Conlisk *et al.*, 2013), modeling algorithms (Lawler *et al.*, 2006; Pearson *et al.*, 2006) or both (Dormann *et al.*, 2008; Diniz-Filho *et al.*, 2009; Mbogga *et al.*, 2010) in terms of the projection of suitable species ranges, no attention has been paid to the influences of these uncertainties on the shift directionality of species, in which circular statistics are most applicable. Furthermore, the incorporation of post-SDM dispersal modeling will increase the uncertainty of the range-shift patterns. Finally, due to the uncertainties that are present in each modeling step, it is unclear whether there will be consistency between the directionality predicted by the modeling approaches and that predicted by the climate-velocity metrics.

The decline of amphibians is one of the most important contemporary conservation problems (Wake, 2007). Approximately 40% of amphibians globally are at risk of extinction; this percentage is the largest among all vertebrate taxonomic groups (Primack, 2014). Climate-driven range loss is one of the prevailing factors threatening amphibians (Lawler *et al.*, 2009; Forero-Medina *et al.*, 2011; Chen *et al.*, 2016). Previous studies have examined the amphibian range-shift magnitudes relative to the species' abilities to keep pace via dispersal (Early & Sax, 2011; Mokhatla *et al.*, 2015). However, little is known about the broad-scale directionality of the potential range shifts of amphibians and its relationship with climate velocity.

In this work, I combined the SDM approaches with dispersal modeling to investigate the possible range-shift directionality and shift distance under climate forces in amphibians in China. I used circular statistical approaches in this study and evaluated the congruence of these estimated directionalities and distances with the climate-velocity index. I also assessed the impacts of various uncertainties, including climatic scenarios and statistical approaches using post-SDM dispersal modeling, on the consensus of the results.

Materials and Methods

Distributional and climatic data

I obtained the distributional ranges of the amphibian species found in China from the IUCN online spatial database (<http://www.iucnredlist.org/technical-documents/spatial-data>). I then measured the presence and absence of each species over a $0.5^\circ \times 0.5^\circ$ grid system covering the whole land surface of China.

Five bioclimatic predictor variables were chosen after removing collinearity using $VIF \geq 5$ from a set of 19 bioclimatic variables in the online database of the Research Program on Climate Change, Agriculture and Food Security (CCFAS; <http://www.ccafs-climate.org/data/>) for the current time period and for four future 20-years periods (2030s, 2050s, 2070s and 2090s). The chosen variables were isothermality (Bio3), the mean temperature of the wettest quarter (Bio8), precipitation

in the driest month (Bio14), precipitation seasonality (Bio15), and precipitation in the warmest quarter (Bio18). These bioclimatic variables reflect the water requirement and thermal limit of amphibians and thus are critical to determine their diversity and distribution (Chen, 2013).

Species distribution models (SDMs)

The potential distributions of the amphibian species in China were modeled using an ensemble SDM approach (Araujo & New, 2007), which is to average the predictive outputs from three modeling algorithms (generalized additive model, random forest and maximum entropy) using the BIOMOD2 package (Thuiller *et al.*, 2009) in the R platform (R Development Core Team, 2013). The area under the curve of the receiver operating characteristic (AUC) was used to evaluate the model performance (Bellard *et al.*, 2013). Values of the AUC ranged from 0.5 to 1.0, with 1.0 indicating a perfect model fit, and 0.5 representing a fit from a perfectly random model. All SDM approaches predicted the probability of species presence as a response. To convert the probability maps into a binary prediction map, a threshold criterion that maximized the sum of the sensitivity and specificity values was used (Liu *et al.*, 2005, 2011).

Dispersal modeling

To account for the dispersal limitation of each species, a deterministic dispersal scenario was implemented after the distribution modeling. This scenario assumed that each species can expand its range only gradually over time. Thus, for the four future time periods (2030s, 2050s, 2070s and 2090s), buffer zones with widths of 50 km, 100 km, 150 km and 200 km were used to encompass the currently projected ranges of each species. These buffer zones represented the maximum allowed distances of range expansion for the species at different future periods.

I also implemented the following two post-SDM dispersal scenarios for comparison: 1) universal dispersal, in which no dispersal limitation of the species is enforced, which allows the species to disperse anywhere instantaneously; and 2) stochastic dispersal, in which the original probabilistic outputs of SDMs were used to conduct a stochastic dispersal simulation using the MIGCLIM package in R (Engler *et al.*, 2012). Specifically, during the stochastic simulation, the occupancy dynamic (lost and gain) of suitable sites for each species was recorded in a progressive manner over time. As my interest is to study the range shift of amphibians between the current time and 2090s, for each species, I conducted 1000 stochastic simulations and took those sites that were always occupied by the species across the 1000 simulations as the evidence of presence. Such a criterion allowed me to convert suitability maps into binary presence-absence maps directly for species at both the current time and 2090s. Other less restrictive site conditions (like sites are identified to present the species if occupied by the species in 70% of the 1000 simulations) may be applied but will result in the prediction of a larger suitable range for the species.

Climate velocity and range shift of the species

I computed the climate velocity using a standard method (Loaire *et al.*, 2009) in which the spatial gradient was divided by the temporal gradient for an individual climate variable. The temporal gradient of the climate variable was computed from the slope of a linear regression model that was built based on the time sequence of the focused grid cell. The spatial gradient was the mean of the slopes of six pairs of neighboring grids from a 3×3 moving window in which the focused grid cell was located at the center (Loaire *et al.*, 2009; Dobrowski *et al.*, 2013). The velocity of each bioclimatic variable used in the SDMs was computed for each of the eight projected climate datasets. Fig. S1 in the Supporting Information shows the spatial distribution of the climate velocity for the MIROC+RCP8.5 climatic data set. In the analyses, I also excluded those grid cells with large velocity scalar values (top 10%) for each bioclimatic variable, but the results were similar.

To quantify the range shift of each species, I measured the geometric centroids of the current and future (2090s) projected distributional ranges of each species (VanDerWal *et al.*, 2013; Gillings *et al.*, 2015; Huang *et al.*, 2016; Zhang *et al.*, 2017). The shift distances were calculated as the distance between the geometric centroids in the current time and the 2090s, while the shift directions were calculated as the direction of a ray pointing from the current to future geometric centroids. The direction was measured in degrees in a counterclockwise manner with the starting

point at due east (0°). Thus, the corresponding due north, west and south were 90° , 180° and 270° , respectively.

Circular statistics for testing range-shift hypotheses

The most basic circular statistic was used to compute the mean direction of the range shift. For a vector of directions measured in degree $\{\theta_i\}$, the calculation formula for the mean direction is given by

$$\bar{\theta} = \begin{cases} \tan^{-1}(X / Y), & Y \geq 0, X > 0 \\ 180^\circ + \tan^{-1}(X / Y), & Y < 0, \\ 360^\circ + \tan^{-1}(X / Y) & Y > 0, X \leq 0 \end{cases} \quad (3-1)$$

where $X = \sum_i \sin \theta_i$; $Y = \sum_i \cos \theta_i$. Here, I defined the resulting length as $R = \sqrt{X^2 + Y^2}$.

To address the question of whether the amphibian range shift is random, I conducted Rayleigh's test of uniformity (Upton & Fingleton, 1989). This test is based on the criterion that a uniform distribution of the shift directions is less likely if the values of R or R^2 are very large. Thus, a standard way of conducting Rayleigh's test should be as follows (Upton & Fingleton, 1989):

$$T = 2R^2 / n \sim \chi_2^2, \quad (3-2)$$

where n is the number of directions in the analysis and χ_2^2 represents the Chi-squared distribution with 2 degrees of freedom.

A rejection in the test implies that there is a degree of a directional preference in the range change, while a non-rejection implies that a directional distribution is not significantly different from a random distribution. Non-uniform shift directions likely follow von Mises distribution (Upton & Fingleton, 1989), of which the probability density function is given by

$$f(\theta) = \frac{1}{2\pi} I_0(\kappa) \exp\{\kappa \cos(\theta - \bar{\theta})\}, \quad (3-3)$$

where $I_0(\bullet)$ is the modified Bessel function of the first type and order zero. The required parameters for the von Mises distribution are κ and $\bar{\theta}$, where κ measures the dispersion of the range shifting directions, and $\bar{\theta}$ measures the mean direction of the range shift in all species. Higher κ values indicate a lower dispersion of the range shift directions. The von Mises distribution becomes a uniform distribution when κ approaches zero. It is possible to fit the generalized von Mises distribution (Gatto & Jammalamadaka, 2007), but this will complicate the present analyses as the central goal of our study is to know whether overall range shift of species is poleward or not. Moreover, there are no R packages for conducting model comparison and selection on the generalized von Mises distribution, which seems to be an open computational question needed to be addressed (Gatto, 2008).

To determine whether the preferred shift direction was significantly different from due north (90°), I conducted the Stephen-Upton's test (Stephens, 1962; Upton, 1973), which is given by

$$SU = 2\kappa(R - Y_0) \sim \chi^2_1, \quad (3-4)$$

Where $Y_0 = Y \cos \mu_0 + X \sin \mu_0$, X , Y and R were as defined above, χ^2_1 represents the Chi-squared distribution with one degree of freedom and μ_0 represents the expected direction (90° in this case). The corresponding null (H_0) and alternative (H_1) hypotheses are as follows:

H_0 : the mean direction of the range shift of amphibians in China is due north ($=90^\circ$) given a known dispersion parameter κ .

H_1 : the mean direction of the range shift of amphibians is not due north ($\neq 90^\circ$).

If the Stephen-Upton's test was not rejected, I concluded that amphibians in China will move northward as the climate warms.

To determine the relationships between the shift direction and the distance of the species and between the shift direction of the species and the magnitude of the climate velocity within the current range of each species, I applied a circular-linear correlation test (Mardia, 1976; Johnson & Wehrly, 1977; Jammalamadaka & Lund, 2006). The calculation formula is given by

$$l = \sqrt{\frac{r^2(y, \cos \theta) + r^2(y, \sin \theta) - 2r(y, \cos \theta)r(y, \sin \theta)}{1 - r^2(\cos \theta, \sin \theta)}}, \quad (3-5)$$

where y and θ represented the linear (e.g., shift distance) and circular (e.g., shift direction) variables, respectively. Here, $r(y, \cos \theta)$ is the Pearson's product-moment correlation between the quantities y and $\cos \theta$. This linear-circular correlation coefficient is always positive and cannot distinguish between positive and negative

associations (Solow *et al.*, 1988). To overcome this issue and make this correlation comparable to Pearson's correlation, I modified the circular-linear coefficient as

$$l^* = l \times sign(b), \quad (3-6)$$

where b is determined from the following regression model:

$E(y) = b_0 + b \cos(\theta - \phi)$, which contains three unknown parameters, b_0 , b and ϕ . The significance of this correlation was tested using a permutation test by randomly shuffling of y , θ or both (e.g., 1000 times); and the above statistic (3-6) was computed repeatedly. The observed l^* could thus be compared with those that were randomly generated, and the significance of the observed circular-linear correlation value could be tested by assessing how many random values were larger or smaller than the observed value.

To determine the associations between the shifting directions and the latitudinal center of the species' current ranges and between the shift directions and the directions of the climate velocity across the species' current ranges, I conducted a circular-circular correlation test as follows (Fisher & Lee, 1983):

$$c = \frac{\sum \sin(\phi_i - \bar{\phi}) \sin(\psi_i - \bar{\psi})}{\sqrt{\sum \sin(\phi_i - \bar{\phi})^2 \sum \sin(\psi_i - \bar{\psi})^2}}, \quad (3-7)$$

where $\bar{\phi}$ and $\bar{\psi}$ are the mean directions for circular variables $\{\phi_i\}$ and $\{\psi_i\}$, respectively. Here, by the same token, I treated the latitude circle in degrees as a circular variable.

Because I implemented three dispersal scenarios, it was interesting to determine whether the corresponding range-shift directions and distances of the species using different post-SDM dispersal scenarios also presented significant differences. A nonparametric Wheeler-Watson test (Wheeler & Watson, 1964; Upton & Fingleton, 1989) and a conventional analysis of variance (ANOVA) test were used to assess the homogeneity of the shift directions and the distances of the species across the different dispersal scenarios, respectively.

For a multi-sample Wheeler-Watson test, the angles in each separate sample should be merged and ranked from low to high to code them and transform them into new angle values as follows: $\theta^* = \frac{360^\circ}{N} \times R(\theta)$. Here, $R(\theta)$ is the overall rank of angle θ across all angles over samples and N is the total number of angles across all samples. The new angles, θ^* , are used to calculate the resultant length of each individual sample i based on the following formulas: $R_i = \sqrt{X_i^2 + Y_i^2}$; $X_i = \sum_j \sin \theta_j^*$; $Y_i = \sum_j \cos \theta_j^*$. The test statistic (Wheeler & Watson, 1964; Mardia & Spurr, 1973) is then given as

$$W = 2 \sum_{i=1}^s R_i^2 / n_i \sim \chi^2_{2(s-1)}, \quad (3-8)$$

where n_i is the number of angles in sample i , and s is the total number of samples. For a single sample, Equation (3-8) is analogous to Rayleigh's test (Eq. 3-2). All the above-mentioned circular statistics were conducted in R using the 'circular' package (Agostinelli & Lund, 2013).

Results

The distribution of the potential range-shift distances and directions of amphibians in China under climate change can be visualized in circular plots (Fig. 3-1). The mean range-shift direction and its 95% confidence interval across all species were $\bar{\theta} = 80.98^\circ (101.01^\circ, 24.15^\circ)$, $64.14^\circ (55.50^\circ, 11.00^\circ)$ and $85.98^\circ (15.12^\circ, 28.12^\circ)$, for the universal, stochastic, and deterministic dispersal scenarios, respectively. The mean directions were similar across all climatic data sets except for the universal and deterministic dispersal scenarios for BCC+RCP2.6 (Figs. 3-S2 to 3-S4 in the Supplementary Information). The range-shift direction of the amphibians tended to differ across the three dispersal modeling scenarios through the multiple-sample Wheeler-Watson test as follows: $W = 9.08$ ($df=4$; $p=0.06$). The results from the ANOVA tests were consistent with these results (data not shown).

Rayleigh's test supported the non-uniformity of the range-shift directions as follows: the statistics for Rayleigh's test were $T = 87.77$ ($p<0.05$), $T = 64.62$ ($p<0.05$) and $T = 82.19$ ($p<0.05$) for the universal, stochastic, and deterministic dispersal scenarios, respectively. When the von Mises distributions were fitted to the range-shift directions of the species, the corresponding fitted dispersion parameter was $\kappa = 0.916$ for the universal dispersal scenario, $\kappa = 0.776$ for the stochastic limited dispersal scenario and $\kappa = 0.891$ for the deterministic limited dispersal scenario.

For both the universal and deterministic dispersal scenarios, the exact northerly shift hypothesis was supported by the Stephen-Upton's test as follows: $SU=2.38$ ($p=0.123$) in the universal scenario and $SU=0.442$ ($p=0.506$) in the deterministic scenario. These results indicated a due-north range shift of Chinese amphibians under climate change. However, in the stochastic dispersal scenario, the due-north shift hypothesis was rejected ($SU=13.88$; $p<0.05$). The mean direction for the stochastic dispersal scenario was $\bar{\theta} = 64.14^\circ$ (50.00° , 77.00°), indicating a northeastern shift rather than a due-north shift.

The range-shift distances of the amphibians were in many cases significantly and positively correlated with the latitudinal centroids of the species' current ranges (Tables 3-1 and 3-S1 to 3-S3). However, in most cases, the range-shift directions of the species were not significantly associated with the range-shift distances of the species or the latitudinal centroid of the species' current ranges (Tables 3-1 and 3-S1 to 3-S3). An exception occurred in the stochastic dispersal scenario, in which the shift distances and directions were mostly significantly correlated (Tables 3-1 and 3-S1 to 3-S3).

Across the three dispersal scenarios, the relationships between the shift directions of the species and both the mean direction and magnitude of the climate velocities were, for the most part, consistently significant for most bioclimatic variables in the species' current ranges (Figs. 3-2A to 3-2B). Results for the other future climatic datasets

(MIRCO+RCP2.6, BCC+RCP2.6 and BCC+RCP8.5) were similar (Figs. 3-S5 to 3-S7).

Regarding the relationships between the range-shift distances of the species and the climate velocity in the species' current ranges (Figs. 3-2C to 3-2D), the significant correlations could be either positive or negative, particularly between the shift distance and velocity direction (Fig. 3-2C). However, in the stochastic and deterministic dispersal scenarios, it was consistently observed that the correlations between the shift distance of the species and the magnitude of the bioclimatic velocities were significantly positive (Fig. 3-2D).

The relationship between certain bioclimatic velocities and the species' range shifts was very strong (Figs. 3-2 and 3-S5 to 3-S7). For example, the scalar values of the velocities for both Bio8 and Bio18 over the species' current ranges were always negatively related to the shift directions of the species regardless of the climatic data sets and the dispersal scenarios used (Figs. 3-2 and 3-S5 to 3-S7). The velocity directions of Bio8 were always positively correlated with the shift directions of the amphibians (Figs. 3-2 and 3-S5 to 3-S7).

Discussion

Amphibian range-shift patterns

The range shifts of amphibians in China under climate change were projected to have selective directions depending on the climatic data and statistical models used. Furthermore, the range-shift distances of the amphibians presented latitudinal gradients as follows: the shift distances of the amphibians tended to be positively associated with the latitudinal centroids of the species' current ranges (Tables 3-1 and 3-S1 to 3-S3). Consequently, the conservation of amphibians in China under climate change might focus on high-latitude areas because their migration requirements (measured as shift distance) would be higher than those of species inhabiting the southern part of the country.

Poleward range shifts may underestimate the impacts of climate change on the patterns of range shifts of the species (VanDerWal *et al.*, 2013), potentially leading to non-optimal planning of climate-change conservation corridors (Alagador *et al.*, 2016). In my study, the shift directions of different amphibian species in China under climate change were diverse and multidirectional (Figs. 3-1 and 3-S2 to 3-S4). From this perspective of species-specific responses, my results regarding amphibians are consistent with some species of birds, the shift directions of which were also multidirectional (VanDerWal *et al.*, 2013; Gillings *et al.*, 2015), but are inconsistent with other earlier findings that emphasized unidirectional poleward species range shifts (Parmesan *et al.*, 1999; Thomas & Lennon, 1999; Hickling *et al.*, 2005).

There were some considerable differences when the different post-SDM dispersal models were incorporated into the prediction of the species' range-shift, particularly

for the directionality. For example, using the MIROC+RCP8.5 climate data set, the mean shift direction of amphibians derived from the stochastic dispersal scenario was markedly smaller than that derived from the universal and deterministic dispersal scenarios ($\bar{\theta} = 64.14^\circ$). Furthermore, the range-shift directions of species in the stochastic dispersal scenario were significantly associated with the shift distances and latitudinal centroids of the species' current ranges (Table 3-1). Finally, the test of homogeneity of both the range-shift direction and distance was also rejected through the Wheeler-Watson and ANOVA tests.

The uncertainty derived from the predicted climatic data were another factor that affected the consensus of not only the projected suitable ranges found in previous studies (Diniz-Filho *et al.*, 2009; Buisson *et al.*, 2010; Conlisk *et al.*, 2013) but also the shift directionality of the amphibian ranges. For example, when the GCM climate dataset BCC+RCP2.6 was used in building the SDMs, the mean shift directions (and their 95% confidence intervals) of the amphibians were very different, i.e $\bar{\theta} = 17.14^\circ (-3.42^\circ, 37.70^\circ)$, $\bar{\theta} = 69.27^\circ (54.69^\circ, 83.86^\circ)$ and $\bar{\theta} = 357.71^\circ (333.51^\circ, 21.90^\circ)$ for the universal, stochastic and deterministic dispersal scenarios, respectively (Fig. 3-S3).

More work may be performed to provide a deeper understanding of the ecological mechanisms underpinning the range shifts of amphibians under climate change. For example, my study has not yet incorporated biotic interactions into the modeling of the species' suitable ranges. Practically, it should be possible to include biotic

competition in the post-SDM stochastic dispersal modeling if the program MIGCLIM (Engler *et al.*, 2012) is re-coded. Moreover, as a case study, and given that thermal and water limitations have been found to be the two most important factors shaping the distribution of amphibians in the region (Chen, 2013), it is sufficient to assess only the impacts of pure climatic effects on the range shift of amphibians in China; nonetheless, the results are similar to those of other range change studies (VanDerWal *et al.*, 2013; Gillings *et al.*, 2015). Therefore, certain other factors, such as land use change and infectious diseases, are also influential and will affect the future distribution of amphibians, as evidenced in previous studies (Hof *et al.*, 2011; Chen *et al.*, 2016).

Climate velocity as a range-shift predictor

The role of the climate velocity calculations in predicting the range-shift directions and distances of species, at least in terms of their consistency with the SDM projections, may depend on the specifics of the SDM implementation. While I found strong correlations between the velocities of most climatic predictors and the unconstrained projected range-shift distances or directions, many significant correlations were negative (Figs. 3-2A to 3-2B and 3-S5 to 3-S7). This finding is contradictory to my expectations, in which a positive correlation between the shift direction of the species and the climate-velocity direction was anticipated. I suspect that this discrepancy may have resulted from the scale mismatch between the

analyses: specifically, I modeled the range shift of amphibians across the whole land surface of China, while the climate velocity was computed by considering only the local climatic heterogeneity (i.e., climate conditions at neighboring sites). Finally, there were significant positive correlations between the range-shift distances versus the velocity directions and scalar values in many cases (Figs. 3-2C to 3-2D and 3-S5 to 3-S7). Thus, the climate velocity could also predict the shift distances of the species' ranges under climate change. All these findings supported the hypothesis that amphibian populations in areas of high climate velocity would tend to move farther away to find areas with analogous climate.

Introducing dispersal limitations to the SDM projections (a more biologically realistic scenario) result in generally positive correlations between the range-shift projections and the climate-velocity calculations, suggesting that on local scales, the migration requirements due to the climate velocities may be consistent with those generated through much more complex species distribution modeling. In this context, the climate velocity could be used to evaluate the potential migration requirements of species needed to keep pace with climate change.

Applying circular statistics in future range change assessments and conservation

My study provides early evidence obtained using circular statistics at the whole community level that the mean directionality of the range shift of species does not always follow the unidirectional due-north pattern. Under climate change, the overall

shift direction of the amphibian assemblage in China would be bidirectional, with northern and northeastern directions being most likely (Figs. 3-1 and 3-S2 to 3-S4). This novel pattern would be impossible to identify whether circular statistics were not adopted in the analyses. Thus, circular statistics can provide adequate and powerful statistical tests to assess hypotheses regarding the community-level range-shift patterns under climate change.

In general, the application of circular statistics to range-shift analyses is similar to the application of conventional statistical methods to linear data. For simplicity, the following circular statistics might be used to address directional data: the test of non-uniformity, the estimation of the parameters in von Mises distributions, the test of hypotheses that are relevant to the mean direction of the range shift of species, the test of the differences in the mean directions and dispersion parameters across multiple samples, the correlation of linear and circular variables, the correlation of circular and circular variables, circular-circular regression and circular-linear regression (Upton & Fingleton, 1989; Jammalamadaka & SenGupta, 2001). In particular, the new circular-linear correlation coefficient developed here (Eq. 3-6) may be useful in range-shift analyses by accounting for both positive and negative associations.

Using circular statistics, my study (1) reported a novel tri-directionality pattern of range shift for amphibians in China, (2) explicitly showed that the climate velocity can influence both the range-shift directionality and spacing of the species, and (3) demonstrated that the uncertainties from models and data could substantially, if not

oppositely, affect the shift directionality of the species. As a prospect for the future, I advocate for the application of circular statistics to address complex range-shift problems in future studies. For example, it would be interesting to investigate how intrinsic and extrinsic factors, such as life-history traits and habitat fragmentation, and their interactions will further affect the climate-induced range shift of amphibians, particularly for the direction of migration. These types of efforts, in a spatially explicit context, would concretely inform the establishment of conservation corridors built upon the migration pathways of amphibians under the complex interactions of climate, habitat and species traits.

Literature cited

Agostinelli C, Lund U (2013) circular: Circular Statistics R package version 0.4-7.

URL: <http://cran.r-project.org/web/packages/circular>.

Alagador D, Cerdeira J, Araujo M (2016) Climate change, species range shifts and dispersal corridors: an evaluation of spatial conservation models. *Methods in Ecology and Evolution*, **7**, 853–866.

Araujo M, New M (2007) Ensemble forecasting of species distributions. *Trends in Ecology & Evolution*, **22**, 42–47.

Bellard C, Thuiller W, Leroy B, Genovesi P, Bakkenes M, Courchamp F (2013) Will climate change promote future invasions? *Global Change Biology*, **19**, 3740–3748.

Buisson L, Thuiller W, Casajus N, Lek S, Grenouillet G (2010) Uncertainty in ensemble forecasting of species distribution. *Global Change Biology*, **16**, 1145–1157.

Burrows M, Schoeman D, Richardson A et al. (2014) Geographical limits to species range-shifts are suggested by climate velocity. *Nature*, **507**, 492–495.

Chen Y (2013) Habitat suitability modeling of amphibian species in southern and central China: environmental correlates and potential richness mapping. *SCIENCE CHINA Life Sciences*, **56**, 476–484.

Chen Y (2015) Analyze causal relations between climatic and biotic velocities using circular statistics so as to inform biodiversity conservation. *Biodiversity and Conservation*, **24**, 3627–3628.

Chen I, Hill J, Ohlemuller R, Roy D, Thomas C (2011) Rapid range shifts of species associated with high levels of climate warming. *Science*, **333**, 1024–1026.

Chen Y, Zhang J, Jiang J, Nielsen S, He F (2016) Assessing the effectiveness of China's protected areas to conserve current and future amphibian diversity. *Diversity and Distributions*, DOI: 10.1111/ddi.12508.

Comte L, Grenouillet G (2015) Distribution shifts of freshwater fish under a variable climate: comparing climatic, bioclimatic and biotic velocities. *Diversity and Distributions*, **21**, 1014–1026.

Conlisk E, Syphard A, Franklin J, Flint L, Flint A, Regan H (2013) Uncertainty in assessing the impacts of global change with coupled dynamic species distribution and population models. *Global Change Biology*, **19**, 858–869.

Cunningham H, Rissler L, Buckley L, Urban M (2016) Abiotic and biotic constraints across reptile and amphibian ranges. *Ecography*, **39**, 1–8.

Diniz-Filho J, Bini L, Rangel T, Loyola R, Hof C, Nogues-Bravo D, Araujo M (2009) Partitioning and mapping uncertainties in ensembles of forecasts of species turnover under climate change. *Ecography*, **32**, 897–906.

Dobrowski S, Abatzoglou J, Swanson A, Greenberg J, Mynsberge A, Holden Z, Schwartz M (2013) The climate velocity of the contiguous United States during the 20th century. *Global Change Biology*, **19**, 241–251.

Dormann C, Purschke O, Garcia-Marquez J, Lautenbach S, Schroder B (2008) Components of uncertainty in species distribution analysis: a case study of the Great Grey Shrike. *Ecology*, **89**, 3371–3386.

Du Y, Mao L, Queenborough S, Freckleton R, Chen B, Ma K (2015) Phylogenetic constraints and trait correlates of flowering phenology in the angiosperm flora of China. *Global Ecology and Biogeography*, **24**, 928–938.

- Early R, Sax D (2011) Analysis of climate paths reveals potential limitations on species range shifts. *Ecology Letters*, **14**, 1125–1133.
- Elith J, Leathwick J (2009) Species distribution models: ecological explanation and prediction across space and time. *Annual Review of Ecology, Evolution, and Systematics*, **40**, 677–697.
- Engler R, Hordijk W, Guisan A (2012) The MIGCLIM R package-seamless integration of dispersal constraints into projections of species distribution models. *Ecography*, **35**, 872–878.
- Fisher N, Lee A (1983) A correlation coefficient for circular data. *Biometrika*, **70**, 327–332.
- Forero-Medina G, Joppa L, Pimm S (2011) Constraints to species' elevational range shifts as climate changes. *Conservation Biology*, **25**, 163–171.
- Franklin J (2009) *Mapping species distributions: spatial inference and prediction*. Cambridge University Press, Cambridge, 1-320 pp.
- Gillings S, Balmer D, Fuller R (2015) Directionality of recent bird distribution shifts and climate change in Great Britain. *Global Change Biology*, **21**, 2155–2168.
- Hickling R, Roy D, Hill J, Thomas C (2005) A northward shift of range margins in British Odonata. *Global Change Biology*, **11**, 502–506.

- Hodgson J, Bennie J, Dale G, Longley N, Wilson R, Thomas C (2015) Predicting microscale shifts in the distribution of the butterfly *Plebejus argus* at the northern edge of its range. *Ecography*, DOI: 10.1111/ecog.00825.
- Hof C, Araujo M, Jetz W, Rahbek C (2011) Additive threats from pathogens, climate and land-use change for global amphibian diversity. *Nature*, **480**, 516–519.
- Huang Q, Sauer J, Swatantran A, Dubayah R (2016) A centroid model of species distribution with applications to the Carolina wren *Thryothorus ludovicianus* and house finch *Haemorhous mexicanus* in the United States. *Ecography*, **39**, 54–66.
- Gatto R (2008) Some computational aspects of the generalized von Mises distribution. *Statistics and Computing*, **18**, 321-331.
- Gatto R, Jammalamadaka SR (2007) The generalized von Mises distribution. *Statistical Methodology*, **4**, 341-353.
- Imbach P, Locatelli B, Molina L, Ciais P, Leadley P (2013) Climate change and plant dispersal along corridors in fragmented landscapes of Mesoamerica. *Ecology and Evolution*, **3**, 2917–2932.
- Jammalamadaka S, Lund U (2006) The effect of wind direction on ozone levels: a case study. *Environmental and Ecological Statistics*, **13**, 287–298.
- Jammalamadaka S, SenGupta A (2001) *Topics in circular statistics*. World Scientific, Singapore, 1-336 pp.

- Johnson R, Wehrly T (1977) Measures and models for angular correlation and angular-linear correlation. *Journal of the Royal Statistical Society, B*, **39**, 222–229.
- Lawler J, White D, Neilson R, Blaustein A (2006) Predicting climate-induced range shifts: model differences and model reliability. *Global Change Biology*, **12**, 1568–1584.
- Lawler J, Shafer S, Bancroft B, Blaustein A (2009) Projected climate impacts for the amphibians of the Western Hemisphere. *Conservation Biology*, **24**, 38–50.
- Liu C, Berry P, Dawson T, Pearson R (2005) Selecting thresholds of occurrence in the prediction of species distributions. *Ecography*, **28**, 385–393.
- Liu C, White M, Newell G (2011) Measuring and comparing the accuracy of species distribution models with presence-absence data. *Ecography*, **34**, 232–243.
- Loaire S, Duffy P, Hamilton H, Asner G, Field C, Ackerly D (2009) The velocity of climate change. *Nature*, **462**, 1052–1057.
- Mardia K (1976) Linear-circular correlation coefficients and rhythmometry. *Biometrika*, **63**, 403–405.
- Mardia K, Spurr B (1973) Multi-sample tests for multi-modal and axial data. *Journal of the Royal Statistical Society, B*, **35**, 422–436.

Mbogga M, Wang X, Hamann A (2010) Bioclimate envelope model predictions for natural resource management: dealing with uncertainty. *Journal of Applied Ecology*, **47**, 731–740.

Mokhatla M, Rodder D, Measey G (2015) Assessing the effects of climate change on distributions of Cape Floristic Region amphibians. *South African Journal of Science*, **111**, 1–7.

Parmesan C, Ryrholm N, Stefanescu C et al. (1999) Poleward shifts in geographical ranges of butterfly species associated with regional warming. *Nature*, **399**, 579–583.

Pearson R, Thuiller W, Araujo M et al. (2006) Model-based uncertainty in species range prediction. *Journal of Biogeography*, **33**, 1704–1711.

Primack R (2014) *Essentials of conservation biology*, 6th edn. Sinauer Associates, Sunderland, Massachusetts, USA, 1-603 pp.

R Development Core Team (2013) R: A Language and Environment for Statistical Computing, Vienna, Austria. ISBN 3-900051-07-0, URL <http://www.R-project.org>.

Roberts D, Hamann A (2016) Climate refugia and migration requirements in complex landscapes. *Ecography*, DOI: 10.1111/ecog.01998.

- Rogelj J, Meinsahusen M, Knutti R (2012) Global warming under old and new scenarios using IPCC climate sensitivity range estimates. *Nature Climate Change*, **2**, 248–253.
- Solow A, Bullister J, Nevison C (1988) An application of circular-linear correlation analysis to the relationship between Freon concentration and wind direction in Woods Hole, Massachusetts. *Environmental Monitoring and Assessment*, **10**, 219–228.
- Stephens M (1962) Exact and approximate tests for directions. I. *Biometrika*, **49**, 463–477.
- Thomas C, Lennon J (1999) Birds extend their ranges northwards. *Nature*, **399**, 213.
- Thuiller W, Lafourcade B, Engler R, Araujo M (2009) BIOMOD-a platform for ensemble forecasting of species distributions. *Ecography*, **32**, 369–373.
- Upton G (1973) Single sample tests for the von Mises distribution. *Biometrika*, **60**, 87–99.
- Upton G, Fingleton B (1989) *Spatial data analysis by example: categorical and directional data*. Wiley, New York, 1-432 pp.
- VanDerWal J, Murphy H, Kutt A, Perkins G, Bateman B, Perry J, Reside A (2013) Focus on poleward shifts in species' distribution underestimates the fingerprint of climate change. *Nature Climate Change*, **3**, 239–243.

- Wake D (2007) Climate change implicated in amphibian and lizard declines. *Proceedings of the National Academy of Science of the United States of America*, **104**, 8201–8202.
- Watanabe M, Suzuki T, O’ishi R et al. (2010) Improved climate simulation by MIROC5: mean states, variability, and climate sensitivity. *Journal of Climate*, **23**, 6312–6335.
- Wheeler S, Watson G (1964) A distribution-free two-sample test on a circle. *Biometrika*, **51**, 256–257.
- Xin X, Wu T, Li J, Wang Z, Li W, Wu F (2013a) How well does BCC_CSM1.1 reproduce the 20th century climate change over China? *Atmospheric and Oceanic Science Letters*, **6**, 21–26.
- Xin X, Zhang L, Zhang J, Wu T, Fang Y (2013b) Climate Change Projections over East Asia with BCC_CSM1.1 Climate Model under RCP Scenarios. *Journal of the Meteorological Society of Japan*, **91**, 413–429.
- Zhang J, Nielsen S, Stolar J, Chen Y, Thuiller W (2015) Gains and losses of plant species and phylogenetic diversity for a northern high-latitude region. *Diversity and Distributions*, **21**, 1441–1454.
- Zhang J, Nielsen S, Chen Y et al. (2017) Extinction risk of North American seed plants elevated by climate and land-use. *Journal of Applied Ecology*, **54**, 303–312.

Tables

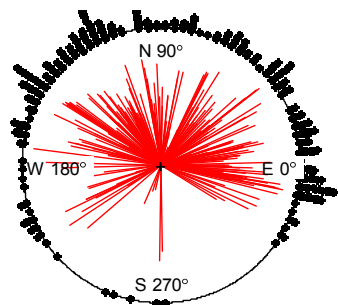
Table 3-1. Associations of range shift distances, directions and latitudinal centroids of current distribution of amphibians of China for MIROC+RCP8.5 climatic data set. Subscripts “a” and “b” denote the circular-circular correlation (Eq. 3-7) and circular-linear correlation (Eq. 3-6) respectively. Significance of the correlations was conducted through a permutation test with 1000 runs.

Universal dispersal scenario		
	Shift distance	Latitudinal centroid
Shift direction	0.120 ^b (p=0.162)	-0.072 ^a (p=0.262)
Shift distance		-0.136 ^b (p=0.096)
Stochastic limited dispersal scenario		
	Shift distance	Latitudinal centroid
Shift direction	-0.174 ^b (p<0.05)	0.147 ^a (p<0.05)
Shift distance		-0.090 ^b (p=0.368)
Deterministic limited dispersal scenario		
	Shift distance	Latitudinal centroid
Shift direction	0.099 ^b (p=0.299)	-0.017 ^a (p=0.76)
Shift distance		0.386 ^b (p<0.05)

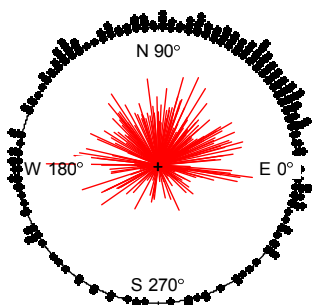
Figures

Fig. 3-1. Shift of range centers of amphibians of China under climate change using universal unlimited dispersal (A), stochastic limited dispersal (B) and deterministic limited dispersal (C) scenarios respectively. Mean directions are given in the titles of the subplots. Length of each line indicates the relative shift distance of geographic centroids of a species' range in the future. Directions are measured in a counterclockwise manner starting from the due East. Individual directions of species are binned together on the circle if they are close to each other to show the density.

A) universal dispersal $\theta=80.98^\circ$



B) stochastic dispersal $\theta=64.14^\circ$



C) deterministic dispersal $\theta=85.98^\circ$

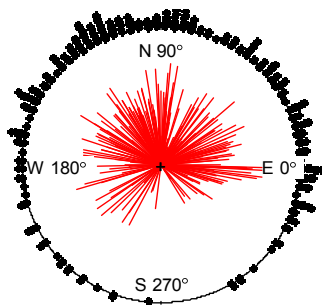
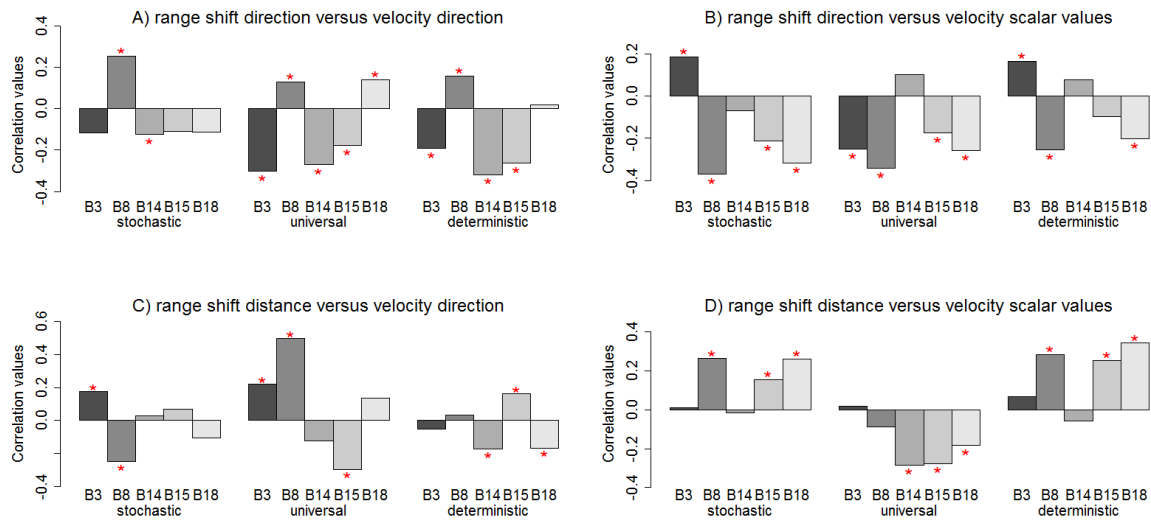


Fig. 3-2. Associations between range shift directions and distances of species versus the mean directions and scalar values of climate velocity in species' current ranges for MIROC+RCP8.5 climatic data set across different dispersal scenarios. Circular-circular correlation (Eq. 3-7), circular-linear correlation (Eq. 3-6) and conventional Pearson's product-moment correlation were applied to subplots A, B-C and D respectively. Significance of the correlations was conducted through a permutation test and marked with asterisks. B3, B8, B14, B15 and B18 indicate the bioclimatic variables Bio3, Bio8, Bio14, Bio 15 and Bio18 respectively.



Supporting Information

Table 3-S1. Associations of range shift distances, directions and latitudinal centroids of current distribution of amphibians of China for MIROC+RCP2.6 climate data set. Subscripts “a” and “b” denote the circular-circular correlation (Eq. 3-7) and circular-linear correlation (Eq. 3-6) respectively. Significance of the correlations was conducted through a permutation test.

Universal dispersal scenario		
	Shift distance	Latitudinal centroid
Shift direction	-0.116 ^b (p=0.182)	-0.181 ^a (p<0.05)
Shift distance		-0.187 ^b (p<0.05)
Stochastic limited dispersal scenario		
	Shift distance	Latitudinal centroid
Shift direction	0.120 ^b (p=0.170)	0.124 ^a (p=0.067)
Shift distance		-0.030 ^b (p=0.899)
Deterministic limited dispersal scenario		
	Shift distance	Latitudinal centroid
Shift direction	0.212 ^b (p<0.05)	0.004 ^a (p=0.918)
Shift distance		0.315 ^b (p<0.05)

Table 3-S2. Associations of range shift distances, directions and latitudinal centroids of current distribution of amphibians of China for BCC+RCP2.6 climate data set. Subscripts “a” and “b” denote the circular-circular correlation (Eq. 3-7) and circular-linear correlation (Eq. 3-6) respectively. Significance of the correlations was conducted through a permutation test.

Universal dispersal scenario		
	Shift distance	Latitudinal centroid
Shift direction	0.139 ^b (p=0.089)	0.033 ^a (p=0.608)
Shift distance		0.043 ^b (p=0.796)
Stochastic limited dispersal scenario		
	Shift distance	Latitudinal centroid
Shift direction	0.160 ^b (p<0.05)	0.077 ^a (p=0.24)
Shift distance		0.193 ^b (p<0.05)
Deterministic limited dispersal scenario		
	Shift distance	Latitudinal centroid
Shift direction	0.068 ^b (p=0.568)	-0.094 ^a (p=0.138)
Shift distance		0.229 ^b (p<0.05)

Table 3-S3. Associations of range shift distances, directions and latitudinal centroids of current distribution of amphibians of China for BCC+RCP8.5 climate data set. Subscripts “a” and “b” denote the circular-circular correlation (Eq. 3-7) and circular-linear correlation (Eq. 3-6) respectively. Significance of the correlations was conducted through a permutation test.

Universal dispersal scenario		
	Shift distance	Latitudinal centroid
Shift direction	0.091 ^b (p=0.353)	-0.040 ^a (p=0.532)
Shift distance		-0.152 ^b (p=0.054)
Stochastic limited dispersal scenario		
	Shift distance	Latitudinal centroid
Shift direction	0.160 ^b (p<0.05)	0.095 ^a (p=0.152)
Shift distance		-0.158 ^b (p<0.05)
Deterministic limited dispersal scenario		
	Shift distance	Latitudinal centroid
Shift direction	-0.092 ^b (p=0.361)	-0.041 ^a (p=0.514)
Shift distance		0.195 ^b (p<0.05)

Fig. 3-S1. Climate velocity magnitude maps of the five bioclimatic variables based on MIROC+RCP8.5 climatic dataset for building SDMs for amphibians of China. Units for the legends are km/year.

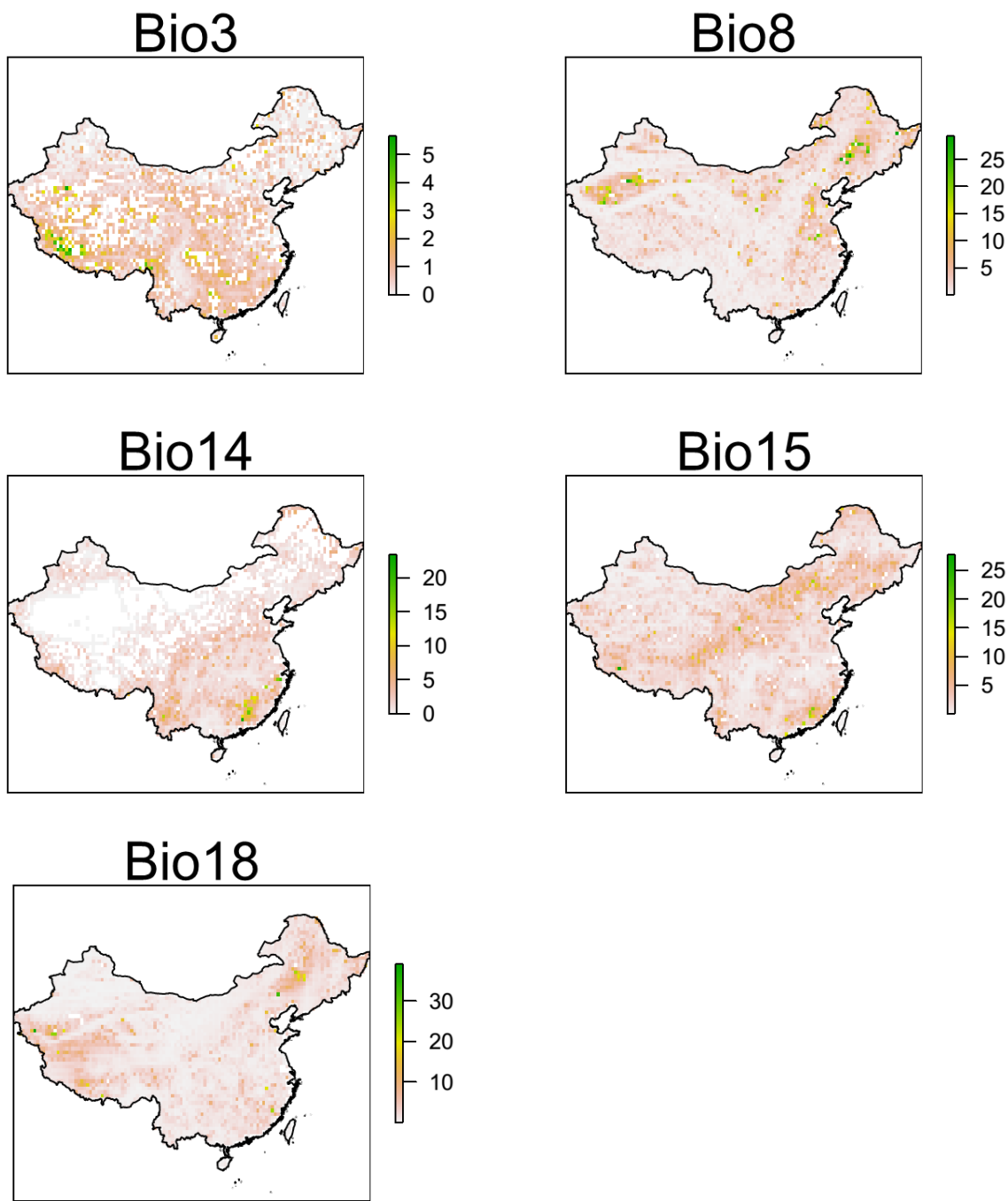


Fig. 3-S2. Shift of range centers of amphibians of China for MIROC+RCP2.6 climatic data set using universal unlimited dispersal (A), stochastic limited dispersal (B) and deterministic limited dispersal (C) scenarios respectively. Mean directions are given in the titles of the subplots. Length of each line indicates the relative shift distance of geographic centroids of a species' range in the future. Directions are measured in a counterclockwise manner starting from the due East. Individual directions are binned together on the circle if they are close to each other.

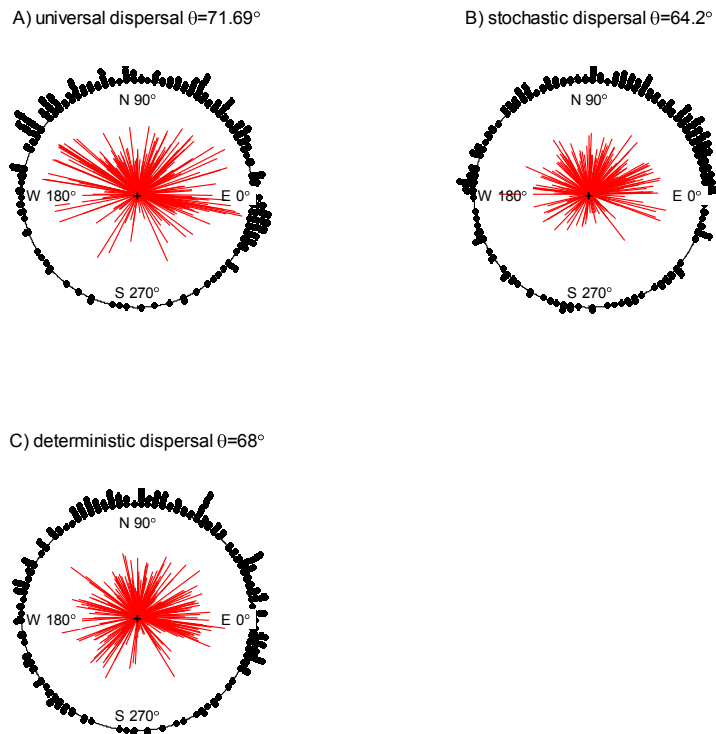


Fig. 3-S3. Shift of range centers of amphibians of China for BCC+RCP2.6 climatic data set using universal unlimited dispersal (A), stochastic limited dispersal (B) and deterministic limited dispersal (C) scenarios respectively. Length of each line indicates the shift distance of geographic centroids of a species' range in the future. Mean directions are given in the titles of the subplots. Length of each line indicates the relative shift distance of geographic centroids of a species' range in the future. Directions are measured in a counterclockwise manner starting from the due East. Individual directions are binned together on the circle if they are close to each other.

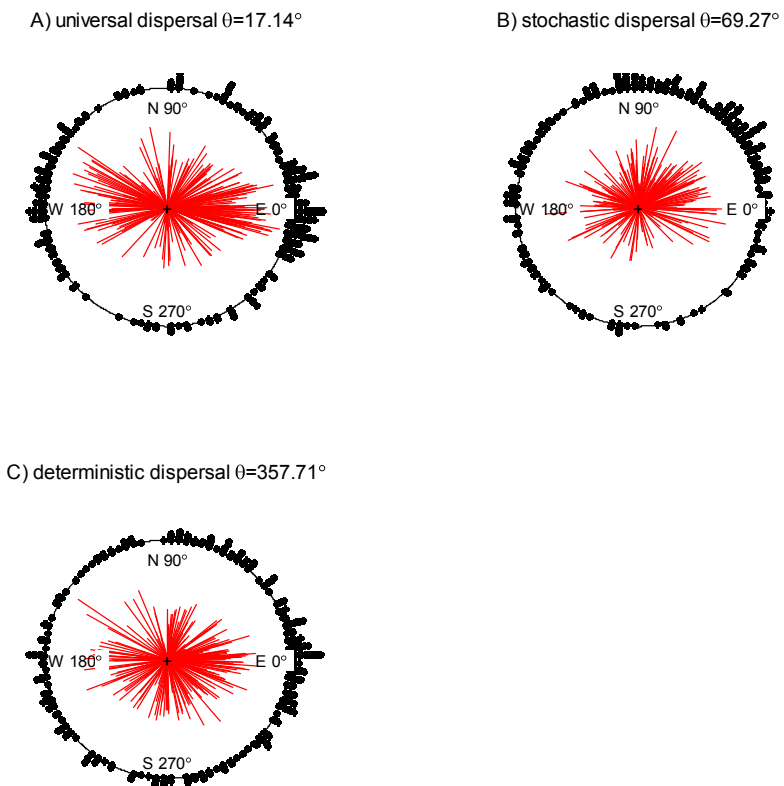


Fig. 3-S4. Shift of range centers of amphibians of China for BCC+RCP8.5 climatic data set using universal unlimited dispersal (A), stochastic limited dispersal (B) and deterministic limited dispersal (C) scenarios respectively. Mean directions are given in the titles of the subplots. Length of each line indicates the relative shift distance of geographic centroids of a species' range in the future. Directions are measured in a counterclockwise manner starting from the due East. Individual directions are binned together on the circle if they are close to each other.

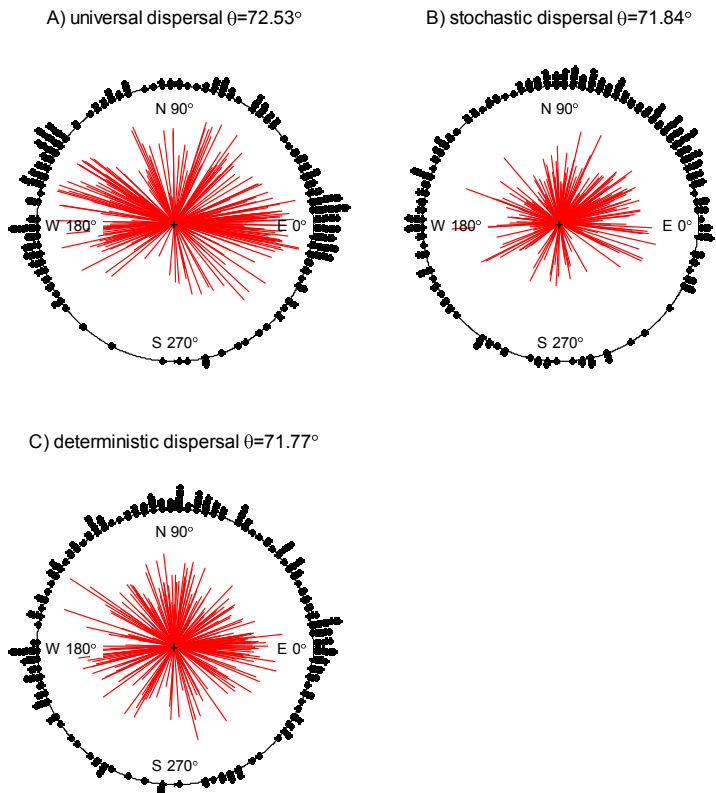


Fig. 3-S5. Associations between range shift direction and shift distance of species versus the mean direction and scalar values of climate velocity in species' current ranges for MIROC+RCP2.6 climatic data set across different dispersal scenarios. Circular-circular correlation (Eq. 3-7), circular-linear correlation (Eq. 3-6) and conventional Pearson's product-moment correlation were applied to subplots A, B-C and D respectively. Significance of the correlations was conducted through a permutation test and marked with asterisks. B3, B8, B14, B15 and B18 indicate the bioclimatic variables Bio3, Bio8, Bio14, Bio 15 and Bio18 respectively.

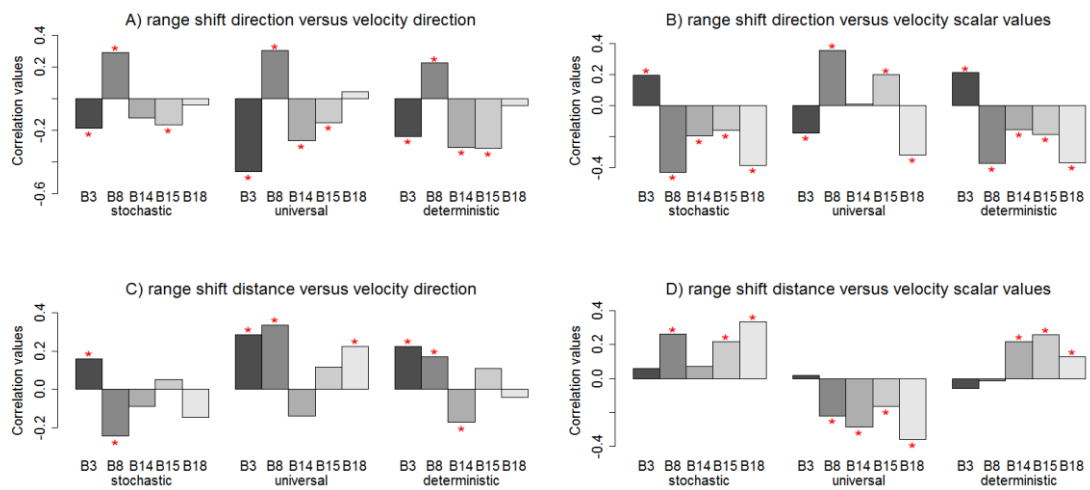


Fig. 3-S6. Associations between range shift direction and shift distance of species versus the mean direction and scalar values of climate velocity in species' current ranges for BCC+RCP2.6 climatic data set across different dispersal scenarios. Circular-circular correlation (Eq. 3-7), circular-linear correlation (Eq. 3-6) and conventional Pearson's product-moment correlation were applied to subplots A, B-C and D respectively. Significance of the correlations was conducted through a permutation test and marked with asterisks. B3, B8, B14, B15 and B18 indicate the bioclimatic variables Bio3, Bio8, Bio14, Bio 15 and Bio18 respectively.

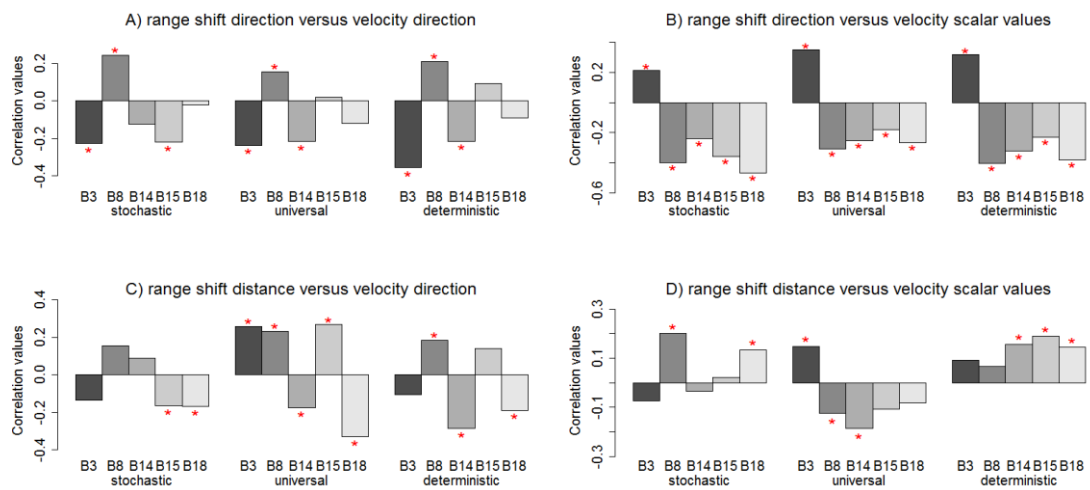
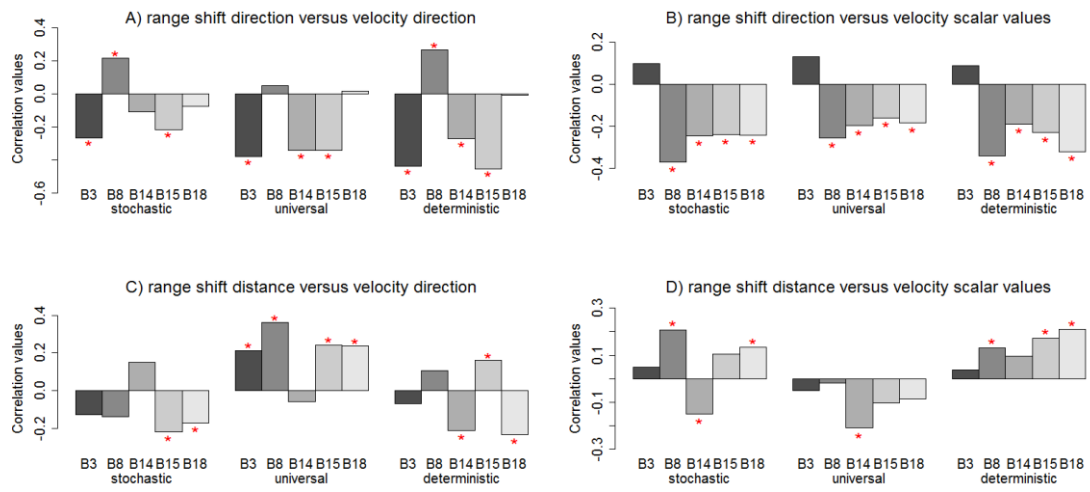


Fig. 3-S7. Associations between range shift direction and shift distance of species versus the mean direction and scalar values of climate velocity in species' current ranges for BCC+RCP8.5 climatic data set across different dispersal scenarios. Circular-circular correlation (Eq. 3-7), circular-linear correlation (Eq. 3-6) and conventional Pearson's product-moment correlation were applied to subplots A, B-C and D respectively. Significance of the correlations was conducted through a permutation test and marked with asterisks. B3, B8, B14, B15 and B18 indicate the bioclimatic variables Bio3, Bio8, Bio14, Bio 15 and Bio18 respectively.



Chapter 4 Predicting the extinction debt for amphibians in China due to deforestation

Summary

Species extinction is a time-delayed process leading to extinction debts. By relying on community-level statistical models, many previous studies have focused on the magnitude of extinction, leaving the cause and extinction (or relaxation) time of these debts understudied. Moreover, these models fail to determine which species are subject to a delayed extinction. They are also very vague in terms of how other ecological processes, such as the Allee effect, contribute to delayed extinction, particularly when extrapolated to the whole ecological community on broad spatial scales. In this study, by applying simple metapopulation models to different future forest datasets, I predicted future time periods triggering the extinction debts of forest-dwelling endemic amphibians in China and measured the relaxation time as the time to half extinction (THE: time required for a species to reduce half of its original occupancy in the forest). The impacts of weak and strong Allee effects on each debt were also assessed. When species occupancy was assumed to be in a steady state at the current time, 27 endemic species were predicted to experience a delayed extinction. This prediction was conservative, and more debts were expected when species occupancy was reduced due to continuing deforestation. The average THEs

for these debt events were 44.9 and 71.8 years in the models with and without Allee effects, respectively. THE was only related to the strength parameter values of the Allee effects. Different metapopulation models predicted the same number of species incurring extinction debts. The spatial distributions of the extinction magnitude and extinction time were largely non-overlapping, thus necessitating the conservation of non-hotspot areas of low debt magnitude in which extinction velocity is increasing quickly. The next 30~50 years, which is the peak period triggering most delayed extinction events, serve as a crucial time window for preventing the debt default of amphibian loss in China by restoring or establishing more forest habitats. Finally, I show that compared with gradual deforestation, rapid and abrupt forest destruction is more detrimental to amphibian conservation.

Introduction

Species extinction is being aggravated worldwide by anthropogenic-related climate change and habitat alteration (Brooks *et al.*, 1999; Thomas *et al.*, 2004; Hanski *et al.*, 2007). Accurately estimating species extinction, thus, becomes a fundamental, if not the most important, target in conservation biology and ecology (Thomas *et al.*, 2004; He, 2012; Hanski *et al.*, 2014). However, it is controversial whether extinction has been accurately estimated (He & Hubbell, 2011). This controversy is further complicated by the fact that biodiversity may not respond to habitat loss and climate

change immediately; this phenomenon can be generally described as an extinction debt (Tilman *et al.*, 1994, 1997; Essl *et al.*, 2015).

A variety of community- and species-based statistical methods have been employed to study the delayed extinction of species (Hanski & Ovaskainen, 2002; Halley & Iwasa, 2011). To date, many previous studies have adopted community-based methods, such as static or dynamic species-area relations (SARs) (Cowlishaw, 1999; Gilbert *et al.*, 2006; Triantis *et al.*, 2010; Wearn *et al.*, 2012; Gibson *et al.*, 2013; Kitzes & Harte, 2015) to estimate the magnitude of extinction debts; these methods usually ignore extinction time (or relaxation time), which is another important component of the debts. More importantly, these methods exclusively measure the number of species and are unable to differentiate the identity of each species subject to debts. In comparison, by studying each species separately, species-based methods, including metapopulation models and species distribution modeling (SDMs) (Tilman *et al.*, 1994; Hanski & Ovaskainen, 2002; Dullinger *et al.*, 2012), are superior to SARs in showing which species will have extinction debts, when each debt event will occur and how much time is required to fulfill the debt process.

Metapopulation models were originally used to quantify extinction debts (Tilman *et al.*, 1994). The relevant theoretical backgrounds, including the latency of the Allee effect, have been well explored in subsequent studies (Tilman *et al.*, 1997; Hanski, 1998; Hanski & Ovaskainen, 2000, 2003; Ovaskainen & Hanski, 2001, 2003; Chen & Hui, 2009). While many empirical studies have extensively applied metapopulation

models to assess extinction debts for various taxa on local spatial scales (Hanski, 1994; Hanski & Gyllenberg, 1997; Hanski *et al.*, 2007; Naujokaitis-Lewis *et al.*, 2013; Schnell *et al.*, 2013), because of the lack of long-term data on habitat change, most of these studies failed to predict the triggering time and relaxation time of the debts.

Species are more prone to a delayed extinction, at least in part, when their populations are near the extinction threshold or their distributional ranges are small. Some interference mechanisms, such as the Allee effect, which describes the positive relationship between the per-capita growth rate and population size of a species (Allee, 1931; Allee & Bowen, 1932; Courchamp *et al.*, 1999), further increase the likelihood of triggering extinction debt. However, as mentioned above, the latent influence of the Allee effect on species extinction has been investigated only in theoretical works (Zhou *et al.*, 2004; Courchamp *et al.*, 2006; Chen & Hui, 2009). No empirical studies have explicitly incorporated the Allee effect, along with climate and land use, into the assessment of extinction of many species on broad spatial scales.

Among the terrestrial vertebrate taxa, amphibians are estimated to have the highest extinction possibility (Stuart *et al.*, 2004), with over 40% of the global taxa being threatened (Wake & Vredenburg, 2008; Primack, 2014). Their high extinction risk is partially caused by their specific habitat requirements, which is a combination of both aquatic and land environments. Amphibian populations are semi-isolated in ponds, streams or other shallow water bodies (Marsh & Trenham, 2001; Smith &

Green, 2005). Naturally, land surfaces serve as dispersal bridges among populations, and the interactions of different populations resemble the dynamics of metapopulations (Marsh & Trenham, 2001). Currently, there is no clear evidence of Allee effects in amphibians (Kramer et al., 2009). However, a recent study (Gaston et al., 2010) showed that a component Allee effect existed in a critically endangered toad species (*Bufo houstonensis*). Given the high extinction risk of global amphibians, it is valuable to evaluate potential Allee effects on amphibian population decline and extinction (Gaston et al., 2010).

In the present study, by applying simple metapopulation models (with or without the Allee effect) to different future forest-change data sets derived from the outputs of earth system models (Hurtt et al., 2011; Reick et al., 2013), I predict the spatiotemporal patterns of extinction debts for forest-dwelling endemic amphibians in China until the end of this century. I study forest-dwelling taxa, which live in forests as a primary habitat and, therefore, are sensitive to forest loss (particularly tree frogs). I work on the amphibians of China because nearly 60% of them are endemic and 30% are threatened (Fei et al., 2012; Chen et al., 2016; Duan et al., 2016). More importantly, the southern part of the country is a hotspot of diversity with a high species richness that is recognized not only at the national level but also on global scales (Stuart et al., 2004; Chen & Bi, 2007; Chen, 2013). Therefore, assessing the extinction debts of amphibians in this region will contribute greatly to global amphibian conservation.

Compared with previous studies using community-based methods (Halley & Iwasa, 2011; Wearn *et al.*, 2012), my study focuses on species-specific estimations of extinction debts. Because of the availability of data on predicted future forest dynamics, my study can appropriately address the following questions on regional spatial scales: Which and how many species will undergo extinction because of forest loss by the end of the century? When will each debt process arise? How much time is required to fulfill half of each debt? Where are the locations of hotspots for high debt magnitude or extinction velocity?

Materials and Methods

Distribution data

The forest-dwelling endemic amphibians in China that were analyzed in the present study were identified based on published monographs (Fei, 1999; Fei *et al.*, 2012) and the IUCN Red List (<http://www.iucnredlist.org/>). To identify the presence and absence of the species in the cells, I overlapped the grid cells covering all terrestrial areas of China with the range map of each endemic amphibian downloaded from the IUCN spatial database (<http://www.iucnredlist.org/technical-documents/spatial-data>) at a $1^\circ \times 1^\circ$ spatial resolution.

Forest data

To construct the annual forest-cover fraction maps in China from the years 1980 to 2100 at the same $1^\circ \times 1^\circ$ spatial resolution, I utilized the harmonized historical land-cover data from 1980 to 2005 and the harmonized future land-cover data from 2005 to 2100, all of which were derived from the Land Use Harmonization (LUH; version 3.1) database (<http://luh.umd.edu/data.php>) (Hurtt *et al.*, 2011).

To account for uncertainty in the forest-cover data, I analyzed and compared

different harmonized future forest-cover datasets from the following four integrated

assessment scenarios of Representative Concentration Pathways (RCPs) (van Vuuren *et al.*, 2011): MESSAGE for RCP 8.5

(<http://webarchive.iiasa.ac.at/Admin/PUB/Documents/WP-95-069.pdf>), AIM for

RCP6.0 (<http://www-iam.nies.go.jp/aim/>), MINICAM for RCP4.5

(http://www.pnl.gov/main/publications/external/technical_reports/PNNL-14337.pdf),

and IMAGE for RCP2.6

(http://themasites.pbl.nl/models/image/index.php>Welcome_to_IMAGE_3.0_Documentation).

For the transition between natural land cover (i.e., forest and natural grassland) and agricultural land cover (i.e., pasture and cropland), I adopted the following transition rules (Jain *et al.*, 2013): 1) a new pasture patch in a grid cell must have been created, in order of priority, from a natural grassland patch or from a forest patch if a natural grassland patch was unavailable in the grid cell (Reick *et al.*, 2013), and 2) a

new cropland patch should have been created from the proportion of the existing forest and natural grassland patches in the grid cell (Brovkin *et al.*, 2013).

Based on the European Space Agency CCI land-cover map from 2005 (<http://www.esa-landcover-cci.org/?q=node/158>), I incorporated the annual changes in the agriculture land from LUH and followed the above-mentioned transition rules to project the future forest-cover maps in a recursively forward manner up to the year 2100 for each of the four scenarios.

Metapopulation models

Levins' metapopulation model, incorporating the dynamics between colonization and extinction of species populations in different patches, is utilized to describe the dynamics of the observed occupancy of an amphibian species i in the forest at time t (Levins, 1969; Levins & Culver, 1971; Hanski, 1999) as

$$\frac{dp_{i,t}}{dt} = c_i p_{i,t} (h_{i,t} - p_{i,t}) - e_i p_{i,t}, \quad (4-1)$$

where $h_{i,t}$ indicates the potential forest occupancy, which is the total forest area size at time t in all the potentially suitable grid cells predicted for the species divided by the area size of the suitable grid cells to standardize its value to $0 \leq h_{i,t} \leq 1$. I utilized species distribution modeling (SDMs) to identify those potentially suitable grid cells at the current time and calculate the percentage of forested habitat within these grid cells for each species. For those species with a few occurrence points (≤ 5), I

employed BIOCLIM, a distance-based SDM algorithm (Busby, 1991; Chen, 2015), with a probability threshold of 0.5 to identify the potentially suitable cells. $p_{i,t}$ indicates the observed forest occupancy, which is the total forest area size at time t in all observed occupied grid cells for the species divided by the area size of all potentially suitable grid cells to standardize its value to $0 \leq p_{i,t} \leq 1$. Moreover, because the observed occupied forested habitat for the species should not be larger than the potentially suitable forested habitat, it can be observed that $p_{i,t} \leq h_{i,t}$. Finally, c_i and e_i are the corresponding colonization and extinction rates for species i (both are non-negative values).

I incorporated both strong and weak Allee effects into the above-mentioned model as follows (Amarasekare, 1998; Zhou & Wang, 2004; Chen & Lin, 2008; Courchamp *et al.*, 2008; Chen & Hui, 2009):

$$\frac{dp_{i,t}}{dt} = c_i p_{i,t} (h_{i,t} - p_{i,t}) \frac{p_{i,t}}{p_{i,t} + a} - e_i p_{i,t} \quad (4-2)$$

$$\frac{dp_{i,t}}{dt} = c_i p_{i,t} (h_{i,t} - p_{i,t}) \frac{p_{i,t} - b}{p_{i,t}} - e_i p_{i,t}, \quad (4-3)$$

where a and b represent the strength parameters of the weak and strong Allee effects, respectively. It was further assumed that the strength of the Allee effect is the same for different species. The difference between the models is as follows: the strong Allee model (Eq. 4-3) has a critical occupancy point ($p_{i,t} = b$), while the weak model (Eq. 4-2) does not.

The forest occupancy of species without the Allee effect was assumed to be in an positive equilibrium by solving the equation (4-1) as

$$p_i^* = h_{i,t} - e_i / c_i . \quad (4-4)$$

Thus, the species occupancy was predicted to reach a positive value if $h_{i,t} > e_i / c_i$. Under this condition, the species could survive in the forest habitat without extinction. However, when $h_{i,t} \leq e_i / c_i$, the observed occupancy of the species at equilibrium is expected to be zero. Under this condition, species extinction is inevitable: the extinction-debt process starts, and the species occupancy will gradually decrease until extermination.

For the metapopulation model with the weak Allee effect (Eq. 4-2), the corresponding stable positive solution is

$$p_i^* = \frac{h_{i,t} - e_i / c_i + \sqrt{(h_{i,t} - e_i / c_i)^2 - 4ae_i / c_i}}{2} . \quad (4-5)$$

For the strong Allee effect (Eq. 4-3), the stable equilibrium point is

$$p_i^* = \frac{b + h_{i,t} - e_i / c_i + \sqrt{(b + h_{i,t} - e_i / c_i)^2 - 4bh_{i,t}}}{2} . \quad (4-6)$$

Because I aimed to predict the future extinction of species based on forest loss, the observed occupancy of each species in the forest at the current time (2000s, $t=0$) was assumed to be in stable equilibrium. Under this assumption, equation (4-4) could be used to estimate the ratio between the species-specific extinction and the colonization rates as

$$e_i / c_i = h_{i,0} - p_i^*, \quad (4-7)$$

where $h_{i,0}$ and p_i^* are the potential and observed forest occupancies of the species at the current time, respectively, which are calculated as

$$\left\{ \begin{array}{l} p_i^* = \frac{\sum_{j=1}^n A_j F_{j,0}}{\sum_{j=1}^m A_j} \\ h_{i,0} = \frac{\sum_{j=1}^m A_j F_{j,0}}{\sum_{j=1}^m A_j} \end{array} \right. , \quad (4-8)$$

where m and n are the total numbers of predicted suitable and observed occupied grid cells, respectively, at the current time. A_j is the area size of grid cell j , and $F_{j,0}$ is the proportion of forested habitat available in grid cell j at the current time (2000s; $t=0$).

The corresponding extinction-colonization ratios for the weak and the strong Allee metapopulation models were calculated as

$$e_i / c_i = \frac{(h_{i,0} - p_i^*) p_i^*}{a + p_i^*} \quad (4-9)$$

and

$$e_i / c_i = \frac{(h_{i,0} - p_i^*)(p_i^* - b)}{p_i^*}, \quad (4-10)$$

where Eq. 4-9 is for the weak Allee model and Eq. 4-10 is the solution for the strong Allee model.

Time point triggering extinction debts

For the different metapopulation models, the specific future time period (measured every twenty years as one time step) τ , in which the extinction-debt process of a species begins, was estimated. The committed loss process is triggered if any of the following quantities becomes negative (Ovaskainen & Hanski, 2002):

$$\left\{ \begin{array}{l} h_{i;\tau} - e_i / c_i \leq 0 \quad (4-11) \\ \frac{h_{i;\tau} - e_i / c_i + \sqrt{(h_{i;\tau} - e_i / c_i)^2 - 4ae_i / c_i}}{2} \leq 0 \quad (4-12) \\ \frac{b + h_{i;\tau} - e_i / c_i + \sqrt{(b + h_{i;\tau} - e_i / c_i)^2 - 4bh_{i;\tau}}}{2} \leq 0 \quad (4-13) \end{array} \right.$$

Here, Eq. 4-11 is for the non-Allee model (Eq. 4-1), Eq. 4-12 is for the weak Allee model (Eq. 4-2), and Eq. 4-13 is for the strong Allee model (Eq. 4-3). In contrast, the species-specific e_i / c_i were estimated using equations (Eqs. 4-7, 4-9 and 4-10) at the current time and were assumed to be constant over time.

Time to half extinction

I computed the time to half extinction (THE, $t_{50}(i;\tau)$) to measure the required time length for species i to reduce half of its original forest occupancy when it begins the extinction-debt process at time point τ (i.e., the time when the inequality (Eq. 4-11) holds). Without the Allee effect, $t_{50}(i;\tau)$ for the metapopulation model (Eq. 4-1) could be calculated analytically (Ovaskainen & Hanski, 2002) as follows:

$$t_{50}(i; \tau)_{\text{No-Allee}} = \frac{\ln \left(\frac{2c_i h_{i;\tau} - c_i p_{i;\tau} - 2e_i}{c_i h_{i;\tau} - p_{i;\tau} c_i - e_i} \right)}{e_i - c_i h_{i;\tau}} \quad (4-14)$$

For the model with the strong Allee effect (Eq. 4-3), the analytical THE is given by

$$t_{50}(i; \tau)_{\text{Strong-Allee}} = \frac{2 \left(\arctan \left(\frac{a_i c_i + c_i h_{i;\tau} - c_i p_{i;\tau} - e_i}{s_i} \right) - \arctan \left(\frac{a_i c_i + c_i h_{i;\tau} - 2c_i p_{i;\tau} - e_i}{s_i} \right) \right)}{s_i} \quad (4-15)$$

where $s_i = \sqrt{-a_i^2 c_i^2 + 2a_i c_i^2 h_{i;\tau}^2 - c_i^2 h_{i;\tau}^2 + 2a_i c_i e_i + 2c_i e_i h_{i;\tau} - e_i^2}$.

For the model with the weak Allee effect (Eq. 4-2), the analytical THE is given by

$$\begin{aligned} t_{50}(i; \tau)_{\text{Weak-Allee}} = & -\frac{1}{2e_i l_i} \left(-2c_i \operatorname{arctanh} \left(\frac{c_i h_{i;\tau} - 2c_i p_{i;\tau} - e_i}{l_i} \right) h_{i;\tau} + 2c_i \operatorname{arctanh} \left(\frac{c_i h_{i;\tau} - c_i p_{i;\tau} - e_i}{l_i} \right) h_{i;\tau} \right) \\ & -\frac{1}{2e_i l_i} \left(\ln(-c_i h_{i;\tau} p_{i;\tau} + c_i p_{i;\tau}^2 + a_i e_i + e_i p_{i;\tau}) l_i \right) \\ & + \frac{1}{2e_i l_i} \left(2 \ln(p_{i;\tau}) l_i + \ln(-\frac{1}{2} c_i h_{i;\tau} p_{i;\tau} + \frac{1}{4} p_{i;\tau}^2 c_i + a_i e_i + \frac{1}{2} e_i p_{i;\tau}) l_i - 2 \ln(\frac{1}{2} p_{i;\tau}) l_i \right) \\ & + \frac{1}{2e_i l_i} \left(2 \operatorname{arctanh} \left(\frac{c_i h_{i;\tau} - 2c_i p_{i;\tau} - e_i}{l_i} \right) e_i - 2 \operatorname{arctanh} \left(\frac{c_i h_{i;\tau} - c_i p_{i;\tau} - e_i}{l_i} \right) e_i \right) \end{aligned} \quad (4-16)$$

where $l_i = \sqrt{c_i^2 h_{i;\tau}^2 - 4a_i c_i e_i - 2c_i e_i h_{i;\tau} + e_i^2}$. Maple code was provided in Appendix 4-1 of the Supporting Information for showing the computation of these formulas.

Finally, to better illustrate the quantities measured in my study, the dynamics of the observed forest occupancy for a single species, which is the time point at which the

extinction-debt process is triggered, the relaxation time required for fulfilling the entire debt process and the corresponding THE are shown in Fig. 4-1.

Comparisons of different metapopulation models and forest scenarios

To predict the extinction debts of amphibians due to future forest loss, four future forest-cover scenario datasets (MESSAGE, AIM, MINICAM and IMAGE) were used in this study. Moreover, three metapopulation models, including the non-Allee model (Eq. 4-1), the weak Allee model (Eq. 4-2) and the strong Allee model (Eq. 4-3), were implemented. Meanwhile, for the weak Allee model (Eq. 4-2), the strength parameter was set to have two values ($a=0.0005$ or 0.001). Finally, the strength parameter could also have two values ($b=0.0005$ or 0.001) for the strong Allee model (Eq. 4-3). Overall, I had five metapopulation models. Therefore, when these models and datasets were combined, I had $4 \times 5 = 20$ groups of results for comparisons.

Results

The future forest changes predicted by the different forest-change scenarios in China until the year 2100 showed remarkable differences (Fig. 4-2). The MESSAGE scenario predicted the most optimistic future, with a very small loss of forest area in China; by contrast, the MINICAM scenario predicted the sharpest decline of forest mid-century, though the forest cover could be recovered to some extent afterwards.

Finally, both the IMAGE and AIM scenarios predicted a gradual decline in forest cover until the end of this century.

Assuming a stationary equilibrium between the forest cover at the current time (2000s) and the species distributions, the estimated extinction-colonization ratios e_i / c_i for different metapopulation models (non-, weak or strong Allee models) of each amphibian species using equations (Eqs. 4-7, 4-9 and 4-10) are summarized in Table S1 in the Supporting Information. The relationship between e_i / c_i in the non-Allee model and the range size of the species measured at the $1^\circ \times 1^\circ$ spatial resolution is presented in Fig. 4-3.

As shown in Fig. 4-3, some species had very small e_i / c_i values even though their relative range sizes are small. Thus, these species were predicted to be more tolerant to forest loss in the future. In contrast, most small-ranged species had high e_i / c_i values (i.e., when their habitat is lost, they are more likely to go extinct). Across the different metapopulation models, usually, the extinction-colonization ratios resulting from the weak and strong Allee models were smaller than those resulting from the non-Allee model (Table S1 in Supporting Information).

In the different forest-cover scenarios and metapopulation models, 27 species were predicted to undergo extinction debts before the end of the 21st century. Across these species, two species, *Rana kunyuensis* and *Nanorana taihangnica* (Table S2 in Supporting Information), were consistently identified as committed to extinction across all 20 combinations of forest scenarios and metapopulation models.

In addition, there were four species with extinction debts that appeared at least 15 times in the 20 sets of results. These species were *Cynops orphicus*, *Batrachuperus londongensis*, *Quasipaa yei* and *Pachyhynobius yunanicus* (Table S2 in Supporting Information). Finally, 15 species were detected to undergo extinction debts no more than 5 times among the 20 sets of results (Table S2 in Supporting Information).

The mid-21st century is a peak period during which extinction debts will be triggered (Fig. 4-4A). The 2050s and the 2070s were the top two time frames for extinction debt triggers, having the largest and second-largest numbers, respectively, of species committed to extinction debts. In the different future forest scenarios (Fig. 4-4B), MINICAM and IMAGE predicted the largest and second largest number of species with extinction debts, respectively. In the different models (Fig. 4-4C), there were no differences in the number of species with extinction debts among the non-, weak and strong Allee models. However, the THEs for species with debts in these models followed a decreasing trend (Fig. 4-4D). Overall, the non-Allee model had a mean THE of 71.8 years, while the weak and strong Allee metapopulation models had mean THEs of 49.1 and 48.9 years, respectively, when the strength parameter of the Allee effects was set to 0.0005. The mean THEs decreased further to 40.9 and 39.8 years in the weak and strong Allee models, respectively, when the strength parameter became 0.001 (Fig. 4-4D).

The spatial patterns for the extinction debts in terms of magnitude and mean relaxation time derived from the suitable ranges for the 27 candidate species are

presented in Fig. 4-5. The magnitude hotspots of the extinction debts (i.e., areas with a number of species committed to extinction ≥ 7) were located in Eastern Tibet, Sichuan Basin, Southeastern Yunnan, the middle part of Guangxi and the Pearl River Delta region in Guangdong (Fig. 4-5A). The averaged THEs of species in non-hotspots of extinction-debt magnitude (i.e., areas with $\text{THE} \leq 70$ years), particularly the southeastern part of the country (Anhui, Jiangxi and Guangdong Provinces), were much shorter than those in magnitude-hotspot areas (Fig. 4-5B).

Discussion

The incorporation of Allee effects into the assessment of species extinction is a necessity (Gaston *et al.*, 2010) because the small-population effect is a key factor driving species extinction (Primack, 2014). In the present study, I explicitly incorporated the Allee effect into simple metapopulation models to detect potential extinction-debt events for amphibians in China resulting from the trade-off between the colonization-extinction dynamic, the future change in forested habitats and the Allee effect. My results showed that if deforestation continues, a considerable number of endemic amphibians are predicted to incur extinction debts, and the THEs of the debt processes followed a decreasing order from the non- and weak to the strong Allee models (Fig. 4-4D).

Surprisingly, there were no differences in the number of species with extinction debts predicted by the different metapopulation models (Fig. 4-4C). This observation

was contradictory to my intuitive expectation that the models that incorporated the Allee effect would predict a higher proportion of endemic species undergoing delayed extinction. For comparison, the different metapopulation models resulted in a significant difference only in the relaxation time of the debts (Fig. 4-4D). As expected, the weak or strong Allee models predicted a much shorter THE. Both models predicted a nearly identical THE if the Allee strength parameters a and b were the same (Fig. 4-4D). Therefore, the relaxation time of debts is dependent only on the numeric value assigned to the strength parameter and is not related to the model structure per se. Moreover, because the computation of THE is related to $h_{i,\tau}$ (see Eqs. 4-14 to 4-16), the change rate of available forested habitat for each species was important to determine the extinction time of species. A greater reduction of forested habitat should predict a shorter extinction time of species when it undergoes delayed extinction.

The relaxation process of extinction debts provides a window of opportunity for conserving biodiversity (Rangel, 2012; Wearn *et al.*, 2012). When each extinction debt relaxes following its activation, measures should be taken to protect the species from final extinction. According to the information of the starting (or triggering) time shown in Fig. 4-4A, the next 30~50 years are a key time window to take measures to prevent amphibian extinction in China. Furthermore, conservation gap areas can be identified through the spatial mapping of the debt magnitudes and THEs. Because of the spatial discordance between the hotspots with a high debt magnitude and extinction velocity (Fig. 4-5), non-hotspot areas with a low debt magnitude are

predicted to lose species more quickly. Therefore, to prevent the debt crisis of species extinction, policymakers should consider refocusing conservation strategies towards low-extinction-risk areas (i.e., the southeastern part of the country) where species will have high extinction velocities (Fig. 4-5B).

The extinction of amphibians is strongly associated with the four integrated assembly scenarios used to predict future forest changes. When comparing the magnitude of the extinction debts across the four forest-cover scenarios (Fig. 4-4B), MINICAM predicted the highest number of extinct amphibians. This result was largely attributed to the fact that the MINICAM scenario predicted the greatest abrupt reduction in forest cover mid-century in comparison to the other forest-cover scenarios (Fig. 4-2). This abrupt forest reduction in approximately the 2040s under the MINICAM scenario would lead to the extinction of some endemic amphibians even though the forest cover could be recovered to a certain intermediate level by the end of the century (Fig. 4-2). In contrast, the forest cover would be predicted to decline very slowly in the MESSAGE scenario (Fig. 4-2), and the number of extinct species was estimated to be the smallest (Fig. 4-4B). These results implied that compared with a gradual forest loss, abrupt and sudden forest destruction events are more detrimental to the conservation of biodiversity.

It is noteworthy that when assessing the possible extinction of species in the future, it is very conservative to assume that the forest occupancy of the species is in a steady equilibrium at the current time (2000s, $t=0$). Such an assumption will result in the

most conservative estimation of the extinction-debt magnitudes because if the occupancy of a species has had a declining tendency due to past- and current-time forest losses, that species will have a higher chance to become extinct as a result of successive forest loss in the future. The extinction risk will further escalate if the additive threats from climate change, invasive species and epidemic diseases, which have not been investigated here, are considered (Hof *et al.*, 2011; Rangel, 2012). Therefore, by implementing the equilibrium assumption, as was performed in my study (i.e., the current species occupancy is in stable equilibrium), the extinction probability of a given species in the future would definitely be lower than if the species occupancy is currently decreasing.

To the best of my knowledge, this synthetic study is the first to (1) estimates the starting time and time length required to fulfill half of the extinction-debt process for each candidate species, (2) differentiates the impacts of the alternative integrated assembly scenarios on the change in future forest and amphibian extinction in China, (3) assesses the confounding influence of the Allee effects, and (4) maps the spatial distributions of the debt events and mean extinction time on a regional scale. These conclusive results convey helpful and tangible take-home messages for conserving Chinese amphibians in forested habitats by identifying the possible species with extinction debts, the conservation time window for preventing the debts and the gap areas with high extinction velocities.

Literature cited

- Allee W (1931) *Animal aggregations, a study in general sociology*. University of Chicago Press, Chicago, IL.
- Allee W, Bowen E (1932) Studies in animal aggregations: mass protection against colloidal silver among goldfishes. *Journal of Experimental Zoology*, **61**, 185–207.
- Amarasekare P (1998) Allee effects in metapopulation dynamics. *American Naturalist*, **152**, 298–302.
- Brooks T, Pimm S, Oyugi J (1999) Time lag between deforestation and bird extinction in tropical forest fragments. *Conservation Biology*, **13**, 1140–1150.
- Brovkin V, Boysen L, Arora V et al. (2013) Effect of anthropogenic land-use and land-cover changes on climate and land carbon storage in CMIP5 projections for the twenty-first century. *Journal of Climate*, **26**, 6859–6881.
- Busby J (1991) BIOCLIM-a bioclimate analysis and prediction system. *Plant Protection Quarterly*, **6**, 8–9.
- Chen Y (2013) Habitat suitability modeling of amphibian species in southern and central China: environmental correlates and potential richness mapping. *Science China Life Sciences*, **56**, 476–484.
- Chen Y (2015) New climate velocity algorithm is nearly equivalent to simple species distribution modeling methods. *Global Change Biology*, **21**, 2832–2833.

- Chen Y, Bi J (2007) Biogeography and hotspots of amphibian species of China: Implications to reserve selection and conservation. *Current Science*, **92**, 480–489.
- Chen L, Hui C (2009) Habitat destruction and the extinction debt revisited: the allee effect. *Mathematical Biosciences*, **221**, 26–32.
- Chen L, Lin Z (2008) The effect of habitat destruction on metapopulations with the Allee-like effect: a study case of Yancheng in Jiangsu Province, China. *Ecological Modelling*, **213**, 356–364.
- Chen Y, Zhang J, Jiang J, Nielsen S, He F (2016) Assessing the effectiveness of China's protected areas to conserve current and future amphibian diversity. *Diversity and Distributions*, DOI: 10.1111/ddi.12508.
- Courchamp F, Clutton-Brock T, Grenfell B (1999) Inverse density dependence and the Allee effect. *TREE*, **14**, 405–410.
- Courchamp F, Angulo E, Rivalan P, Hall R, Signoret L, Bull L, Meinard Y (2006) Rarity value and species extinction: the anthropogenic Allee effect. *PLoS Biology*, **4**, e415.
- Courchamp F, Berec J, Gascoigne J (2008) *Allee effects in ecology and conservation*. Oxford University Press, New York, USA.
- Cowlishaw G (1999) Predicting the pattern of decline of African primate diversity: an extinction debt from historical deforestation. *Conservation Biology*, **13**, 1183.

Duan R, Kong X, Huang M, Varela S, Ji X (2016) The potential effects of climate change on amphibian distribution, range fragmentation and turnover in China. *PeerJ*, **4**, e2185.

Dullinger S, Gatringer A, Thuiller W et al. (2012) Extinction debt of high-mountain plants under twenty-first-century climate change. *Nature Climate Change*, **2**, 619–622.

Essl F, Dullinger S, Rabitsch W, Hulme P, Pysek P, Wilson J, Richardson D (2015) Delayed biodiversity change: no time to waste. *Trends in Ecology and Evolution*, In press.

Fei L (1999) *Atlas of amphibians of China*. Henan Science and Technology Press, Zhengzhou, China.

Fei L, Ye C, Jiang J (2012) *Colored atlas of Chinese amphibians and their distributions*. Sichuan Science & Technology Press, Chengdu, China, 1-619 pp.

Gaston M, Fuji A, Weckerly F, Forstner M (2010) Potential component Allee effects and their impact on wetland management in the conservation of endangered Anuarans. *PLoS ONE*, **5**, e10102.

Gibson L, Lynam A, Bradshaw C et al. (2013) Near-complete extinction of native small mammal fauna 25 years after forest fragmentation. *Science*, **341**, 1508–1510.

Gilbert B, Laurance W, Leigh E, Nascimento H (2006) Can neutral theory predict changes in Amazonian forest fragments? *American Naturalist*, **168**, 304–317.

Halley J, Iwasa Y (2011) Neutral theory as a predictor of avifaunal extinctions after habitat loss. *PNAS*, **108**, 2316–2321.

Hanski I (1994) A practical model of metapopulation dynamics. *Journal of Animal Ecology*, **63**, 151–162.

Hanski I (1998) Metapopulation dynamics. *Nature*, **396**, 41–49.

Hanski I (1999) *Metapopulation ecology*. Oxford University Press, Oxford.

Hanski I, Gyllenberg M (1997) Uniting two general patterns in the distribution of species. *Science*, **275**, 397–400.

Hanski I, Ovaskainen O (2000) The metapopulation capacity of a fragmented landscape. *Nature*, **404**, 755–758.

Hanski I, Ovaskainen O (2002) Extinction debt at extinction threshold. *Conservation Biology*, **16**, 666–673.

Hanski I, Ovaskainen O (2003) Metapopulation theory for fragmented landscapes. *Theoretical Population Biology*, **64**, 119–127.

Hanski I, Koivulehto H, Cameron A, Rahagalala P (2007) Deforestation and apparent extinctions of endemic forest beetles in Madagascar. *Biology letters*, **3**, 344–347.

Hanski I, Zurita G, Bellocq M, Rybicki J (2014) Species-fragmented area relationship. *PNAS*, doi: 10.1073/pnas.1311491110.

- He F (2012) Area-based assessment of extinction risk. *Ecology*, **93**, 974–980.
- He F, Hubbell S (2011) Species-area relationships always overestimate extinction rates from habitat loss. *Nature*, **473**, 368–371.
- Hof C, Araujo M, Jetz W, Rahbek C (2011) Additive threats from pathogens, climate and land-use change for global amphibian diversity. *Nature*, **480**, 516–519.
- Hurtt G, Chini L, Frolking S et al. (2011) Harmonization of land-use scenarios for the period 1500-2100: 600 years of global gridded annual land-use transitions, wood harvest, and resulting secondary lands. *Climatic Change*, **109**, 117–161.
- Jain A, Meiyappan P, Song Y, House J (2013) CO₂ emissions from land-use change affected more by nitrogen cycle, than by the choice of land-cover data. *Global Change Biology*, **19**, 2893–2906.
- Kramer AM, Dennis B, Liebhold AM, Drake JM (2009) The evidence for Allee effects. *Population Ecology*, **51**, 341–354.
- Kitzes J, Harte J (2015) Predicting extinction debt from community patterns. *Ecology*, **96**, 2127–2136.
- Levins R (1969) Some demographic and genetic consequences of environmental heterogeneity for biological control. *Bulletin of Entomology Society of America*, **15**, 237–240.
- Levins R, Culver D (1971) Regional coexistence of species and competition between rare species. *PNAS*, **68**, 1246–1248.

- Marsh D, Trenham P (2001) Metapopulation dynamics and amphibian conservation. *Conservation Biology*, **15**, 40–49.
- Naujokaitis-Lewis I, Curtis J, Tischendorf L, Badzinski D, Lyndsay K, Fortin M (2013) Uncertainties in coupled species distribution-metapopulation dynamics models for risk assessments under climate change. *Diversity and Distributions*, **19**, 541–554.
- Ovaskainen O, Hanski I (2001) Spatially structured metapopulation models: global and local assessment of metapopulation capacity. *Theoretical Population Biology*, **60**, 281–302.
- Ovaskainen O, Hanski I (2002) Transient dynamics in metapopulation response to perturbation. *Theoretical Population Biology*, **61**, 285–295.
- Ovaskainen O, Hanski I (2003) Extinction threshold in metapopulation models. *Annales Zoologici Fennici*, **40**, 81–97.
- Primack R (2014) *Essentials of conservation biology*, 6th edn. Sinauer Associates, Sunderland, Massachusetts, USA, 1-603 pp.
- Rangel T (2012) Amazonian extinction debts. *Science*, **337**, 162–163.
- Reick C, Raddatz T, Brovkin V, Gayler V (2013) Representation of natural and anthropogenic land cover change in MPI-ESM. *Journal of Advances in Modeling Earth Systems*, **5**, 459–482.

- Schnell J, Harris G, Pimm S, Russell G (2013) Estimating extinction risk with metapopulation models of large-scale fragmentation. *Conservation Biology*, **27**, 520–530.
- Smith M, Green D (2005) Dispersal and the metapopulation paradigm in amphibian ecology and conservation: are all amphibian populations metapopulations? *Ecography*, **28**, 110–128.
- Stuart S, Chanson J, Cox N, Young B, Rodrigues A, Fischman D, Waller R (2004) Status and trends of amphibian declines and extinctions worldwide. *Science*, **306**, 1783–1786.
- Thomas C, Cameron A, Green R et al. (2004) Extinction risk from climate change. *Nature*, **427**, 145–148.
- Tilman D, May R, Lehman C, Nowak M (1994) Habitat destruction and the extinction debt. *Nature*, **371**, 65–66.
- Tilman D, Lehman C, Yin C (1997) Habitat destruction, dispersal, and deterministic extinction in competitive communities. *American Naturalist*, **149**, 407–435.
- Triantis K, Borges P, Ladle R et al. (2010) Extinction debt on oceanic islands. *Ecography*, **33**, 285–294.
- van Vuuren D, Edmonds J, Kainuma M et al. (2011) The representative concentration pathways: an overview. *Climatic Change*, **109**, 5–31.

- Wake D, Vredenburg V (2008) Are we in the midst of the sixth mass extinction? A view from the world of amphibians. *PNAS*, **105**, 11466–11473.
- Wearn O, Reuman D, Ewers R (2012) Extinction debt and windows of conservation opportunity in the Brazilian Amazon. *Science*, **337**, 228–232.
- Zhou S, Wang G (2004) Allee-like effects in metapopulation dynamics. *Mathematical Biosciences*, **189**, 103–113.
- Zhou S, Liu C, Wang G (2004) The competitive dynamics of metapopulations subject to the Allee-like effect. *Theoretical Population Biology*, **65**, 29–37.

Figures

Fig. 4-1. Extinction-debt process of the observed occupancy of a species and the corresponding quantities quantified by the metapopulation models used in the present study.

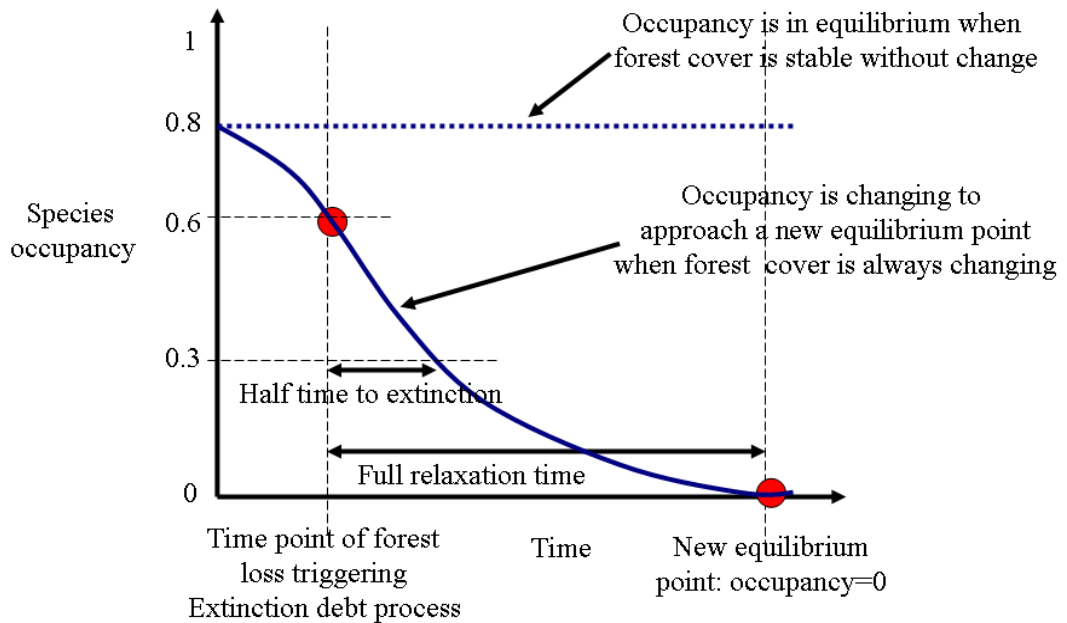


Fig. 4-2. Projected future forest-cover change in China based on the harmonized data sets from the four integrated assembly scenarios.

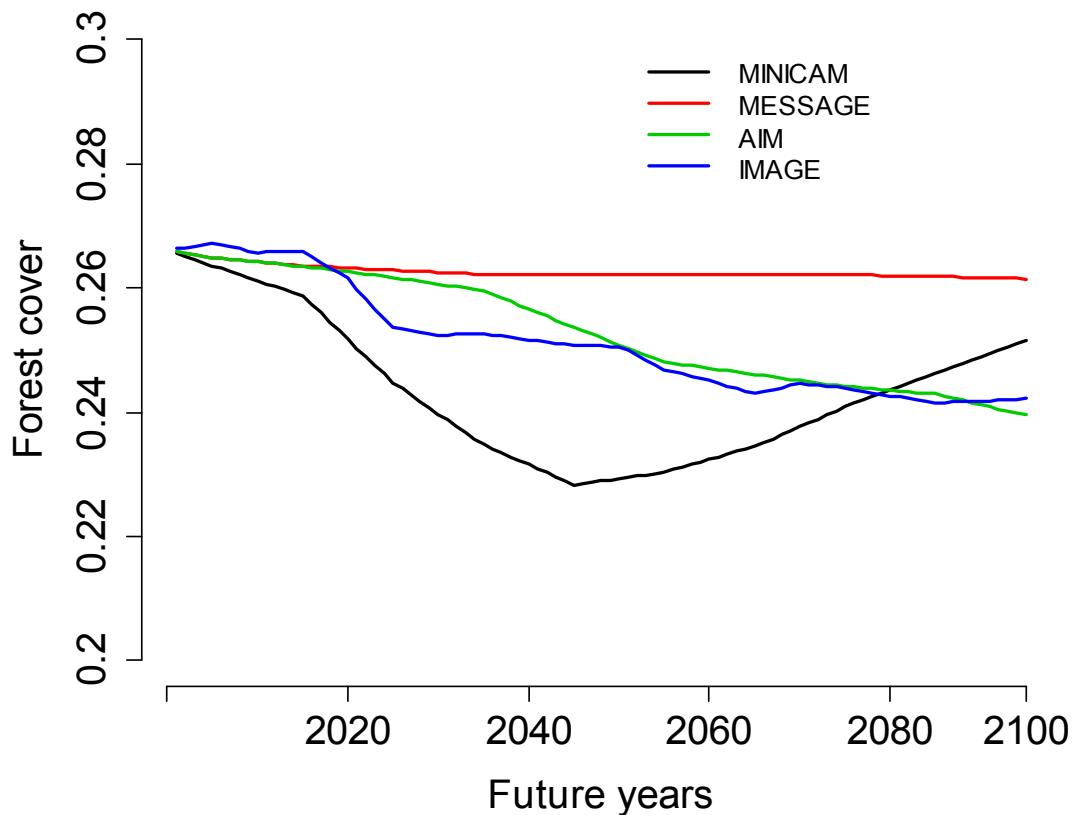


Fig. 4-3. Relationship between the estimated extinction-colonization ratio (e/c) and the range size observed for the amphibian species in the non-Allee metapopulation model.

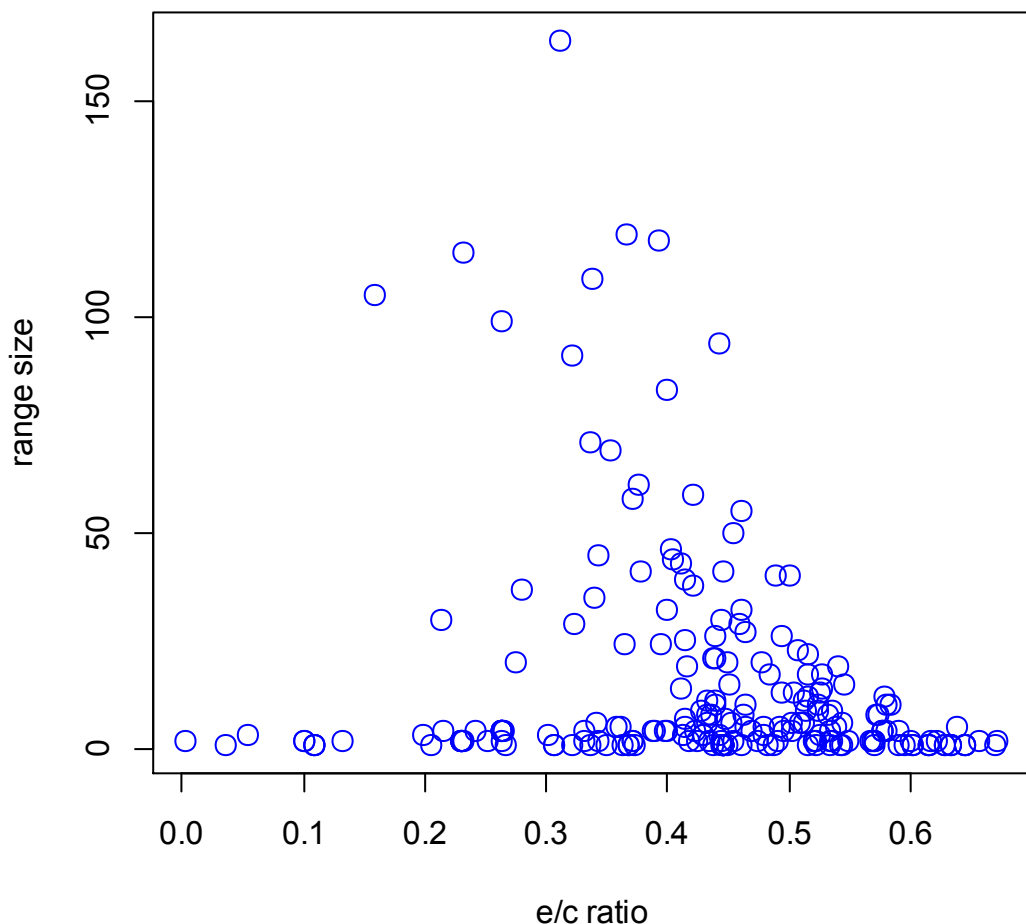


Fig. 4-4. Comparisons of the number and relaxation time of species subjected to extinction-debt processes in different future time periods (measured every twenty years) (A), under different forest-cover scenarios (B) or using different metapopulation models (C). Finally, a comparison of the time to half extinction in the different metapopulation models is presented (D). Error bars indicate the standard errors; the letters “a-c” above the bars in (D) indicate the significance of the model indicated by two-sample *t*-tests.

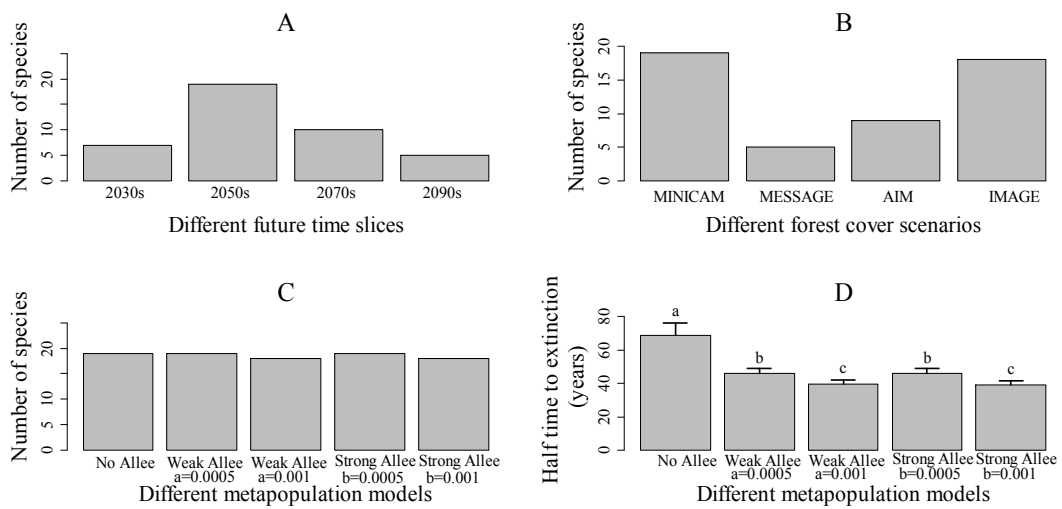
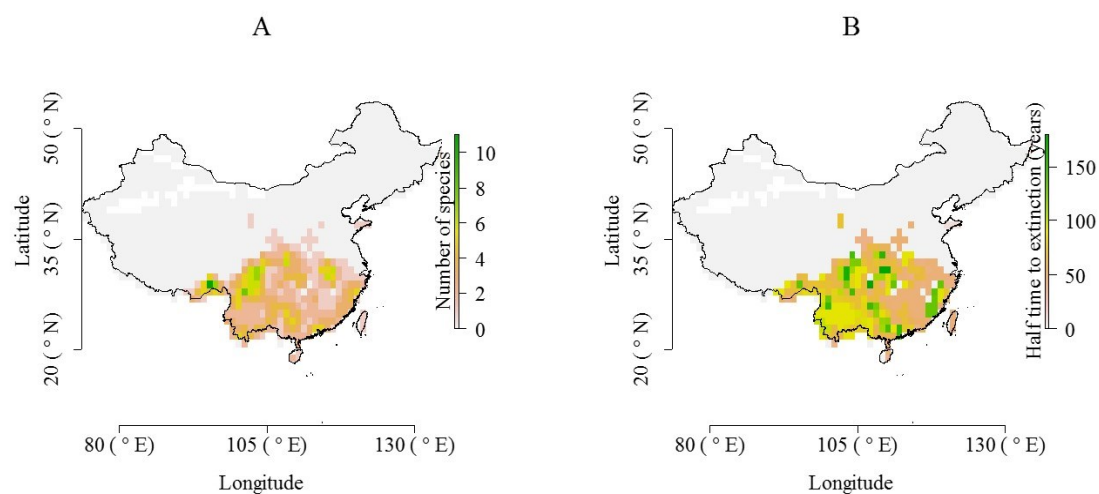


Fig. 4-5. Spatial extinction-debt patterns for forest-dwelling endemic amphibians in China in terms of magnitude (A) and mean time to half extinction (B). Results were obtained by combining the distributions from all 27 species that are prone to future extinction (detected at least once in the results of 20 combinations of different forest-cover scenarios and metapopulation models).



Supporting Information

Appendix 4-1. Maple code for the computation of time to half extinction for non-, weak- and strong-Allee models (Eqs. 4-14, 4-15 and 4-16).

1. Computation code for non-Allee model:

$$classical := \{diff(p(t), t) = (c \cdot p(t) \cdot (h - p(t)) - e \cdot p(t)), p(0) = p0\}$$

$$\left\{ \frac{d}{dt} p(t) = c p(t) (h - p(t)) - e p(t), p(0) = p0 \right\}$$

$$outc := dsolve(classical, p(t))$$

$$p(t) = \frac{(ch - e) p0}{e^{-(ch - e)t} ch - e^{-(ch - e)t} p0 c - e^{-(ch - e)t} e + p0 c}$$

$$t50.c := solve\left(rhs(outc) = \frac{p0}{2}, t\right)$$

$$-\frac{\ln\left(\frac{2ch - cp0 - 2e}{ch - p0c - e}\right)}{ch - e}$$

2. Computation code for strong-Allee model:

$$sys.ch1 := \left\{ diff(p(t), t) = \left(\frac{c \cdot p(t) \cdot (h - p(t)) \cdot (p(t) - a)}{p(t)} - e \cdot p(t) \right), p(0) = p0 \right\}$$

$$\left\{ \frac{d}{dt} p(t) = c (h - p(t)) (p(t) - a) - e p(t), p(0) = p0 \right\}$$

$$out.ch1 := dsolve(sys.ch1, p(t))$$

$$p(t) = -\frac{1}{2} \frac{1}{c} \left(\tan\left(\frac{1}{2} t \sqrt{-a^2 c^2 + 2 a c^2 h - c^2 h^2 + 2 a c e + 2 c e h - e^2}\right) + \arctan\left(\frac{a c + c h - 2 c p0 - e}{\sqrt{-a^2 c^2 + 2 a c^2 h - c^2 h^2 + 2 a c e + 2 c e h - e^2}}\right) \right) \sqrt{-a^2 c^2 + 2 a c^2 h - c^2 h^2 + 2 a c e + 2 c e h - e^2} - c a - c h + e$$

$$t50.ch1 := solve\left(rhs(out.ch1) = \frac{p0}{2}, t\right)$$

$$\left(2 \left(-\arctan \left(\frac{ac + ch - 2cp0 - e}{\sqrt{-a^2c^2 + 2ac^2h - c^2h^2 + 2ace + 2ceh - e^2}} \right) \right. \right. \\ \left. \left. + \arctan \left(\frac{ac + ch - cp0 - e}{\sqrt{-a^2c^2 + 2ac^2h - c^2h^2 + 2ace + 2ceh - e^2}} \right) \right) \right) \Bigg) \\ \Bigg/ \sqrt{-a^2c^2 + 2ac^2h - c^2h^2 + 2ace + 2ceh - e^2}$$

3. Computation code for weak-Allee model:

$$sys.lin := \left\{ diff(p(t), t) = \left(\frac{c \cdot p(t) \cdot (h - p(t)) \cdot p(t)}{p(t) + a} - e \cdot p(t) \right), p(0) = p0 \right\}$$

$$\left\{ \frac{d}{dt} p(t) = \frac{cp(t)^2(h - p(t))}{p(t) + a} - ep(t), p(0) = p0 \right\}$$

$$out.lin := dsolve(sys.lin, p(t))$$

$$p(t) = RootOf \left(-\ln(-chp0 + cp0^2 + ae + ep0) \sqrt{c^2h^2 - 4ace - 2ceh + e^2} \right. \\ \left. + 2c \operatorname{arctanh} \left(\frac{ch - 2cp0 - e}{\sqrt{c^2h^2 - 4ace - 2ceh + e^2}} \right) h \right. \\ \left. + 2 \operatorname{arctanh} \left(\frac{ch - 2cp0 - e}{\sqrt{c^2h^2 - 4ace - 2ceh + e^2}} \right) e \right. \\ \left. + 2 \ln(p0) \sqrt{c^2h^2 - 4ace - 2ceh + e^2} - 2te \sqrt{c^2h^2 - 4ace - 2ceh + e^2} \right. \\ \left. + 2c \operatorname{arctanh} \left(\frac{2_Zc - ch + e}{\sqrt{c^2h^2 - 4ace - 2ceh + e^2}} \right) h + \ln(_Z^2c - _Zch + _Ze \right. \\ \left. + ae) \sqrt{c^2h^2 - 4ace - 2ceh + e^2} - 2 \ln(_Z) \sqrt{c^2h^2 - 4ace - 2ceh + e^2} \right. \\ \left. + 2 \operatorname{arctanh} \left(\frac{2_Zc - ch + e}{\sqrt{c^2h^2 - 4ace - 2ceh + e^2}} \right) e \right)$$

$$t50.lin := solve \left(rhs(out.lin) = \frac{p0}{2}, t \right)$$

$$\begin{aligned}
& -\frac{1}{2} \frac{1}{e \sqrt{c^2 h^2 - 4 a c e - 2 c e h + e^2}} \left(-2 c \operatorname{arctanh} \left(\frac{c h - 2 c p 0 - e}{\sqrt{c^2 h^2 - 4 a c e - 2 c e h + e^2}} \right) h \right. \\
& + 2 c \operatorname{arctanh} \left(\frac{c h - p 0 c - e}{\sqrt{c^2 h^2 - 4 a c e - 2 c e h + e^2}} \right) h + \ln(-c h p 0 + c p 0^2 + a e \\
& + e p 0) \sqrt{c^2 h^2 - 4 a c e - 2 c e h + e^2} - 2 \ln(p 0) \sqrt{c^2 h^2 - 4 a c e - 2 c e h + e^2} - \ln \left(\right. \\
& - \frac{1}{2} c h p 0 + \frac{1}{4} p 0^2 c + a e + \frac{1}{2} e p 0 \left. \right) \sqrt{c^2 h^2 - 4 a c e - 2 c e h + e^2} \\
& + 2 \ln \left(\frac{1}{2} p 0 \right) \sqrt{c^2 h^2 - 4 a c e - 2 c e h + e^2} \\
& - 2 \operatorname{arctanh} \left(\frac{c h - 2 c p 0 - e}{\sqrt{c^2 h^2 - 4 a c e - 2 c e h + e^2}} \right) e \\
& \left. + 2 \operatorname{arctanh} \left(\frac{c h - p 0 c - e}{\sqrt{c^2 h^2 - 4 a c e - 2 c e h + e^2}} \right) e \right)
\end{aligned}$$

Table 4-S1. Estimated extinction-colonization ratios for different metapopulation models (with or without Allee effects) for each amphibian species using the equations (Eq. 4-7, 4-9 and 4-10) in the main text.

Species	No Allee	Weak Allee <i>a=0.0005</i>	Weak Allee <i>a=0.001</i>	Strong Allee <i>b=0.0005</i>	Strong Allee <i>b=0.001</i>
<i>Oreolalax rhodostigmatus</i>	0.398938	0.397934	0.396934	0.397931	0.396924
<i>Amolops tuberodepressus</i>	0.495059	0.494119	0.493183	0.494117	0.493176
<i>Rhacophorus arvalis</i>	0.109077	0.108279	0.107493	0.108274	0.10747
<i>Rana sauteri</i>	0.109077	0.108279	0.107493	0.108274	0.10747
<i>Scutiger brevipes</i>	0.449663	0.447845	0.446041	0.447837	0.446012
<i>Amolops kangtingensis</i>	0.478936	0.477499	0.47607	0.477494	0.476053
<i>Pseudorana sangzhiensis</i>	0.508692	0.507341	0.505998	0.507338	0.505984
<i>Oreolalax xiangchengensis</i>	0.523862	0.521939	0.52003	0.521932	0.520002
<i>Brachytarsophrys platyparietus</i>	0.443091	0.441974	0.440862	0.441971	0.440851
<i>Odorrana hejiangensis</i>	0.520202	0.517992	0.5158	0.517982	0.515762
<i>Xenophrys medogensis</i>	0.541662	0.539116	0.536593	0.539104	0.536545
<i>Oreolalax puxiongensis</i>	0.621557	0.618727	0.615922	0.618714	0.61587
<i>Leptobrachium liui</i>	0.404375	0.40346	0.40255	0.403458	0.402542
<i>Tylototriton taliangensis</i>	0.572513	0.570583	0.568666	0.570577	0.56864
<i>Hylarana spinulosa</i>	0.230039	0.22954	0.229043	0.229539	0.229039
<i>Xenophrys omeimontis</i>	0.428091	0.427256	0.426424	0.427254	0.426417
<i>Xenophrys caudoprocta</i>	0.520295	0.518817	0.517347	0.518813	0.51733
<i>Rhacophorus taipeianus</i>	0.263286	0.262786	0.262289	0.262786	0.262286
<i>Quasipaa yei</i>	0.368024	0.364793	0.361618	0.364764	0.361505
<i>Oreolalax pingii</i>	0.569984	0.568363	0.56675	0.568358	0.566731
<i>Odorrana junlianensis</i>	0.414379	0.413761	0.413144	0.41376	0.41314
<i>Cynops orientalis</i>	0.335669	0.334806	0.333947	0.334804	0.333938
<i>Quasipaa jiulongensis</i>	0.578517	0.575873	0.573252	0.575861	0.573204

<i>Xenophrys zhangi</i>	0.133099	0.132838	0.132578	0.132837	0.132576
<i>Odorrana nasuta</i>	0.230039	0.22954	0.229043	0.229539	0.229039
<i>Rhacophorus aurantiventralis</i>	0.252417	0.251958	0.2515	0.251957	0.251497
<i>Bufo kabischi</i>	0.443718	0.442689	0.441664	0.442686	0.441654
<i>Rhacophorus minimus</i>	0.436541	0.434701	0.432878	0.434694	0.432847
<i>Amolops wuyiensis</i>	0.514816	0.512709	0.510618	0.5127	0.510583
<i>Hynobius formosanus</i>	0.197879	0.197578	0.197278	0.197578	0.197277
<i>Buergeria oxycephala</i>	0.230039	0.22954	0.229043	0.229539	0.229039
<i>Amolops hainanensis</i>	0.100848	0.100684	0.100521	0.100684	0.10052
<i>Micryletta steinegeri</i>	0.109077	0.108279	0.107493	0.108274	0.10747
<i>Tylototriton hainanensis</i>	0.306719	0.305946	0.305176	0.305944	0.305169
<i>Leptolalax ventripunctatus</i>	0.644143	0.641957	0.639785	0.641949	0.639755
<i>Amolops caelumnoctis</i>	0.542779	0.541487	0.540201	0.541484	0.540189
<i>Paramesotriton fuzhongensis</i>	0.388824	0.387975	0.387129	0.387973	0.387122
<i>Odorrana margaretae</i>	0.399958	0.399008	0.398061	0.399005	0.398052
<i>Ingerana medogensis</i>	0.533586	0.527974	0.52248	0.527915	0.522244
<i>Hyla immaculata</i>	0.232018	0.231099	0.230187	0.231095	0.230172
<i>Rhacophorus zhaojuensis</i>	0.439785	0.438985	0.438187	0.438983	0.438181
<i>Pseudohynobius kuankuoshuiensis</i>	0.515174	0.513318	0.511475	0.513311	0.511449
<i>Odorrana kuangwuensis</i>	0.43461	0.433208	0.431815	0.433203	0.431796
<i>Liua tsinpaensis</i>	0.436469	0.435526	0.434588	0.435524	0.43458
<i>Bufo andrewsi</i>	0.391724	0.390978	0.390234	0.390976	0.390229
<i>Oreolalax granulosus</i>	0.632323	0.630461	0.628611	0.630456	0.628589
<i>Scutiger gongshanensis</i>	0.49057	0.489745	0.488923	0.489744	0.488918
<i>Amolops jinjiangensis</i>	0.580412	0.577501	0.574618	0.577486	0.57456
<i>Tylototriton shanjing</i>	0.463624	0.462684	0.461748	0.462682	0.46174
<i>Rhacophorus yaoshanensis</i>	0.396702	0.394409	0.392143	0.394396	0.39209

<i>Pseudohynobius flavomaculatus</i>	0.439462	0.438381	0.437305	0.438378	0.437295
<i>Protohynobius puxiongensis</i>	0.601047	0.598795	0.59656	0.598787	0.596526
<i>Xenophrys giganticus</i>	0.413544	0.412943	0.412345	0.412942	0.412341
<i>Oreolalax chuanbeiensis</i>	0.388114	0.387203	0.386296	0.387201	0.386287
<i>Tylototriton wenxianensis</i>	0.527468	0.524926	0.522409	0.524914	0.52236
<i>Rhacophorus yinggelingensis</i>	0.306719	0.305946	0.305176	0.305944	0.305169
<i>Rana kunyuensis</i>	0.035852	0.035271	0.034709	0.035262	0.034672
<i>Odorrana anlungensis</i>	0.568924	0.567344	0.565774	0.56734	0.565756
<i>Rhacophorus moltrechti</i>	0.263286	0.262786	0.262289	0.262786	0.262286
<i>Parapelophryne scalpta</i>	0.230039	0.22954	0.229043	0.229539	0.229039
<i>Hynobius chinensis</i>	0.357234	0.356085	0.354942	0.356081	0.354928
<i>Oreolalax popei</i>	0.450616	0.449821	0.449028	0.449819	0.449023
<i>Rhacophorus hungfuensis</i>	0.5018	0.498744	0.495724	0.498725	0.495649
<i>Amolops mantzorum</i>	0.506265	0.504488	0.502724	0.504482	0.502699
<i>Xenophrys spinata</i>	0.461029	0.459495	0.457972	0.45949	0.457952
<i>Nanorana maculosa</i>	0.511513	0.510487	0.509465	0.510485	0.509457
<i>Oreolalax multipunctatus</i>	0.577045	0.575426	0.573816	0.575421	0.573798
<i>Scutiger mammatus</i>	0.279753	0.278823	0.277899	0.27882	0.277886
<i>Oreolalax omeimontis</i>	0.535638	0.534419	0.533205	0.534416	0.533194
<i>Amolops loloensis</i>	0.432367	0.431674	0.430984	0.431673	0.43098
<i>Oreolalax jingdongensis</i>	0.576496	0.574817	0.573148	0.574812	0.573129
<i>Odorrana hainanensis</i>	0.370344	0.36914	0.367944	0.369136	0.367929
<i>Rhacophorus verrucopus</i>	0.444992	0.443682	0.44238	0.443679	0.442365
<i>Rana omeimontis</i>	0.421341	0.420295	0.419254	0.420292	0.419243
<i>Amolops daiyunensis</i>	0.340514	0.339806	0.339102	0.339805	0.339096
<i>Amolops chunganensis</i>	0.461146	0.460088	0.459036	0.460086	0.459027
<i>Nanorana unculuanus</i>	0.432413	0.43172	0.431029	0.431719	0.431024

<i>Xenophrys huangshanensis</i>	0.54889	0.547297	0.545713	0.547292	0.545695
<i>Scutiger tuberculatus</i>	0.464107	0.463297	0.462489	0.463295	0.462483
<i>Cynops orphicus</i>	0.33175	0.327736	0.323819	0.327687	0.323625
<i>Amolops granulosus</i>	0.459083	0.457986	0.456895	0.457984	0.456885
<i>Hyla sanchiangensis</i>	0.370448	0.369514	0.368585	0.369512	0.368575
<i>Scutiger liupanensis</i>	0.321981	0.319451	0.316961	0.319431	0.316882
<i>Rhacophorus prasinatus</i>	0.336556	0.336032	0.335509	0.336031	0.335506
<i>Bufo wolongensis</i>	0.461205	0.459861	0.458525	0.459858	0.45851
<i>Leptobrachium hainanense</i>	0.230039	0.22954	0.229043	0.229539	0.229039
<i>Nanorana conaensis</i>	0.34245	0.340595	0.338759	0.340585	0.338719
<i>Rana multidenticulata</i>	0.300898	0.300099	0.299304	0.300097	0.299296
<i>Ingerana liui</i>	0.44697	0.446252	0.445536	0.446251	0.445532
<i>Xenophrys shapingensis</i>	0.540633	0.538848	0.537075	0.538842	0.537052
<i>Odorrana schmackeri</i>	0.312126	0.311529	0.310933	0.311527	0.310929
<i>Odorrana versabilis</i>	0.44379	0.442809	0.441832	0.442807	0.441824
<i>Rana zhenhaiensis</i>	0.321036	0.320319	0.319606	0.320318	0.319599
<i>Limnonectes fragilis</i>	0.230039	0.22954	0.229043	0.229539	0.229039
<i>Scutiger ruginosus</i>	0.521936	0.520092	0.518261	0.520085	0.518235
<i>Rana chaochiaoensis</i>	0.454558	0.45369	0.452825	0.453688	0.452819
<i>Odorrana tormota</i>	0.452469	0.451707	0.450947	0.451706	0.450942
<i>Xenophrys binchuanensis</i>	0.655502	0.641183	0.627476	0.640864	0.626225
<i>Quasipaa shini</i>	0.43893	0.437639	0.436355	0.437635	0.43634
<i>Odorrana exiliversabilis</i>	0.514564	0.512981	0.511408	0.512976	0.511389
<i>Ingerana alpina</i>	0.444992	0.443682	0.44238	0.443679	0.442365
<i>Leptolalax alpinus</i>	0.532635	0.531195	0.529762	0.531191	0.529747
<i>Rhacophorus puerensis</i>	0.644143	0.641957	0.639785	0.641949	0.639755
<i>Pachyhynobius yunanicus</i>	0.368024	0.364793	0.361618	0.364764	0.361505
<i>Pachyhynobius shangchengensis</i>	0.36114	0.359217	0.357315	0.359207	0.357274

<i>Hynobius maoershanensis</i>	0.486309	0.484674	0.483049	0.484668	0.483027
<i>Brachytarsophrys chuannanensis</i>	0.617126	0.589375	0.564012	0.588068	0.55901
<i>Rana hanluica</i>	0.477936	0.476375	0.474825	0.47637	0.474805
<i>Oreolalax liangbeiensis</i>	0.601047	0.598795	0.59656	0.598787	0.596526
<i>Kalophrynx menglienicus</i>	0.429004	0.428347	0.427691	0.428346	0.427687
<i>Rhacophorus hui</i>	0.502109	0.50082	0.499538	0.500817	0.499525
<i>Batrachuperus pinchonii</i>	0.493543	0.492299	0.491061	0.492296	0.491049
<i>Leptobrachium boringii</i>	0.464109	0.463125	0.462144	0.463122	0.462136
<i>Xenophrys daweimontis</i>	0.399935	0.399276	0.398618	0.399275	0.398614
<i>Pseudohynobius shuichengensis</i>	0.594182	0.592325	0.59048	0.59232	0.590457
<i>Rhacophorus chenfui</i>	0.487977	0.48648	0.484992	0.486475	0.484973
<i>Hynobius arisanensis</i>	0.262954	0.261109	0.25929	0.261096	0.259238
<i>Bombina lichuanensis</i>	0.525536	0.524125	0.522721	0.524121	0.522706
<i>Hynobius sonani</i>	0.2318	0.231407	0.231016	0.231407	0.231014
<i>Leptobrachium leishanense</i>	0.590254	0.588885	0.587522	0.588882	0.587509
<i>Ingerana reticulata</i>	0.444992	0.443682	0.44238	0.443679	0.442365
<i>Bufo bankorensis</i>	0.263286	0.262786	0.262289	0.262786	0.262286
<i>Nanorana quadranus</i>	0.351975	0.35091	0.349852	0.350907	0.349839
<i>Hynobius yiwuensis</i>	0.433083	0.431895	0.430713	0.431891	0.4307
<i>Rhacophorus omeimontis</i>	0.500677	0.499177	0.497687	0.499173	0.497669
<i>Nanorana medogensis</i>	0.444992	0.443682	0.44238	0.443679	0.442365
<i>Leptobrachium huashen</i>	0.415481	0.414839	0.4142	0.414838	0.414196
<i>Scutiger glandulatus</i>	0.364829	0.363957	0.363089	0.363955	0.363081
<i>Paramesotriton caudopunctatus</i>	0.511685	0.510198	0.50872	0.510194	0.508702
<i>Leptobrachium ailaonicum</i>	0.590466	0.588786	0.587116	0.588782	0.587097
<i>Bufo ailaoanus</i>	0.627662	0.625446	0.623246	0.625438	0.623215

<i>Rana zhengi</i>	0.615046	0.613322	0.611607	0.613317	0.611588
<i>Theloderma albopunctata</i>	0.491523	0.49	0.488488	0.489996	0.488469
<i>Amolops lifanensis</i>	0.638472	0.632296	0.626237	0.632235	0.625998
<i>Rana longicrus</i>	0.054539	0.054481	0.054423	0.054481	0.054423
<i>Bufo aspinius</i>	0.468664	0.467739	0.466819	0.467737	0.466811
<i>Batrachuperus londongensis</i>	0.670052	0.656397	0.643287	0.656113	0.642174
<i>Rhacophorus nigropunctatus</i>	0.394068	0.393315	0.392564	0.393313	0.392558
<i>Oreolalax major</i>	0.531333	0.530138	0.528948	0.530135	0.528938
<i>Xenophrys pachyproctus</i>	0.628441	0.625486	0.622559	0.625472	0.622503
<i>Xenophrys shuichengensis</i>	0.599776	0.597426	0.595094	0.597417	0.595057
<i>Ichthyophis bannanicus</i>	0.274635	0.274086	0.27354	0.274085	0.273535
<i>Ingerana xizangensis</i>	0.453578	0.452477	0.451382	0.452475	0.451372
<i>Hynobius guabangshanensis</i>	0.362647	0.35994	0.357273	0.35992	0.357193
<i>Echinotriton chinhaiensis</i>	0.482839	0.481536	0.480241	0.481533	0.480227
<i>Liuixalus ocellatus</i>	0.370344	0.36914	0.367944	0.369136	0.367929
<i>Oreolalax schmidti</i>	0.572018	0.570234	0.56846	0.570228	0.568438
<i>Rana chevronta</i>	0.615046	0.613322	0.611607	0.613317	0.611588
<i>Liuixalus hainanus</i>	0.444412	0.442549	0.440701	0.442541	0.440669
<i>Oreolalax nanjiangensis</i>	0.417545	0.416702	0.415862	0.4167	0.415855
<i>Cynops cyanurus</i>	0.49393	0.492817	0.491709	0.492815	0.491699
<i>Xenophrys mangshanensis</i>	0.535076	0.533116	0.531171	0.533109	0.531142
<i>Odorrana swinhoana</i>	0.263286	0.262786	0.262289	0.262786	0.262286
<i>Odorrana lungshengensis</i>	0.483264	0.481803	0.480351	0.481799	0.480334
<i>Oreolalax lichuanensis</i>	0.4775	0.476193	0.474893	0.476189	0.474878
<i>Theloderma kwangsiense</i>	0.331446	0.330091	0.328748	0.330086	0.328726
<i>Liua shihi</i>	0.409996	0.408251	0.406521	0.408243	0.406491
<i>Andrias davidianus</i>	0.337498	0.33658	0.335666	0.336577	0.335656

<i>Nanorana taihangnica</i>	0.348888	0.341378	0.334184	0.341212	0.333537
<i>Scutiger ningshanensis</i>	0.67115	0.666859	0.662623	0.666831	0.662513
<i>Leptolalax liui</i>	0.402864	0.401925	0.400991	0.401923	0.400982
<i>Quasipaa exilispinosa</i>	0.438091	0.436648	0.435213	0.436643	0.435194
<i>Amolops hongkongensis</i>	0.266862	0.265423	0.263999	0.265415	0.263968
<i>Paramesotriton hongkongensis</i>	0.215248	0.213506	0.211791	0.213491	0.211734

Table 4-S2. Future time periods triggering the delayed extinctions of 27 endemic amphibians in 20 combinations of different forest-cover scenarios and metapopulation models.

Models	No Allee	No Allee	No Allee	No Allee	Weak Allee <i>a=0.000</i>	Weak Allee <i>a=0.000</i>
					5	5
Scenarios	MINIC AM	MESSA GE	AIM	IMA GE	MINIC AM	MESSA GE
<i>Rana kunyuensis</i>	2030s	2030s	2030s	2070s	2030s	2030s
<i>Cynops orphicus</i>	2030s	2050s	2050s	2070s	2030s	2070s
<i>Xenophrys binchuanensis</i>	2030s	-	-	2030s	2050s	-
<i>Brachytarsophrys chuannanensis</i>	2030s	2030s	2030s	2030s	2030s	-
<i>Batrachuperus londongensis</i>	2030s	2050s	2050s	2030s	2030s	-
<i>Nanorana taihangnica</i>	2030s	2030s	2030s	2030s	2030s	2030s
<i>Quasipaa yei</i>	2050s	-	2050s	2070s	2050s	-
<i>Quasipaa jiulongensis</i>	2050s	-	-	-	2070s	-
<i>Rhacophorus hungfuensis</i>	2050s	-	-	-	2050s	-
<i>Scutiger liupanensis</i>	2050s	-	-	-	2050s	-
<i>Pachyhynobius yunanicus</i>	2050s	-	2050s	2070s	2050s	-
<i>Amolops lifanensis</i>	2050s	-	-	2050s	2050s	-
<i>Hynobius guabangshanensis</i>	2050s	-	2090s	-	2050s	-
<i>Scutiger ningshanensis</i>	2050s	-	-	2050s	2050s	-
<i>Amolops hongkongensis</i>	2050s	-	-	-	2050s	-
<i>Paramesotriton hongkongensis</i>	2050s	-	2090s	-	2050s	-

<i>Tylototriton wenxianensis</i>	2070s	-	-	-	2070s	-
<i>Pachyhynobius shangchengensis</i>	2070s	-	-	-	2070s	-
<i>Liuixalus hainanus</i>	2070s	-	-	-	2070s	-
<i>Leptolalax ventripunctatus</i>	-	-	-	2030s	-	-
<i>Rhacophorus puerensis</i>	-	-	-	2030s	-	-
<i>Scutiger brevipes</i>	-	-	-	2050s	-	-
<i>Xenophrys medogensis</i>	-	-	-	2050s	-	-
<i>Ingerana medogensis</i>	-	-	-	2050s	-	-
<i>Scutiger ruginosus</i>	-	-	-	2050s	-	-
<i>Xenophrys pachyproctus</i>	-	-	-	2050s	-	-
<i>Oreolalax puxiongensis</i>	-	-	-	2090s	-	-

Table 4-S2 (continued)

Models	Weak Allele	Strong Allele					
	<i>a=0.0</i>	<i>a=0.0</i>	<i>a=0.0</i>	<i>a=0.0</i>	<i>a=0.0</i>	<i>a=0.0</i>	<i>b=0.00</i>
	005	005	01	01	01	01	05
Scenarios	AIM	IMA GE	MINI CAM	MESS AGE	AIM	IMA GE	MINI CAM
<i>Rana kunyuensis</i>	2030s	2070s	2030s	2030s	2030s	2070s	2030s
<i>Cynops orphicus</i>	2050s	2090s	2050s	2090s	2070s	-	2030s
<i>Xenophrys binchuanensis</i>	-	2050s	2050s	-	-	2050s	2050s
<i>Brachytarsophrys chuannanensis</i>	2070s	2050s	2050s	-	-	2070s	2030s
<i>Batrachuperus londongensis</i>	2070s	2050s	2050s	-	2090s	2070s	2030s
<i>Nanorana taihangnica</i>	2030s						
<i>Quasipaa yei</i>	2050s	2070s	2050s	-	2050s	2070s	2050s
<i>Quasipaa jiulongensis</i>	-	-	2070s	-	-	-	2070s
<i>Rhacophorus hungfuensis</i>	-	-	2050s	-	-	-	2050s
<i>Scutiger liupanensis</i>	-	-	2050s	-	-	-	2050s
<i>Pachyhynobius yunanicus</i>	2050s	2070s	2050s	-	2050s	2070s	2050s
<i>Amolops lifanensis</i>	-	2050s	2050s	-	-	2050s	2050s
<i>Hynobius guabangshanensis</i>	2090s	-	2050s	-	-	-	2050s
<i>Scutiger ningshanensis</i>	-	2050s	2050s	-	-	2050s	2050s
<i>Amolops hongkongensis</i>	-	-	2050s	-	-	-	2050s
<i>Paramesotriton hongkongensis</i>	2090s	-	2070s	-	2090s	-	2050s

<i>Tylototriton wenxianensis</i>	-	-	2070s	-	-	-	2070s
<i>Pachyhynobius shangchengensis</i>	-	-	-	-	-	-	2070s
<i>Liuixalus hainanus</i>	-	-	2070s	-	-	-	2070s
<i>Leptolalax ventripunctatus</i>	-	2030s	-	-	-	2030s	-
<i>Rhacophorus puerensis</i>	-	2030s	-	-	-	2030s	-
<i>Scutiger brevipes</i>	-	2050s	-	-	-	2050s	-
<i>Xenophrys medogensis</i>	-	2050s	-	-	-	2050s	-
<i>Ingerana medogensis</i>	-	2050s	-	-	-	2050s	-
<i>Scutiger ruginosus</i>	-	2050s	-	-	-	2050s	-
<i>Xenophrys pachyproctus</i>	-	2050s	-	-	-	2050s	-
<i>Oreolalax puxiongensis</i>	-	-	-	-	-	-	-

Table 4-S2 (continued)

	Stron g Allele	Stron g Allele	Stron g Allele	Stron g Allele	Stron g Allele	Stron g Allele	Stron g Allele
Models	b=0.00 05	b=0.00 05	b=0.00 05	b=0.00 1	b=0.00 1	b=0.00 1	b=0.00 1
Scenarios	MESS AGE	AIM	IMAG E	MINI CAM	MESS AGE	AIM	IMAG E
<i>Rana kunyuensis</i>	2030s	2030s	2070s	2030s	2030s	2030s	2070s
<i>Cynops orphicus</i>	2070s	2050s	2090s	2050s	2090s	2070s	-
<i>Xenophrys binchuanensis</i>	-	-	2050s	2050s	-	-	2050s
<i>Brachytarsophrys chuannanensis</i>	-	2070s	2050s	2050s	-	-	2070s
<i>Batrachuperus londongensis</i>	-	2070s	2050s	2050s	-	2090s	2070s
<i>Nanorana taihangnica</i>	2030s	2030s	2030s	2030s	2030s	2030s	2030s
<i>Quasipaa yei</i>	-	2050s	2070s	2050s	-	2050s	2070s
<i>Quasipaa jiulongensis</i>	-	-	-	2070s	-	-	-
<i>Rhacophorus hungfuensis</i>	-	-	-	2050s	-	-	-
<i>Scutiger liupanensis</i>	-	-	-	2050s	-	-	-
<i>Pachyhynobius yunanicus</i>	-	2050s	2070s	2050s	-	2050s	2070s
<i>Amolops lifanensis</i>	-	-	2050s	2050s	-	-	2050s
<i>Hynobius guabangshanensi s</i>	-	2090s	-	2050s	-	-	-
<i>Scutiger ningshanensis</i>	-	-	2050s	2050s	-	-	2050s
<i>Amolops hongkongensis</i>	-	-	-	2050s	-	-	-

<i>Paramesotriton hongkongensis</i>	-	2090s	-	2070s	-	2090s	-
<i>Tylototriton wenxianensis</i>	-	-	-	2070s	-	-	-
<i>Pachyhynobius shangchengensis</i>	-	-	-	-	-	-	-
<i>Liuixalus hainanus</i>	-	-	-	2070s	-	-	-
<i>Leptolalax ventripunctatus</i>	-	-	2030s	-	-	-	2030s
<i>Rhacophorus puerensis</i>	-	-	2030s	-	-	-	2030s
<i>Scutiger brevipes</i>	-	-	2050s	-	-	-	2050s
<i>Xenophrys medogensis</i>	-	-	2050s	-	-	-	2050s
<i>Ingerana medogensis</i>	-	-	2050s	-	-	-	2050s
<i>Scutiger ruginosus</i>	-	-	2050s	-	-	-	2050s
<i>Xenophrys pachyproctus</i>	-	-	2050s	-	-	-	2050s
<i>Oreolalax puxiongensis</i>	-	-	-	-	-	-	-

Chapter 5 Discussion and conclusions

In the thesis, by applying and developing a variety of statistical methods and calculating different diversity indices, I evaluated the potential impacts of climate change and land use on broad-scale diversity, distribution and extinction patterns of amphibian species in China. In particular, the effectiveness of current protected areas is assessed in terms of the coverage of amphibian ranges, suitable habitat and climate conditions. I found that although current protected areas can well cover amphibian diversity and ranges. Climate velocity of temperature in protected areas was typically higher, and correspondingly, the residence time of temperature was significantly lower than those in other reference sites (e.g., non-protected areas). By using a simple scoring method, I found that southern parts of the Hengduan Mountain and Tibet were two large and spatially continuous conservation gap zones that were recommended to be a part of the current protected area network. By using circular statistics, I found general associations between range shift (for both shift distance and direction) of amphibians and climatic variables including climate velocity magnitude and direction. Finally, by developing three metapopulation models, I quantified the impacts of spatial Allee effects on extinction debts of forest-dwelling endemic amphibians in China. It was found that Allee effects can shorten extinction time of amphibians. The overall goal of these studies in the three chapters is to provide a comprehensive understanding on the impacts of habitat loss and climate change on amphibian

extinction in China, one of the worldwide biodiversity hotspots for both flora and fauna.

Limitations

As discussed earlier in the Chapter 2, distributional data and biological information are largely limited for some amphibians in the country, which may underestimate threatened status of amphibians in China. Furthermore, I utilized range maps as the proxy to model range shift of species in both Chapters 2 and 3, which might be too coarse to accurately reflect the true distributional status of species (even though many macroecological studies also utilize range maps as baseline data in their papers). Moreover, my research utilizes the distributional data (for both range maps and occurrence points) that have been archived over the past century. Current distribution of some amphibian species might be largely different from the historically documented distributional information because of species migration and extinction. Fourth, the present research only focuses on the evaluation of extinction risk of amphibians exclusively based on the distributional information of species, which might not be sufficient. Other than distributional data, other biological traits can also play deterministic roles of extinction risk, for instance, population size and generation length (Pearson *et al.*, 2014).

Conservation challenges

One big challenge for protecting amphibians in China is the limited information on the population status and range size of species (these species usually are classified as Data Deficit in the IUCN Red List) (Howard & Bickford, 2014). Population dynamics are an important aspect of extinction risk of species (Lande, 1987; Lande *et al.*, 2003; Ovaskainen & Meerson, 2010). It would be difficult to determine the threatened status of amphibian species without detailed population information. A substantial proportion of amphibian species in the country has not been well assessed on their populations and behaviors. Moreover, since amphibians are nocturnal (Bartlett & Bartlett, 2006), they are secretive species and are hidden from human beings (Pough, 2007). Field surveys have to be conducted in an active way at night if ecologists want to better assess the population status of data-deficit species. In summary, labor-extensive field surveys under legal registration are needed to provide a full and accurate assessment on the conservation priorities of data-deficit amphibians in the country.

Protection of natural habitats for amphibians should be enforced. As discussed previously, many amphibians are habitat specialists and may be present in freshwater environments at specific elevational ranges of the mountains (Bartlett & Bartlett, 2006; Fei *et al.*, 2012). Destruction and degeneration of amphibian habitats would drive the extinction of endemic species immediately. Currently, pollution of water bodies in China is very severe because of rapid urbanization and industrialization over

the past decades (Shao *et al.*, 2006; Wang & Yu, 2014). According to recent governmental reports, nearly 70% of water bodies in China have been polluted (Bowman, 2011). Therefore, natural habitats of amphibians, in particular water bodies like wetlands, streams and rivers in mountain ranges, should be given a high protection priority in the design of nature reserves at national, provincial or local levels.

Literature cited

Bartlett R, Bartlett P (2006) *Guide and reference to the amphibians of eastern and central North America*. University Press of Florida, Gainesville, FL, USA, 312 pp.

Bowman R (2011) Chapter 30: Adaptation challenges for water and waste management in the US and China. In: *Climate: Global Change and Local Adaptation* (eds Linkov L, Bridges T), pp. 561–574. Springer Science+Business Media, BV.

Fei L, Ye C, Jiang J (2012) *Colored atlas of Chinese amphibians and their distributions*. Sichuan Science & Technology Press, Chengdu, China, 1-619 pp.

Howard S, Bickford D (2014) Amphibians over the edge: silent extinction risk of Data Deficient species. *Diversity and Distributions*, **20**, 837–846.

- Lande R (1987) Extinction thresholds in demographic models of territorial populations. *American Naturalist*, **130**, 624–635.
- Lande R, Engen S, Sather B (2003) *Stochastic population dynamics in ecology and conservation*. Oxford University Press, New York, USA.
- Ovaskainen O, Meerson B (2010) Stochastic models of population extinction. *Trends in Ecology and Evolution*, **25**, 643–652.
- Pearson R, Stanton J, Shoemaker K et al. (2014) Life history and spatial traits predict extinction risk due to climate change. *Nature Climate Change*, **4**, 217.
- Pough F (2007) Amphibian biology and husbandry. *ILAR Journal*, **48**, 203–213.
- Shao M, Tang X, Zhang Y, Li W (2006) City clusters in China: air and surface water pollution. *Frontiers in Ecology and the Environment*, **4**, 353–361.
- Wang H, Yu X (2014) A review of the protection of sources of drinking water in China. *Natural Resources Forum*, **38**, 99–108.

Bibliography

- Agostinelli C, Lund U (2013) circular: Circular Statistics R package version 0.4-7. URL: <http://cran.r-project.org/web/packages/circular>.
- Alagador D, Cerdeira J, Araujo M (2014) Shifting protected areas: scheduling spatial priorities under climate change. *Journal of Applied Ecology*, 51, 703–713.
- Alagador D, Cerdeira J, Araujo M (2016) Climate change, species range shifts and dispersal corridors: an evaluation of spatial conservation models. *Methods in Ecology and Evolution*, 7, 853–866.
- Alkemade R, Oorschot M, Miles L, Nellemann C, Bakkenes M, ten Brink B (2009) GLOBIO3: a framework to investigate options for reducing global terrestrial biodiversity loss. *Ecosystems*, 12, 374–390.
- Allee W (1931) Animal aggregations, a study in general sociology. University of Chicago Press, Chicago, IL.
- Allee W, Bowen E (1932) Studies in animal aggregations: mass protection against colloidal silver among goldfishes. *Journal of Experimental Zoology*, 61, 185–207.
- Alroy J (2015) Current extinction rates of reptiles and amphibians. *PNAS*, 112, 13003–13008.
- Amarasekare P (1998) Allee effects in metapopulation dynamics. *American Naturalist*, 152, 298–302.
- Araujo M, Alagador D, Cabeza M, Nogues-Bravo D, Thuiller W (2011) Climate change threatens European conservation areas. *Ecology Letters*, 14, 484–492.

Araujo M, New M (2007) Ensemble forecasting of species distributions. *Trends in Ecology & Evolution*, 22, 42–47.

Araujo M, Thuiller W, Pearson R (2006) Climate warming and the decline of amphibians and reptiles in Europe. *Journal of Biogeography*, 33, 1712–1728.

Bai C, Liu X, Fisher M, Garner T, Li Y (2012) Global and endemic Asian lineages of the emerging pathogenic fungus *Batrachochytrium dendrobatidis* widely infect amphibians in China. *Diversity and Distributions*, 18, 307–318.

Bartlett R, Bartlett P (2006) Guide and reference to the amphibians of eastern and central North America. University Press of Florida, Gainesville, FL, USA, 312 pp.

Bellard C, Thuiller W, Leroy B, Genovesi P, Bakkenes M, Courchamp F (2013) Will climate change promote future invasions? *Global Change Biology*, 19, 3740–3748.

Bowman R (2011) Chapter 30: Adaptation challenges for water and waste management in the US and China. In: *Climate: Global Change and Local Adaptation* (eds Linkov L, Bridges T), pp. 561–574. Springer Science+Business Media, BV.

Braid A, Nielsen S (2015) Prioritizing sites for protection and restoration for Grizzly Bears (*Ursus arctos*) in Southwestern Alberta, Canada. *PLoS ONE*, 10, e0132501.

Brooks T, Mittermeier R, Mittermeier C et al. (2002) Habitat loss and extinction in the hotspots of biodiversity. *Conservation Biology*, 16, 909–923.

Brooks T, Pimm S, Oyugi J (1999) Time lag between deforestation and bird extinction in tropical forest fragments. *Conservation Biology*, 13, 1140–1150.

Brovkin V, Boysen L, Arora V et al. (2013) Effect of anthropogenic land-use and land-cover changes on climate and land carbon storage in CMIP5 projections for the twenty-first century. *Journal of Climate*, 26, 6859–6881.

Brown C, Bode M, Venter O et al. (2015) Effective conservation requires clear objectives and prioritizing actions, not places or species. *Proceedings of the National Academy of Sciences of the United States of America*, 112, E4342.

Buisson L, Thuiller W, Casajus N, Lek S, Grenouillet G (2010) Uncertainty in ensemble forecasting of species distribution. *Global Change Biology*, 16, 1145–1157.

Burrows M, Schoeman D, Richardson A et al. (2014) Geographical limits to species range-shifts are suggested by climate velocity. *Nature*, 507, 492–495.

Busby J (1991) BIOCLIM-a bioclimate analysis and prediction system. *Plant Protection Quarterly*, 6, 8–9.

Cao M, Peng L, Liu S (2015) Analysis of the network of protected areas in China based on a geographic perspective: current status, issues and integration. *Sustainability*, 7, 15617–15631.

Chades I, Nicol S, van Leeuwen S et al. (2015) Benefits of integrating complementarity into priority threat management. *Conservation Biology*, 29, 525–536.

Chaplin G (2005) Physical geography of the Gaoligong Shan Area of southwest China in relation to biodiversity. *Proceedings of the California Academy of Sciences*, 56, 527–556.

Chen I, Hill J, Ohlemuller R, Roy D, Thomas C (2011) Rapid range shifts of species associated with high levels of climate warming. *Science*, 333, 1024–1026.

Chen L (2004) The precise biogeographic division of Palearctic and Oriental Realm in the East of China: based on data of amphibians. *Zoological Research*, 25, 369–377.

Chen L, Hui C (2009) Habitat destruction and the extinction debt revisited: the allee effect. *Mathematical Biosciences*, 221, 26–32.

Chen L, Lin Z (2008) The effect of habitat destruction on metapopulations with the Allee-like effect: a study case of Yancheng in Jiangsu Province, China. *Ecological Modelling*, 213, 356–364.

Chen Y (2013) Biotic element analysis of reptiles of China: a test of vicariance model. *Current Zoology*, 59, 447–455.

Chen Y (2013) Habitat suitability modeling of amphibian species in southern and central China: environmental correlates and potential richness mapping. *Science China Life Sciences*, 56, 476–484.

Chen Y (2015) Analyze causal relations between climatic and biotic velocities using circular statistics so as to inform biodiversity conservation. *Biodiversity and Conservation*, 24, 3627–3628.

Chen Y (2015) New climate velocity algorithm is nearly equivalent to simple species distribution modeling methods. *Global Change Biology*, 21, 2832–2833.

Chen Y, Bi J (2007) Biogeography and hotspots of amphibian species of China: Implications to reserve selection and conservation. *Current Science*, 92, 480–489.

Chen Y, Srivastava D (2015) Latitudinal concordance between biogeographic regionalization, community structure and richness patterns: a study on the reptiles of China. *The Science of Nature*, 102, 1253.

Chen Y, Zhang J, Jiang J, Nielsen S, He F (2016) Assessing the effectiveness of China's protected areas to conserve current and future amphibian diversity. *Diversity and Distributions*, DOI: 10.1111/ddi.12508.

Comte L, Grenouillet G (2015) Distribution shifts of freshwater fish under a variable climate: comparing climatic, bioclimatic and biotic velocities. *Diversity and Distributions*, 21, 1014–1026.

Conlisk E, Syphard A, Franklin J, Flint L, Flint A, Regan H (2013) Uncertainty in assessing the impacts of global change with coupled dynamic species distribution and population models. *Global Change Biology*, 19, 858–869.

Courchamp F, Angulo E, Rivalan P, Hall R, Signoret L, Bull L, Meinard Y (2006) Rarity value and species extinction: the anthropogenic Allee effect. *PLoS Biology*, 4, e415.

Courchamp F, Berec J, Gascoigne J (2008) *Allee effects in ecology and conservation*. Oxford University Press, New York, USA.

Courchamp F, Clutton-Brock T, Grenfell B (1999) Inverse density dependence and the Allee effect. *TREE*, 14, 405–410.

Cowlishaw G (1999) Predicting the pattern of decline of African primate diversity: an extinction debt from historical deforestation. *Conservation Biology*, 13, 1183.

- Crisp M, Laffan S, Linder H, Monro A (2001) Endemism in the Australian flora. *Journal of Biogeography*, 28, 183–198.
- Culter D, Edwards T, Beard K, Culter A, Hess K, Gibson J, Lawler J (2007) Random forests for classification in ecology. *Ecology*, 88, 2783–2792.
- Cunningham H, Rissler L, Buckley L, Urban M (2016) Abiotic and biotic constraints across reptile and amphibian ranges. *Ecography*, 39, 1–8.
- Davis M (1986) Climatic stability, time lags and community disequilibrium. In: *Community Ecology* (eds Diamond J, Case T), pp. 269–284. Harper & Row, New York.
- Diniz-Filho J, Bini L, Rangel T, Loyola R, Hof C, Nogues-Bravo D, Araujo M (2009) Partitioning and mapping uncertainties in ensembles of forecasts of species turnover under climate change. *Ecography*, 32, 897–906.
- Dobrowski S, Abatzoglou J, Swanson A, Greenberg J, Mynsberge A, Holden Z, Schwartz M (2013) The climate velocity of the contiguous United States during the 20th century. *Global Change Biology*, 19, 241–251.
- Dong B, Che J, Ding L, Huang S, Murphy R, Zhao E, Zhang Y (2012) Testing hypotheses of Pleistocene population history using coalescent simulations: refugial isolation and secondary contact in *Pseudepidalea raddei* (Amphibia: Bufonidae). *Asian Herpetological Research*, 3, 103–113.
- Dormann C, Purschke O, Garcia-Marquez J, Lautenbach S, Schroder B (2008) Components of uncertainty in species distribution analysis: a case study of the Great Grey Shrike. *Ecology*, 89, 3371–3386.

Du Y, Mao L, Queenborough S, Freckleton R, Chen B, Ma K (2015) Phylogenetic constraints and trait correlates of flowering phenology in the angiosperm flora of China. *Global Ecology and Biogeography*, 24, 928–938.

Duan R, Kong X, Huang M, Varela S, Ji X (2016) The potential effects of climate change on amphibian distribution, range fragmentation and turnover in China. *PeerJ*, 4, e2185.

Dudley N, Shadie P, Stolton S (2013) Guidelines for applying protected area management categories including IUCN WCPA best practice guidance on recognising protected areas and assigning management categories and governance types. IUCN, 1-86 pp.

Dullinger S, Gattringer A, Thuiller W et al. (2012) Extinction debt of high-mountain plants under twenty-first-century climate change. *Nature Climate Change*, 2, 619–622.

Early R, Sax D (2011) Analysis of climate paths reveals potential limitations on species range shifts. *Ecology Letters*, 14, 1125–1133.

Elith J, Leathwick J (2009) Species distribution models: ecological explanation and prediction across space and time. *Annual Review of Ecology, Evolution, and Systematics*, 40, 677–697.

Elith J, Phillips S, Hastie T, Dudik M, Chee Y, Yates C (2011) A statistical explanation of MaxEnt for ecologists. *Diversity and Distributions*, 17, 43–57.

Engler R, Hordijk W, Guisan A (2012) The MIGCLIM R package-seamless integration of dispersal constraints into projections of species distribution models. *Ecography*, 35, 872–878.

Essl F, Dullinger S, Rabitsch W, Hulme P, Pysek P, Wilson J, Richardson D (2015) Delayed biodiversity change: no time to waste. *Trends in Ecology and Evolution*, In press.

Fahrig L (2001) How much habitat is enough? *Biological Conservation*, 100, 65–74.

Faith D (1992) Conservation evaluation and phylogenetic diversity. *Biological Conservation*, 61, 1–10.

Fang F, Sun H, Zhao Q et al. (2013) Patterns of diversity, areas of endemism, and multiple glacial refuges for freshwater crabs of the genus *Sinopotamon* in China (Decapoda: Brachyura: Potamidae). *PLoS ONE*, 8, e53143.

Fei L (1999) *Atlas of amphibians of China*. Henan Science and Technology Press, Zhengzhou, China.

Fei L, Ye C, Jiang J (2012) *Colored atlas of Chinese amphibians and their distributions*. Sichuan Science & Technology Press, Chengdu, China, 1-619 pp.

Feng G, Mao L, Sandel B, Swenson N, Svenning J (2015) High plant endemism in China is partially linked to reduced glacial-interglacial climate change. *Journal of Biogeography*, DOI: 10.1111/jbi.12613.

Feng X, Lau M, Stuart S, Chanson J, Cox N, Fischman D (2007) Conservation needs of amphibians in China: a review. *Science in China Series C: Life Sciences*, 50, 265.

Fernandez-Palacios J, Rijsdijk K, Norder S et al. (2015) Towards a glacial-sensitive model of island biogeography. *Global Ecology and Biogeography*, DOI: 10.1111/geb.12320.

Fisher N, Lee A (1983) A correlation coefficient for circular data. *Biometrika*, 70, 327–332.

Forero-Medina G, Joppa L, Pimm S (2011) Constraints to species' elevational range shifts as climate changes. *Conservation Biology*, 25, 163–171.

Franklin J (2009) Mapping species distributions: spatial inference and prediction. Cambridge University Press, Cambridge, 1-320 pp.

Fritz S, Rahbek C (2012) Global patterns of amphibian phylogenetic diversity. *Journal of Biogeography*, 39, 1373–1382.

Gao Y, Zhang Y, Gao X, Zhu Z (2015) Pleistocene glaciations,demographic expansion and subsequent isolation promoted morphological heterogeneity: a phylogeographic study of the alpine Rosa sericea complex (Rosaceae). *Scientific Reports*, 5, 11698.

Gaston M, Fuji A, Weckerly F, Forstner M (2010) Potential component Allee effects and their impact on wetland management in the conservation of endangered Anuarans. *PLoS ONE*, 5, e10102.

Gatto R (2008) Some computational aspects of the generalized von Mises distribution. *Statistics and Computing*, 18, 321-331.

Gatto R, Jammalamadaka SR (2007) The generalized von Mises distribution. *Statistical Methodology*, 4, 341-353.

Geldmann J, Barnes M, Coad L, Craigie I, Hockings M, Burgess N (2013) Effectiveness of terrestrial protected areas in reducing habitat loss and population declines. *Biological Conservation*, 161, 230–238.

Gibson L, Lynam A, Bradshaw C et al. (2013) Near-complete extinction of native small mammal fauna 25 years after forest fragmentation. *Science*, 341, 1508–1510.

Gilbert B, Laurance W, Leigh E, Nascimento H (2006) Can neutral theory predict changes in Amazonian forest fragments? *American Naturalist*, 168, 304–317.

Gillings S, Balmer D, Fuller R (2015) Directionality of recent bird distribution shifts and climate change in Great Britain. *Global Change Biology*, 21, 2155–2168.

Goin C, Goin O, Zug G (1978) *Introduction to Herpetology*, 3rd ed. WH Freeman and Company, San Francisco.

Gong W, Chen C, Dobes C, Fu C, Koch M (2008) Phylogeography of a living fossil: pleistocene glaciations forced *Ginkgo biloba* L. (Ginkgoaceae) into two refuge areas in China with limited subsequent postglacial expansion. *Molecular Phylogenetics and Evolution*, 48, 1094–1105.

Halley J, Iwasa Y (2011) Neutral theory as a predictor of avifaunal extinctions after habitat loss. *PNAS*, 108, 2316–2321.

Hamann A, Roberts D, Barber Q, Carroll C, Nielsen S (2015) Velocity of climate change algorithms for guiding conservation and management. *Global Change Biology*, 21, 997–1004.

Hanski I (1994) A practical model of metapopulation dynamics. *Journal of Animal Ecology*, 63, 151–162.

Hanski I (1998) Metapopulation dynamics. *Nature*, 396, 41–49.

Hanski I (1999) *Metapopulation ecology*. Oxford University Press, Oxford.

Hanski I, Gyllenberg M (1997) Uniting two general patterns in the distribution of species. *Science*, 275, 397–400.

Hanski I, Koivulehto H, Cameron A, Rahagalala P (2007) Deforestation and apparent extinctions of endemic forest beetles in Madagascar. *Biology letters*, 3, 344–347.

Hanski I, Ovaskainen O (2000) The metapopulation capacity of a fragmented landscape. *Nature*, 404, 755–758.

Hanski I, Ovaskainen O (2002) Extinction debt at extinction threshold. *Conservation Biology*, 16, 666–673.

Hanski I, Ovaskainen O (2003) Metapopulation theory for fragmented landscapes. *Theoretical Population Biology*, 64, 119–127.

Hanski I, Zurita G, Bellocq M, Rybicki J (2014) Species-fragmented area relationship. *PNAS*, doi: 10.1073/pnas.1311491110.

Harris G, Pimm S (2008) Range size and extinction risk in forest birds. *Conservation Biology*, 22, 163–171.

Hastie T, Tibshirani R (1990) Generalized additive models. Chapman and Hall/CRC.

He F (2009) Price of prosperity: economic development and biological conservation in China. *Journal of Applied Ecology*, 46, 511–515.

He F (2012) Area-based assessment of extinction risk. *Ecology*, 93, 974–980.

He F, Hubbell S (2011) Species-area relationships always overestimate extinction rates from habitat loss. *Nature*, 473, 368–371.

- Heaney L (1985) Zoogeographic evidence for middle and late Pleistocene land bridges to Philippine islands. *Modern Quaternary Research in Southeast Asia*, 9, 127–143.
- Hickling R, Roy D, Hill J, Thomas C (2005) A northward shift of range margins in British Odonata. *Global Change Biology*, 11, 502–506.
- Hijmans R, Cameron S, Parra J, Jones P, Jarvis A (2005) Very high resolution interpolated climate surfaces for global land areas. *International Journal of Climatology*, 25, 1965–1978.
- Hiley J, Bradbury R, Holling M, Thomas C (2013) Protected areas act as establishment centres for species colonizing the UK. *PRSB*, 280, 20122310.
- Hodgson J, Bennie J, Dale G, Longley N, Wilson R, Thomas C (2015) Predicting microscale shifts in the distribution of the butterfly *Plebejus argus* at the northern edge of its range. *Ecography*, DOI: 10.1111/ecog.00825.
- Hof C, Araujo M, Jetz W, Rahbek C (2011) Additive threats from pathogens, climate and land-use change for global amphibian diversity. *Nature*, 480, 516–519.
- Howard S, Bickford D (2014) Amphibians over the edge: silent extinction risk of Data Deficient species. *Diversity and Distributions*, 20, 837–846.
- Huang Q, Sauer J, Swatantran A, Dubayah R (2016) A centroid model of species distribution with applications to the Carolina wren *Thryothorus ludovicianus* and house finch *Haemorhous mexicanus* in the United States. *Ecography*, 39, 54–66.
- Hurt G, Chini L, Frolking S et al. (2011) Harmonization of land-use scenarios for the period 1500–2100: 600 years of global gridded annual land-use transitions, wood harvest, and resulting secondary lands. *Climatic Change*, 109, 117–161.

Imbach P, Locatelli B, Molina L, Ciais P, Leadley P (2013) Climate change and plant dispersal along corridors in fragmented landscapes of Mesoamerica. *Ecology and Evolution*, 3, 2917–2932.

Isaac N, Redding D, Meredith H, Safi K (2012) Phylogenetically-informed priorities for amphibian conservation. *Plos One*, 7, e43912.

Jain A, Meiyappan P, Song Y, House J (2013) CO₂ emissions from land-use change affected more by nitrogen cycle, than by the choice of land-cover data. *Global Change Biology*, 19, 2893–2906.

Jammalamadaka S, Lund U (2006) The effect of wind direction on ozone levels: a case study. *Environmental and Ecological Statistics*, 13, 287–298.

Jammalamadaka S, SenGupta A (2001) Topics in circular statistics. World Scientific, Singapore, 1-336 pp.

Jenkins C, Joppa L (2009) Expansion of the global terrestrial protected area system. *Biological Conservation*, 142, 2166–2174.

Jenkins C, van Houtan K, Pimm S, Sexton J (2015) US protected lands mismatch biodiversity priorities. *Proceedings of the National Academy of Sciences of the United States of America*, 112, 5081–5086.

Jetz W, Freckleton R (2015) Toward a general framework for predicting threat status of data-deficient species from phylogenetic, spatial and environmental information. *Philosophical Transactions of the Royal Society B*, 370, 20140016.

Johnson R, Wehrly T (1977) Measures and models for angular correlation and angular-linear correlation. *Journal of the Royal Statistical Society, B*, 39, 222–229.

Jones C, Hughes J, Bellouin N et al. (2011) The HadGEM2-ES implementation of CMIP5 centennial simulations. *Geoscientific Model Development*, 4, 543–570.

Kirkpatrick J (1983) An iterative method for establishing priorities for the selection of nature reserves: an example from Tasmania. *Biological Conservation*, 25, 127–134.

Kitzes J, Harte J (2015) Predicting extinction debt from community patterns. *Ecology*, 96, 2127–2136.

Kramer AM, Dennis B, Liebhold AM, Drake JM (2009) The evidence for Allee effects. *Population Ecology*, 51, 341–354.

Lande R (1987) Extinction thresholds in demographic models of territorial populations. *American Naturalist*, 130, 624–635.

Lande R, Engen S, Sather B (2003) Stochastic population dynamics in ecology and conservation. Oxford University Press, New York, USA.

Lawler J, Shafer S, Bancroft B, Blaustein A (2009) Projected climate impacts for the amphibians of the Western Hemisphere. *Conservation Biology*, 24, 38–50.

Lawler J, White D, Neilson R, Blaustein A (2006) Predicting climate-induced range shifts: model differences and model reliability. *Global Change Biology*, 12, 1568–1584.

Lehtomaki J, Moilanen A (2013) Methods and workflow for spatial conservation prioritization using Zonation. *Environmental Modelling & Software*, 47, 128–137.

Levins R (1969) Some demographic and genetic consequences of environmental heterogeneity for biological control. *Bulletin of Entomology Society of America*, 15, 237–240.

Levins R, Culver D (1971) Regional coexistence of species and competition between rare species. *PNAS*, 68, 1246–1248.

Li B, Pimm S (2016) China's endemic vertebrates sheltering under the protective umbrella of the giant panda. *Conservation Biology*, 30, 329–339.

Lin Z, Zhao X (1996) Spatial characteristics of changes in temperature and precipitation of the Qinghai-Xizang (Tibet) Plateau. *Science in China (Series D)*, 39, 442–448.

Linder H (2000) Plant diversity and endemism in sub-Saharan tropical Africa. *Journal of Biogeography*, 28, 169–182.

Liu C, Berry P, Dawson T, Pearson R (2005) Selecting thresholds of occurrence in the prediction of species distributions. *Ecography*, 28, 385–393.

Liu C, White M, Newell G (2011) Measuring and comparing the accuracy of species distribution models with presence-absence data. *Ecography*, 34, 232–243.

Loaire S, Duffy P, Hamilton H, Asner G, Field C, Ackerly D (2009) The velocity of climate change. *Nature*, 462, 1052–1057.

Loaire S, Duffy P, Hamilton H, Asner G, Field C, Ackerly D (2009) The velocity of climate change. *Nature*, 462, 1052–1057.

Lomolino M, Riddle B, Brown J (2005) *Biogeography*. Sinauer Associates, Sunderland, Massachusetts, 845 pp.

Loyola R, Lemes P, Brum F, Provete D, Duarte L (2014) Clade-specific consequences of climate change to amphibians in Atlantic forest protected areas. *Ecography*, 37, 65–72.

Mardia K (1976) Linear-circular correlation coefficients and rhythmometry. *Biometrika*, 63, 403–405.

Mardia K, Spurr B (1973) Multi-sample tests for multi-modal and axial data. *Journal of the Royal Statistical Society, B*, 35, 422–436.

Margules C, Pressey R (2000) Systematic conservation planning. *Nature*, 405, 243–253.

Marsh D, Trenham P (2001) Metapopulation dynamics and amphibian conservation. *Conservation Biology*, 15, 40–49.

Mbogga M, Wang X, Hamann A (2010) Bioclimate envelope model predictions for natural resource management: dealing with uncertainty. *Journal of Applied Ecology*, 47, 731–740.

Meller L, Cabeza M, Pironon S, Barbet-Massin M, Maiorano L, Georges D, Thuiller W (2014) Ensemble distribution models in conservation prioritization: from consensus predictions to consensus reserve networks. *Diversity and Distributions*, 20, 309–321.

Meng L, Chen G, Li Z, Yang Y, Wang Z, Wang L (2015) Refugial isolation and range expansions drive the genetic structure of *Oxyria sinensis* (Polygonaceae) in the Himalaya-Hengduan Mountains. *Scientific Reports*, 5, 10396.

Mokhatla M, Rodder D, Measey G (2015) Assessing the effects of climate change on distributions of Cape Floristic Region amphibians. *South African Journal of Science*, 111, 1–7.

- Naujokaitis-Lewis I, Curtis J, Tischendorf L, Badzinski D, Lyndsay K, Fortin M (2013) Uncertainties in coupled species distribution-metapopulation dynamics models for risk assessments under climate change. *Diversity and Distributions*, 19, 541–554.
- Nicholson E, Possingham H (2006) Objectives for multiple-species conservation planning. *Conservation Biology*, 20, 871–881.
- Ning B, Yang X, Chang L (2012) Changes of temperature and precipitation extremes in Hengduan Mountains, Qinghai-Tibet Plateau in 1961-2008. *Chinese Geographical Science*, 22, 422–436.
- Otto-Bliesner B, Brady E, Clauzet G, Tomas R, Levis S, Kothavala Z (2006) Last glacial maximum and Holocene climate in CCSM3. *Journal of Climate*, 19, 2526–2544.
- Ovaskainen O, Hanski I (2001) Spatially structured metapopulation models: global and local assessment of metapopulation capacity. *Theoretical Population Biology*, 60, 281–302.
- Ovaskainen O, Hanski I (2002) Transient dynamics in metapopulation response to perturbation. *Theoretical Population Biology*, 61, 285–295.
- Ovaskainen O, Hanski I (2003) Extinction threshold in metapopulation models. *Annales Zoologici Fennici*, 40, 81–97.
- Ovaskainen O, Meerson B (2010) Stochastic models of population extinction. *Trends in Ecology and Evolution*, 25, 643–652.
- Parmesan C, Ryrholm N, Stefanescu C et al. (1999) Poleward shifts in geographical ranges of butterfly species associated with regional warming. *Nature*, 399, 579–583.

Pavon-Jordan D, Fox A, Clausen P et al. (2015) Climate-driven changes in winter abundances of a migratory waterbird in relation to EU protected areas. *Diversity and Distributions*, 21, 571–582.

Pearson R, Stanton J, Shoemaker K et al. (2014) Life history and spatial traits predict extinction risk due to climate change. *Nature Climate Change*, 4, 217.

Pearson R, Thuiller W, Araujo M et al. (2006) Model-based uncertainty in species range prediction. *Journal of Biogeography*, 33, 1704–1711.

Phillips S, Dudik M (2008) Modeling of species distributions with Maxent: new extensions and a comprehensive evaluation. *Ecography*, 31, 161–175.

Pough F (2007) Amphibian biology and husbandry. *ILAR Journal*, 48, 203–213.

Pounds J, Bustamante M, Coloma L et al. (2006) Widespread amphibian extinctions from epidemic disease driven by global warming. *Nature*, 439, 161–167.

Pouzols F, Toivonen T, Minin E et al. (2014) Global protected area expansion s compromised by projected land-use and parochialism. *Nature*, 516, 383–386.

Pressey R, Cabeza M, Watts M, Cowling R, Wilson K (2007) Conservation planning in a changing world. *Trends in Ecology and Evolution*, 22, 583–592.

Pressey R, Humphries C, Margules C, Vane-Wright R, Williams P (1993) Beyond opportunism: key principles for systematic reserve selection. *Trends in Ecology and Evolution*, 8, 124–128.

Primack R (2014) Essentials of conservation biology, 6th edn. Sinauer Associates, Sunderland, Massachusetts, USA, 1-603 pp.

R Development Core Team (2013) R: A Language and Environment for Statistical Computing, Vienna, Austria. ISBN 3-900051-07-0, URL <http://www.R-project.org>.

Rangel T (2012) Amazonian extinction debts. *Science*, 337, 162–163.

Reick C, Raddatz T, Brovkin V, Gayler V (2013) Representation of natural and anthropogenic land cover change in MPI-ESM. *Journal of Advances in Modeling Earth Systems*, 5, 459–482.

Ren G, Young S, Wang L et al. (2015) Effectiveness of China's national forest protection program and nature reserves. *Conservation Biology*, 29, 1368–1377.

Rickart E, Heaney L, Utzurum R (1991) Distribution and ecology of small mammals along an elevational transect in southeastern Luzon, Philippines. *Journal of Mammalogy*, 72, 458–469.

Roberts D, Hamann A (2016) Climate refugia and migration requirements in complex landscapes. *Ecography*, DOI: 10.1111/ecog.01998.

Rodrigues A, Brooks T (2007) Shortcuts for biodiversity conservation planning: the effectiveness of surrogates. *Annual Review of Ecology, Evolution and Systematics*, 38, 713–737.

Rogelj J, Meinsahusen M, Knutti R (2012) Global warming under old and new scenarios using IPCC climate sensitivity range estimates. *Nature Climate Change*, 2, 248–253.

Rosauer D, Jetz W (2015) Phylogenetic endemism in terrestrial mammals. *Global Ecology and Biogeography*, 24, 168–179.

Rosauer D, Laffan S, Crisp M, Donnellan S, Cook L (2009) Phylogenetic endemism: a new approach for identifying geographical concentrations of evolutionary history. *Molecular Ecology*, 18, 4061–4072.

Sandel B, Arge L, Dalsgaard B, Davies R, Gaston K, Sutherland W, Svenning J (2011) The influence of late Quaternary climate-change velocity on species endemism. *Science*, 334, 660.

Schnell J, Harris G, Pimm S, Russell G (2013) Estimating extinction risk with metapopulation models of large-scale fragmentation. *Conservation Biology*, 27, 520–530.

Shao M, Tang X, Zhang Y, Li W (2006) City clusters in China: air and surface water pollution. *Frontiers in Ecology and the Environment*, 4, 353–361.

Sinsch U (2014) Movement ecology of amphibians: from individual migratory behaviour to spatially structured populations in heterogeneous landscapes. *Canadian Journal of Zoology*, 92, 491-502.

Smith M, Green D (2005) Dispersal and the metapopulation paradigm in amphibian ecology and conservation: are all amphibian populations metapopulations? *Ecography*, 28, 110–128.

Smith MA, Green DM (2006) Sex, isolation and fidelity: unbiased long-distance dispersal in a terrestrial amphibian. *Ecography*, 29, 649-658.

Solow A, Bullister J, Nevison C (1988) An application of circular-linear correlation analysis to the relationship between Freon concentration and wind direction in Woods Hole, Massachusetts. *Environmental Monitoring and Assessment*, 10, 219–228.

Soutullo A, De Castro M, Urios V (2008) Linking political and scientifically derived targets for global biodiversity conservation: implications for the expansion of the global network of protected areas. *Diversity and Distributions*, 14, 604–613.

Stephens M (1962) Exact and approximate tests for directions. I. *Biometrika*, 49, 463–477.

Stockwell D, Peterson A (2002) Effects of sample size on accuracy of species distribution models. *Ecological Modelling*, 148, 1–13.

Stuart S, Chanson J, Cox N, Young B, Rodrigues A, Fischman D, Waller R (2004) Status and trends of amphibian declines and extinctions worldwide. *Science*, 306, 1783–1786.

Thomas C, Cameron A, Green R et al. (2004) Extinction risk from climate change. *Nature*, 427, 145–148.

Thomas C, Gillingham P, Bradbury R et al. (2012) Protected areas facilitate species' range expansions. *Proceedings of the National Academy of Sciences*, 109, 14063–14068.

Thomas C, Lennon J (1999) Birds extend their ranges northwards. *Nature*, 399, 213.

Thuiller W, Lafourcade B, Engler R, Araujo M (2009) BIOMOD-a platform for ensemble forecasting of species distributions. *Ecography*, 32, 369–373.

Thuiller W, Maiorano L, Mazel F et al. (2015) Conserving the functional and phylogenetic trees of life of European tetrapods. *Philosophical Transactions of the Royal Society B*, 370, 20140005.

Tilman D, Lehman C, Yin C (1997) Habitat destruction, dispersal, and deterministic extinction in competitive communities. *American Naturalist*, 149, 407–435.

Tilman D, May R, Lehman C, Nowak M (1994) Habitat destruction and the extinction debt. *Nature*, 371, 65–66.

Triantis K, Borges P, Ladle R et al. (2010) Extinction debt on oceanic islands. *Ecography*, 33, 285–294.

Tulloch A, Chades I, Possingham H (2013) Accounting for complementarity to maximize monitoring power for species management. *Conservation Biology*, 27, 988–999.

Upton G (1973) Single sample tests for the von Mises distribution. *Biometrika*, 60, 87–99.

Upton G, Fingleton B (1989) Spatial data analysis by example: categorical and directional data. Wiley, New York, 1-432 pp.

van Proosdij A, Sosef M, Wieringa J, Raes N (2015) Minimum required number of specimen records to develop accurate species distribution models. *Ecography*, 38, 1–11.

van Vuuren D, Edmonds J, Kainuma M et al. (2011) The representative concentration pathways: an overview. *Climatic Change*, 109, 5–31.

van Vuuren D, Stehfest E, den Elzen M et al. (2011) RCP2.6: exploring the possibility to keep global mean temperature increase below 2 Celsius degree. *Climatic Change*, 109, 95–116.

- VanDerWal J, Murphy H, Kutt A, Perkins G, Bateman B, Perry J, Reside A (2013) Focus on poleward shifts in species' distribution underestimates the fingerprint of climate change. *Nature Climate Change*, 3, 239–243.
- von Wissmann H (1937) The Pleistocene glaciation in China. *Bulletin of the Geological Society of China*, 17, 145–168.
- Wake D (1991) Declining amphibian populations. *Science*, 253, 860.
- Wake D (2007) Climate change implicated in amphibian and lizard declines. *Proceedings of the National Academy of Science of the United States of America*, 104, 8201–8202.
- Wake D, Vredenburg V (2008) Are we in the midst of the sixth mass extinction? A view from the world of amphibians. *PNAS*, 105, 11466–11473.
- Wang C, Wan J, Zhang Z, Zhang G (2016) Identifying appropriate protected areas for endangered fern species under climate change. *SpringerPlus*, 5, 904.
- Wang H, Yu X (2014) A review of the protection of sources of drinking water in China. *Natural Resources Forum*, 38, 99–108.
- Wang P (2000) Protection of the habitat of giant salamanders should be realized. *Sichuan Journal of Zoology*, 19, 164.
- Watanabe M, Suzuki T, O'ishi R et al. (2010) Improved climate simulation by MIROC5: mean states, variability, and climate sensitivity. *Journal of Climate*, 23, 6312–6335.
- Watts M, Bal I, Stewart R et al. (2009) Marxan with zones: software for optimal conservation based land- and sea-use zoning. *Environmental Modelling & Software*, 1513–1521.

Wearn O, Reuman D, Ewers R (2012) Extinction debt and windows of conservation opportunity in the Brazilian Amazon. *Science*, 337, 228–232.

Wei Y, Xu K, Zhu D, Chen X, Wang X (2010) Early-spring survey for Batrachochytrium dendrobatidis in wild *Rana dybowskii* in Heilongjiang Province, China. *Diseases of Aquatic Organisms*, 92, 241–244.

Wen J, Zhang J, Nie Z, Zhong Y, Sun H (2014) Evolutionary diversifications of plants on the Qinghai-Tibetan Plateau. *Frontiers in Genetics*, 5, 4.

Wheeler S, Watson G (1964) A distribution-free two-sample test on a circle. *Biometrika*, 51, 256–257.

Williams P, Gibbons D, Margules C, Rebelo A, Humphries C, Pressey R (1996) A comparison of richness hotspots, rarity hotspots, and complementary areas for conserving diversity of British birds. *Conservation Biology*, 10, 155–174.

Wintle B, Bekessy S, Keith D et al. (2011) Ecological-economic optimization of biodiversity conservation under climate change. *Nature Climate Change*, 1, 355–359.

Wood S (2006) Generalized additive models: an introduction with R. Chapman and Hall/CRC.

Xin X, Wu T, Li J, Wang Z, Li W, Wu F (2013a) How well does BCC_CSM1.1 reproduce the 20th century climate change over China? *Atmospheric and Oceanic Science Letters*, 6, 21–26.

Xin X, Zhang L, Zhang J, Wu T, Fang Y (2013b) Climate Change Projections over East Asia with BCC_CSM1.1 Climate Model under RCP Scenarios. *Journal of the Meteorological Society of Japan*, 91, 413–429.

Xu H, Wu J, Liu Y et al. (2008) Biodiversity congruence and conservation strategies: a national test. *BioScience*, 58, 632–639.

Yap T, Koo M, Ambrose R, Wake D, Vredenburg V (2015) Averting a North American biodiversity crisis. *Science*, 349, 481–482.

Yip J, Corlett R, Dudgeon D (2006) Selecting small reserves in a human-dominated landscape: a case study of Hong Kong, China. *Journal of Environmental Management*, 78, 86–96.

Yokohata T, Emori S, Nozawa T et al. (2007) Different transient climate responses of two versions of an atmosphere-ocean coupled general circulation model. *Geophysical Research Letters*, 34, L02707.

You Y, Sun K, Xu L et al. (2010) Pleistocene glacial cycle effects on the phylogeography of the Chinese endemic bat species, *Myotis davidii*. *BMC Evolutionary Biology*, 10, 208.

Yue L, Sun H (2013) Montane refugia isolation and plateau population expansion: phylogeography of Sino-Himalayan endemic *Spenceria ramalana* (Rosaceae). *Journal of Systematics and Evolution*, 52, 326–340.

Zhang J, Nielsen S, Chen Y et al. (2017) Extinction risk of North American seed plants elevated by climate and land-use. *Journal of Applied Ecology*, 54, 303–312.

Zhang J, Nielsen S, Stolar J, Chen Y, Thuiller W (2015) Gains and losses of plant species and phylogenetic diversity for a northern high-latitude region. *Diversity and Distributions*, 21, 1441–1454.

Zhang R (2004) Relict distribution of land vertebrates and Quaternary glaciation in China. *Acta Zoologica Sinica*, 50, 841–851.

- Zhang Z, Liu R (1991) The Holocene along the coast of Hainan Island, China. Chinese Geographical Science, 1, 188–196.
- Zhong D, Ding L (1996) Rising process of the Qinghai-Xizang (Tibet) Plateau and its mechanism. Science in China (Series D), 39, 369–379.
- Zhou S, Liu C, Wang G (2004) The competitive dynamics of metapopulations subject to the Allee-like effect. Theoretical Population Biology, 65, 29–37.
- Zhou S, Wang G (2004) Allee-like effects in metapopulation dynamics. Mathematical Biosciences, 189, 103–113.
- Zhu W, Bai C, Wang S, Soto-Azat C, Li X, Liu X, Li Y (2014) Retrospective survey of museum specimens reveals historically widespread presence of *Batrachochytrium dendrobatidis* in China. EcoHealth, 11, 241–250.